Supplement of Atmos. Chem. Phys., 24, 4029–4046, 2024
https://doi.org/10.5194/acp-24-4029-2024-supplement

Atmospheric Chemistry and Physics
Open Access
EGU

Supplement of

Reaction of SO_3 with H_2SO_4 and its implications for aerosol particle formation in the gas phase and at the air–water interface

Rui Wang et al.

Correspondence to: Tianlei Zhang (ztianlei88@163.com) and Hao Li (haol@rcees.ac.cn)

Figure S1 Schematic energy diagrams for the formation of H_2SO_4 from the SO_3 + H_2O reaction without and with H_2O at the CCSD(T)-F12/cc-pVDZ-F12//M06-2X/6-311++G(2*df*,2*pd*) level of theory

Table S1 Relative energies (ΔE and $\Delta(E$ + ZPE)/(kcal·mol^{-1})), enthalpies (ΔH/(kcal·mol^{-1})), entropy (S(298 K)/(cal·mol^{-1}·K^{-1})) and free energies (ΔG(298 K)/(kcal·mol^{-1})) for the reactants, intermediates, transition states and products involved in the reaction of SO_3 + H_2SO_4 without and with H_2O along with the hydrolysis reaction of SO_3 without and with H_2O

Table S2 Equilibrium constants (cm^3·molecule^{-1}) for SO_3···H_2SO_4, SO_3···H_2O, H_2SO_4···H_2O and $(H_2O)_2$ within the temperature range of 280-320 K

Table S3 Concentrations (molecules·cm^{-3}) of H_2O and H_2SO_4 within the temperature range of 280-320 K

Part 1 The calculation details of high-pressure-limit (HPL) rate constants

Table S4 The high-pressure limiting rate constants (cm^3·molecule^{-1}·s^{-1}) for the reactants to pre-reactive complex process in the SO_3 + H_2SO_4 reaction without and with H_2O, and the hydrolysis of SO_3 without and with H_2O calculated by the master equation within the temperature range of 280-320 K

Part 2 The details of Master Equation Solver for Multi-Energy Well Reactions

Table S5 Rate constants (cm^3·molecule^{-1}·s^{-1}) for the SO_3 + H_2SO_4 reaction with H_2O and the hydrolysis of SO_3 without and with H_2O within the temperature range of 280-320 K

Table S6 The rate constant (cm^3·molecule^{-1}·s^{-1}) for the SO_3 + H_2SO_4 reaction for the SO_3 + H_2SO_4 reaction without and with H_2O within the temperature range of 280-320 K by using transition state theory

Part 3 Calculations of effective rate constants

Table S7 The rate ratio between the SO_3 + H_2SO_4 reaction and the hydrolysis of SO_3 within the temperature range of 280-320 K at 0 km altitude

Table S8 The rate ratio between the SO_3 + H_2SO_4 reaction and the hydrolysis of SO_3 within the altitude range of 5-30 km in the atmospheres of Earth

Part 4 The details of the equilibrium process for the droplet system with 191 water molecules

Figure S2 The z coordinates of SO_3 (A), H_2SO_4 (B) and $H_2S_2O_7$ (C) molecule as the function of simulation time, (a) the density profile of water (b) and the pie chart with the occurrence percentages (c) at the air-water interface and in water phase

Figure S3 Snapshot structures taken from the BOMD simulations of H_2SO_4 reaction at the air-water interface. The white, red and yellow spheres represent H, O and S atoms, respectively

Figure S4 Two BOMD trajectories and snapshots for H_2O-induced the formation of $S_2O_7^{2-}$ •••H_3O^+ ion pair from the reaction of SO_3 with HSO_4^- at the air-water interface (Top panel: Snapshot structures taken from the BOMD simulations, which illustrate H_2O-induced the formation of $S_2O_7^{2-}$•••H_3O^+ ion pair from the reaction of SO_3 with HSO_4^- at the air-water interface. Lower panel: time evolution of key bond distances (S-O1, O2-H1, and O3-H1) involved in the induced mechanism.)

Figure S5 Two BOMD trajectories and snapshots for the direct HSO_4^--mediated formation of HSO_4^-⋯H_3O^+ ion pair at the air water interface (Top panel: Snapshot structures taken from the BOMD simulations, which illustrate the direct HSO_4^--mediated formation of HSO_4^-⋯H_3O^+ ion pair at the air water interface. Lower panel: time evolution of key bond distances (S1-O1, O1-H1 and H1-O2) involved in the hydration mechanism.)

Figure S6 Two BOMD trajectories and snapshots for the indirect HSO_4^--mediated formation of HSO_4^-⋯H_3O^+ ion pair at the air water interface (Top panel: Snapshot structures taken from the BOMD simulations, which illustrate the indirect HSO_4^--mediated formation of HSO_4^-⋯H_3O^+ ion pair at the air water interface. Lower panel: time evolution of key bond distances (S1-O1, O1-H1 and H1-O2) involved in the hydration mechanism.)

Figure S7 Two BOMD trajectories and snapshots for the deprotonation of $H_2S_2O_7$ at the air water interface (Top panel: Snapshot structures taken from the BOMD simulations, which illustrate the deprotonation of $H_2S_2O_7$ at the air water interface. Lower panel: time evolution of key bond distances (O1-H1, H1-O2, O3-H2 and H2-O4) involved in the hydration mechanism.)

Figure S8 The optimized geometrical structures of $HS_2O_7^-$, $S_2O_7^{2-}$ and HSO_4^- ion at M06-2X/6-311++G(2*df*,2*pd*) level of theory

Figure S9 The most stable configurations of the $(SA)_1(A)_1(Acid)_1$ clusters identified at the M06-2X/6-311++G(2*df*,2*pd*) level of theory. SA^-, SA, A, MOA, GSA, MHS, ASP and GA are respectively $HS_2O_4^-$, H_2SO_4, NH_3, $HOOCCH_2COOH$, $HOCCOOSO_3H$, CH_3OSO_3H, $HOOCC(H)NH_2COOH$ and $HOCH_2COOH$.The lengths of hydrogen bonds are given in Å. (blue = nitrogen, yellow = sulfur, red = oxygen, gray = carbon, and white = hydrogen.)

Table S9 Gibbs free energy (ΔG, kcal·mol^{-1}), equilibrium constant (K_{eq}, cm^3·molecule^{-1}) and the concentrations of SA, SO_3 and DSA computed at the CCSD(T)-F12/cc-pVDZ-F12//M06-2X/6-311++G(2*df*,2*pd*) level of theory

Part 5 Atmospheric concentrations of DSA under different SO_3 scenarios

Figure S10 Concentration (unit: molecules·cm^{-3}) of DSA with respect to different concentrations of SO_3 as function of altitude. We consider the possible concentrations of SO_3 with the injection

of SO_3.

Figure S11 The most stable configurations of the DSA-SA-A-based clusters identified at the M06-2X/6-311++G(2*df*,2*pd*) level of theory. DSA, SA, A are the shorthand for disulfuric acid, sulfuric acid and ammonia, respectively. The lengths of hydrogen bonds are given in Å. (blue = nitrogen, yellow = sulfur, red = oxygen, gray = carbon, and white = hydrogen.)

Table S10 The Gibbs free energy ΔG (kcal·mol$^{-1)}$ of formation of all clusters at pressure of 1 atm and the temperature range of 218.15-298.15 K, calculated at DLPNO-CCSD(T)/aug-cc-pVTZ//M06-2X/6-311++G(2*df*,2*pd*) level of theory

Figure S12 A typical actual ΔG surface at 218.15 K. [SA] is the concentration of sulfuric acid monomers, [A] the concentration of ammonia monomers and [DSA] is disulfuric acid

Figure S13 A typical actual ΔG surface at 238.15 K. [SA] is the concentration of sulfuric acid monomers, [A] the concentration of ammonia monomers and [DSA] is disulfuric acid

Part 6 Collision coefficients and evaporation coefficients

Part 7 Enhancement factor *R*

Table S10 Collision coefficients (β, cm^3·s^{-1}) for each cluster in the present study

Table S11 Evaporation rates (s^{-1}) of the studied clusters at different temperatures of 298.15, 278.15, 258.15, 238.15 and 218.15 K

Table S12 Total evaporation coefficients ($\sum\gamma$, s^{-1}) for each cluster in the present study

Table S13 The formation rate J of DSA at the conditions of T = 218.15 K, [SA] = 10^6-10^8 molecules·cm^{-3}, [A] = 10^7-10^{11} molecules·cm^{-3}, and [DSA] = 0, 10^4-10^7 molecules·cm^{-3}. SA, A and DSA represent sulfuric acid, ammonia and disulfuric acid, respectively

Table S14 The formation rate J of DSA at the conditions of T = 238.15 K, [SA] = 10^6-10^8 molecules·cm^{-3}, [A] = 10^7-10^{11} molecules·cm^{-3}, and [DSA] = 0, 10^4-10^7 molecules·cm^{-3}. SA, A and DSA represent sulfuric acid, ammonia and disulfuric acid, respectively

Table S15 The formation rate J of DSA at the conditions of T = 258.15 K, [SA] = 10^6-10^8 molecules·cm^{-3}, [A] = 10^7-10^{11} molecules·cm^{-3}, and [DSA] = 0, 10^4-10^7 molecules·cm^{-3}. SA, A and DSA represent sulfuric acid, ammonia and disulfuric acid, respectively

Table S16 The formation rate J of DSA at the conditions of T = 278.15 K, [SA] = 10^6-10^8 molecules·cm^{-3}, [A] = 10^7-10^{11} molecules·cm^{-3}, and [DSA] = 0, 10^4-10^7 molecules·cm^{-3}. SA, A

and DSA represent sulfuric acid, ammonia and disulfuric acid, respectively

Table S17 The formation rate J of DSA at the conditions of T = 298.15 K, [SA] = 10^6-10^8 molecules·cm^{-3}, [A] = 10^7-10^{11} molecules·cm^{-3}, and [DSA] = 0, 10^4-10^7 molecules·cm^{-3}. SA, A and DSA represent sulfuric acid, ammonia and disulfuric acid, respectively

Figure S14 The enhancement strength R of DSA as a function of [DSA] from 10^4 to 10^7 molecules·cm^{-3} under different temperatures (218.15, 238.15, 258.15, 278.15 and 298.15 K) where [SA] = 10^7 molecules·cm^{-3} and [A] = 10^9 molecules·cm^{-3}

Figure S15 Simulated cluster formation rates J (cm^{-3} s^{-1}) as a function of (a) [SA], (b) [A], with different concentrations of disulfuric acid [DSA] of 10^4 (red), 10^5 (blue), 10^6 (green) ,10^7 (purple) and 0 molecules·cm^{-3} (black, pure-SA-A), at T = 218.15 K

Figure S16 Simulated cluster formation rates J (cm^{-3} s^{-1}) as a function of (a) [SA], (b) [A], with different concentrations of disulfuric acid [DSA] of 10^4 (red), 10^5 (blue), 10^6 (green) ,10^7 (purple) and 0 molecules·cm^{-3} (black, pure-SA-A), at T = 238.15 K

Figure S17 Simulated cluster formation rates J (cm^{-3} s^{-1}) as a function of (a) [SA], (b) [A], with different concentrations of disulfuric acid [DSA] of 10^4 (red), 10^5 (blue), 10^6 (green) ,10^7 (purple) and 0 molecules·cm^{-3} (black, pure-SA-A), at T = 278.15 K

Figure S18 Simulated cluster formation rates J (cm^{-3} s^{-1}) as a function of (a) [SA], (b) [A], with different concentrations of disulfuric acid [DSA] of 10^4 (red), 10^5 (blue), 10^6 (green) ,10^7 (purple) and 0 molecules·cm^{-3} (black, pure-SA-A), at T = 298.15 K

Figure S19 Particle formation rates (J, cm^{-3}·s^{-1}) with varying ratios of [DSA]:[SA] at 258.15 K under different A concentrations ((a)10^7 molecules·cm^{-3}, (b)10^9 molecules·cm^{-3}, (c)10^{11} molecules·cm^{-3}). [DSA] + [SA] = 10^4-10^8 molecules·cm^{-3}

Figure S20 (a) The main pathways of clusters growing out of the research system under the conditions where 278.15 K, and 298.15 K, [SA] = 10^8 molecules·cm^{-3}, [A] = 10^9 molecules·cm^{-3}, and [DSA] = 10^6 molecules·cm^{-3}; (b) The contribution of different concentrations of DSA to the main cluster formation pathway at 278.15 K, and 298.15 K is shown in the pie charts.

Figure S21 The contribution of different concentrations of SA to the major cluster formation pathways at different temperatures (218.15 K, 238.15 K, 258.15 K, 278.15 K, and 298.15 K) and at [DSA] = 10^6 molecules·cm^{-3}, [A] = 10^9 molecules·cm^{-3} is shown in the pie charts.

Figure S22 The contribution of different concentrations of A to the major cluster formation pathways at different temperatures (218.15 K, 238.15 K, 258.15 K, 278.15 K, and 298.15 K) and at [DSA] = 10^6 molecules·cm^{-3}, [SA] = 10^8 molecules·cm^{-3} is shown in the pie charts.

Table S18. Cartesian coordinates of all molecules and clusters in the studied system

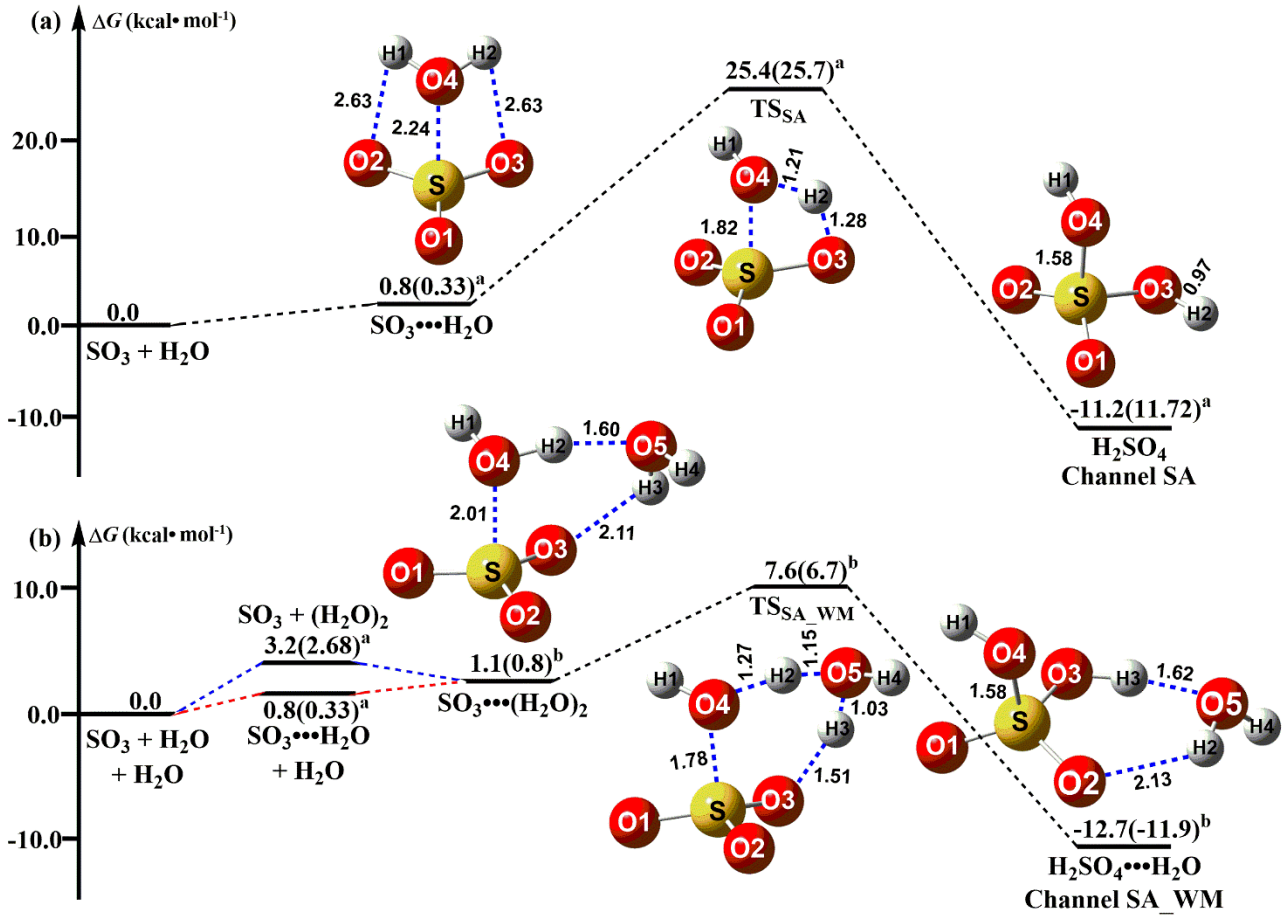

Figure S1 Schematic energy diagrams for the formation of H_2SO_4 from the SO_3 + H_2O reaction without and with H_2O at the CCSD(T)-F12/cc-pVDZ-F12//M06-2X/6-311++G(2*df*,2*pd*) level of theory

[a] The value was taken from reference (***Chem. Phys. Lett.***, **2013**, 581, 26-29.)

[b] The value was taken from reference (***J. Phys. Chem. A***, **2021**, 123, 3131–3141.)

Table S1 Relative energies (ΔE and $\Delta(E + ZPE)$/(kcal·mol^{-1})), enthalpies (ΔH/(kcal·mol^{-1})), entropy (S(298 K)/(cal·mol^{-1}·K^{-1})) and free energies (ΔG(298 K)/(kcal·mol^{-1})) for the reactants, intermediates, transition states and products involved in the reaction of SO_3 + H_2SO_4 without and with H_2O along with the hydrolysis reaction of SO_3 without and with H_2O

Species	ZPE	ΔE	S	ΔG	$\Delta(E+ZPE)$	ΔH
$SO_3 + H_2SO_4$	33.1	0.0	133.5	0.0	0.0	0.0
$SO_3\cdots H_2SO_4$	34.6	-14.3	93.8	-1.6	-12.9	-13.4
TS_{DSA}	32.9	-11.6	87.1	0.7	-11.9	-13.1
$H_2S_2O_7$	35.4	-21.6	89.5	-7.0	-19.4	-20.2
$SO_3 + H_2SO_4 + H_2O$	46.7	0.0	178.6	0.0	0.0	0.0
$SO_3\cdots H_2O + H_2SO_4$	24.0	-9.4	77.9	0.8	-7.0	-7.6
$H_2SO_4\cdots H_2O + SO_3$	40.9	-12.4	87.0	-1.9(-1.82)[a]	-10.2	-10.9
IM_{DSA_WM}'	49.3	-18.0	119.4	2.1	-15.4	-15.6
TS_{DSA_WM}'	49.2	-18.0	112.8	3.3	-15.6	-16.3
IM_{DSA_WM}	49.8	-27.8	104.5	-4.0	-24.7	-26.1
TS_{DSA_WM}	49.3	-27.5	99.9	-3.5	-24.9	-26.9
$H_2S_2O_7\cdots H_2O$	50.7	-34.6	102.8	-9.5	-30.6	-32.1
$SO_3 + H_2O + H_2SO_4$	46.7	0.0	178.6	0.0	0.0	0.0
$SO_3\cdots H_2O + H_2SO_4$	24.0	-9.4	77.9	0.8	-7.0	-7.6
$H_2SO_4\cdots H_2O + SO_3$	40.9	-12.4	87.0	-1.9(-1.82)[a]	-10.2	-10.9
IM_{SA_SA}'	49.5	-18.5	118.6	3.6	-15.5	-15.9
TS_{SA_SA}'	49.6	-18.4	111.0	5.4	-15.3	-16.3
IM_{SA_SA}	50.2	-27.0	104.6	-1.2	-23.3	-24.9
TS_{SA_SA}	49.1	-26.8	99.4	-1.2	-24.2	-26.5
$H_2SO_4\cdots H_2SO_4$	50.8	-34.1	103.0	-7.3	-29.8	-31.4
$SO_3 + H_2O$	21.6	0.0	106.2	0.0	0.0	0.0
$SO_3\cdots H_2O$	24.0	-9.4	77.9	0.8(0.33)[b] (0.62)[c]	-7.0	-7.6
TS_{SA}	22.3	15.7	70.4	25.4 (25.7)[b]	16.4	14.7
H_2SO_4	25.2	-23.6	71.8	-11.2(-10.72)[b]	-20.0	-21.4
$SO_3 + H_2O + H_2O$	35.2	0.0	151.3	0.0	0.0	0.0
$SO_3\cdots H_2O + H_2O$	24.0	-9.4	77.9	0.8(0.33)[b] (0.62)[c]	-7.0	-7.6
$SO_3 + (H_2O)_2$	29.5	-5.0	68.6	3.2(2.68)[b]	-2.7	-3.3
$SO_3\cdots(H_2O)_2$	40.7	-21.6	87.4	1.1(0.8)[d]	-16.0	-17.9
TS_{SA_WM}	39.1	-14.5	80.1	7.6(6.7)[d]	-10.6	-13.6
$H_2SO_4\cdots H_2O$	41.0	-36.0	85.5	-12.7(-11.9)[d]	-30.2	-32.3

[a] The value was taken from reference (Long, B., Tan, X. F., Chang, C. R., Zhao, W. X., Long, Z. W., Ren, D. S., and Zhang, W. J.: Theoretical studies on gas-phase reactions of sulfuric acid catalyzed hydrolysis of formaldehyde and formaldehyde with sulfuric acid and $H_2SO_4\cdots H_2O$ complex, J. Phys. Chem. A 117, 5106-5116, 2013.)

[b] The value was taken from reference (Long, B., Chang, C. R., Long, Z. W., Wang, Y. B., Tan, X. F., and Zhang, W. J.: Nitric acid catalyzed hydrolysis of SO_3 in the formation of sulfuric acid: A theoretical study, Chem. Phys. Lett., 581, 26-29, 2013.)

[c] The value was taken from reference (Long, B., Long, Z. W., Wang, Y. B., Tan, X. F., Han, Y. W., Long, C. W., Qin, S. J., and Zhang, W. J.: Formic acid catalyzed gas-phase reaction of H_2O with SO_3 and the reverse reaction: A theoretical study, ChemPhysChem, 13, 323-329, 10.1002/cphc.201100558, 2012.)

[d] The value was taken from reference (Sarkar, S., Oram, B. K., and Bandyopadhyay, B.: Influence of ammonia and water on the fate of sulfur trioxide in the troposphere: theoretical investigation of sulfamic acid and sulfuric acid formation pathways, J. Phys. Chem. A, 123, 3131-3141, 2019.)

Table S2 Equilibrium constants ($cm^3 \cdot molecule^{-1}$) for $SO_3 \cdots H_2SO_4$, $SO_3 \cdots H_2O$, $H_2SO_4 \cdots H_2O$ and $(H_2O)_2$ within the temperature range of 280-320 K

T/K	$SO_3 \cdots H_2SO_4$	$SO_3 \cdots H_2O$	$H_2SO_4 \cdots H_2O$	$(H_2O)_2$
280	2.54×10^{-18}	2.45×10^{-20}	3.00×10^{-118}	2.86×10^{-22}
290	1.15×10^{-18}	1.59×10^{-20}	2.66×10^{-19}	2.42×10^{-22}
298	6.33×10^{-19}	1.14×10^{-20} (6.44×10^{-20})[a]	1.67×10^{-19} (5.16×10^{-20})[b]	2.14×10^{-22} (2.34×10^{-21})[c]
300	5.48×10^{-19}	1.06×10^{-20}	1.49×10^{-19}	2.08×10^{-22}
310	2.75×10^{-19}	7.25×10^{-21}	8.68×10^{-20}	1.80×10^{-22}
320	1.44×10^{-20}	5.10×10^{-21}	5.24×10^{-20}	1.58×10^{-22}

[a] The value was taken from reference (Long, B., Long, Z. W., Wang, Y. B., Tan, X. F., Han, Y. W., Long, C. W., Qin, S. J., and Zhang, W. J.: Formic Acid Catalyzed Gas-Phase Reaction of H_2O with SO_3 and the Reverse Reaction: A Theoretical Study, ChemPhysChem, 13, 323-329, 10.1002/cphc.201100558, 2012.)

[b] The value was taken from reference (Wang, R., Wen, M., Chen, X., Mu, R., Zeng, Z., Chai, G., Lily, M., Wang, Z., and Zhang, T.: Atmospheric Chemistry of CH_2OO: The Hydrolysis of CH_2OO in Small Clusters of Sulfuric Acid, J. Phys. Chem. A, 125, 2642-2652, 10.1021/acs.jpca.1c02006, 2021.)

[c] The value was taken from reference (Torrent-Sucarrat, M., Francisco, J. S., and Anglada, J. M.: Sulfuric acid as autocatalyst in the formation of sulfuric acid, J. Am. Chem. Soc., 134, 20632-20644, 2012.)

Table S3 Concentrations (molecules·cm^{-3}) of H_2O and H_2SO_4 within the temperature range of 280-320 K

Catalysts	RH	280 K	290 K	298 K	300 K	310 K	320 K
H_2O	20%RH[a]	5.16×10^{16}	9.60×10^{16}	1.50×10^{17}	1.72×10^{17}	2.92×10^{17}	4.70×10^{17}
	40%RH[a]	1.03×10^{17}	1.91×10^{17}	3.10×10^{17}	3.43×10^{17}	5.84×10^{17}	9.40×10^{17}
	60%RH[a]	1.55×10^{17}	2.87×10^{17}	4.50×10^{17}	5.15×10^{17}	8.77×10^{17}	1.41×10^{18}
	80%RH[a]	2.07×10^{17}	3.82×10^{17}	6.20×10^{17}	6.86×10^{17}	1.17×10^{18}	1.88×10^{18}
	100%RH[a]	2.58×10^{17}	4.78×10^{17}	7.70×10^{17}	8.58×10^{17}	1.46×10^{18}	2.35×10^{18}
H_2SO_4	[SA][b] = 10^6	3.90×10^{6}	3.80×10^{6}	3.70×10^{6}	3.60×10^{6}	3.50×10^{6}	3.40×10^{6}
	[SA][c] = 10^7	5.00×10^{7}	5.00×10^{7}	5.00×10^{7}	5.00×10^{7}	5.00×10^{7}	5.00×10^{7}
	[SA][b] = 10^8	3.90×10^{8}	3.80×10^{8}	3.70×10^{8}	3.60×10^{8}	3.50×10^{8}	3.40×10^{8}
$H_2SO_4 \cdots H_2O$	[SA][e] = 10^6	20%RH	6.03×10^{5}	5.76×10^{5}	5.42×10^{5}	5.39×10^{5}	5.10×10^{5}
		40%RH	1.20×10^{6}	1.15×10^{6}	1.12×10^{6}	1.07×10^{6}	1.02×10^{6}
		60%RH	1.81×10^{6}	1.72×10^{6}	1.63×10^{6}	1.61×10^{6}	1.53×10^{6}
		80%RH	2.42×10^{6}	2.29×10^{6}	2.24×10^{6}	2.15×10^{6}	2.04×10^{6}
		100%RH	3.01×10^{6}	2.87×10^{6}	2.78×10^{6}	2.69×10^{6}	2.55×10^{6}
	[SA][c] = 10^7	20%RH	7.73×10^{6}	7.58×10^{6}	7.33×10^{6}	7.48×10^{6}	7.29×10^{6}
		40%RH	1.54×10^{7}	1.51×10^{7}	1.51×10^{7}	1.49×10^{7}	1.46×10^{7}
		60%RH	2.32×10^{7}	2.27×10^{7}	2.20×10^{7}	2.24×10^{7}	2.19×10^{7}
		80%RH	3.10×10^{7}	3.02×10^{7}	3.03×10^{7}	2.98×10^{7}	2.92×10^{7}
		100%RH	3.86×10^{7}	3.77×10^{7}	3.76×10^{7}	3.73×10^{7}	3.64×10^{7}
	[SA][e] = 10^8	20%RH	6.03×10^{7}	5.76×10^{7}	5.42×10^{7}	5.39×10^{7}	5.10×10^{7}
		40%RH	1.20×10^{8}	1.15×10^{8}	1.12×10^{8}	1.07×10^{8}	1.02×10^{8}
		60%RH	1.81×10^{8}	1.72×10^{8}	1.63×10^{8}	1.61×10^{8}	1.53×10^{8}
		80%RH	2.42×10^{8}	2.29×10^{8}	2.24×10^{8}	2.15×10^{8}	2.04×10^{8}
		100%RH	3.01×10^{8}	2.87×10^{8}	2.78×10^{8} (2.40×10^{7})[c] (1.11×10^{8})[d]	2.69×10^{8}	2.55×10^{8}

[a] The values were reported from reference (Anglada, J. M., Hoffman, G. J., Slipchenko, L. V., M. Costa, M., Ruiz-Lopez, M. F., and Francisco, J. S.: Atmospheric significance of water clusters and ozone-water complexes, J. Phys. Chem. A, 117, 10381-10396, 2013.)

[b] The values were taken from reference (Liu, J., Fang, S., Wang, Z., Yi, W., Tao, F. M., and Liu, J. Y.: Hydrolysis of sulfur dioxide in small clusters of sulfuric acid: Mechanistic and kinetic study, Environ. Sci. Technol., 49, 13112-13120, 2015.)

[c] The values were taken from reference (Liu, L., Zhong, J., Vehkamäki, H., Kurtén, T., Du, L., Zhang, X., Francisco, J. S., and Zeng, X. C.: Unexpected quenching effect on new particle formation from the atmospheric reaction of methanol with SO_3, Proc. Natl. Acad. Sci. U.S.A., 116, 24966-24971, 2019.)

[d] The values were taken from reference (Wang, R., Wen, M., Chen, X., Mu, R., Zeng, Z., Chai, G., Lily, M., Wang, Z., and Zhang, T.: Atmospheric Chemistry of CH_2OO: The Hydrolysis of CH_2OO in Small Clusters of Sulfuric Acid, J. Phys. Chem. A, 125, 2642-2652, 10.1021/acs.jpca.1c02006, 2021.)

Part 1 The calculation details of high-pressure-limit (HPL) rate constants

The VRC-VTST calculations were carried out with the potential surface obtained by using CCSD(T)-F12/cc-pVDZ-F12//M06-2X/6-311++G(2*df*,2*pd*) and were performed by variationally minimizing the rate constant with respect to the distance *s* between pivot points and with respect to the location of the pivot points. Specifically, using two pivot points produces a single-faceted dividing surface for the SO_3 + H_2SO_4 reaction without and with H_2O. Such as, using two pivot points produces a single-faceted dividing surface for the reaction of SO_3 + H_2SO_4. One pivot point is located at a distance *d* from the center of mass (COM) of SO_3, where the vector connecting the pivot point with SO_3's COM is perpendicular to the SO_3 plane, and the other pivot point is located at a distance *d* from the COM of catalyst H_2SO_4, where the vector connecting the pivot point with catalyst H_2SO_4's COM is perpendicular to catalyst H_2SO_4 plane. The lengths of these vectors are fixed successively at 0.2 Å. The reaction coordinate *s* is the distance between a pivot point on one reactant and a pivot point on the other reactant. The distance *s* between pivot points is varied from 2.5 to 8.0 Å for SO_3 + H_2SO_4 in each case with a 0.2 Å grid increment. The details of the VRC-VTST calculations can be seen in the supporting information of reference (Bao et al., 2016).

Reference

Bao, J. L.; Zhang, X.; Truhlar, D. G.: Barrierless association of CF_2 and dissociation of C_2F_4 by variational transition-state theory and system-specific quantum Rice-Ramsperger-Kassel theory, Proc. Natl. Acad. Sci. U. S. A., 113, 13606-13611, 2016

Table S4 The high-pressure limiting rate constants ($cm^3 \cdot molecule^{-1} \cdot s^{-1}$) for the reactants to pre-reactive complex process in the SO_3 + H_2SO_4 reaction without and with H_2O, and the hydrolysis of SO_3 without and with H_2O calculated by the master equation within the temperature range of 280-320 K

T(K)	$SO_3 + H_2SO_4 \rightarrow SO_3\cdots H_2SO_4$	$SO_3 + H_2SO_4\cdots H_2O \rightarrow IM_{DSA\_WM\_a'}$	$SO_3\cdots H_2O + H_2SO_4 \rightarrow SO_3\cdots H_2SO_4\cdots H_2O$
280	9.75×10^{-11}	1.69×10^{-10}	7.23×10^{-11}
290	9.93×10^{-11}	1.72×10^{-10}	7.35×10^{-11}
298	1.01×10^{-10}	1.75×10^{-10}	7.46×10^{-11}
300	1.01×10^{-10}	1.75×10^{-10}	7.48×10^{-11}
310	1.03×10^{-10}	1.78×10^{-10}	7.60×10^{-11}
320	1.04×10^{-10}	1.81×10^{-10}	7.73×10^{-11}
T(K)	$SO_3 + H_2O \rightarrow SO_3\cdots H_2O$	$SO_3\cdots H_2O + H_2O \rightarrow SO_3\cdots (H_2O)_2$	
280	1.45×10^{-10}	2.24×10^{-10}	
290	1.47×10^{-10}	2.28×10^{-10}	
298	1.49×10^{-10}	2.32×10^{-10}	
300	1.50×10^{-10}	2.32×10^{-10}	
310	1.52×10^{-10}	2.36×10^{-10}	
320	1.55×10^{-10}	2.40×10^{-10}	

Part 2 The details of Master Equation Solver for Multi-Energy Well Reactions

The rate constants for the SO_3 + H_2SO_4 reaction without and with H_2O within the temperature range of 280-320 K were calculated by using the Master Equation Solver for Multi-Energy Well Reactions (MESMER) (Miller and Klippenstein, 2006). Specifically, as for the SO_3 + H_2SO_4 reaction without and with H_2O, the barrierless bimolecular reaction steps were evaluated by using Inverse Laplace Transform (ILT) method (Horváth et al., 2020), whereas the rate determining steps were obtained by employing the RRKM theory. The ILT methods and RRKM theory can be respectively expressed in Eq. (S1)-Eq. (S2).

$$k(E) = \frac{W(E - E_0)}{h\rho(E)} \tag{S1}$$

$$k^{\infty}(\beta) = \frac{1}{Q(\beta)} \int_0^{\infty} k(E)\rho(E)\exp(-\beta E)dE \tag{S2}$$

In Eq. (S1) and Eq. (S2), $W(E\text{-}E_0)$ is the rovibrational sum of states (SOS) at the optimized transition state (TS) geometry, E_0 is the reaction threshold energy, h is Planck's constant, $\rho(E)$ is the density of rovibrational states of the reactant, and $Q(\beta)$ is the corresponding canonical partition function. Moreover, the electronic geometries, vibrational frequencies, and rotational constants were calculated at the M06-2X/6-311+G(2*df*,2*pd*) level; single-point energy calculations were refined at the CCSD(T)-F12/cc-pVDZ-F12 level for the modeling. The one-dimensional asymmetric Eckart potential was used to treat the tunneling effect in the RRKM calculation. In addition, the Lennard-Jones (L-J) parameters ε/k_B = 71.4 K and σ = 3.798 Å were used for N_2, while ε/k_B = 420.08 K and σ = 2.89 Å were estimated for H_2SO_4 and its isomer.

Reference

Horváth, G., Horváth, I., Almousa, S. A. D., and Telek, M.: Numerical inverse Laplace transformation using concentrated matrix exponential distributions, Perform. Evaluation, 137, 102067, 2020.

Miller, J. A., and Klippenstein, S. J.: Master equation methods in gas phase chemical kinetics, J. Phys. Chem. A, 110, 10528-10544, 2006.

Table S5 Rate constants ($cm^3 \cdot molecule^{-1} \cdot s^{-1}$) for the $SO_3 + H_2SO_4$ reaction with H_2O and the hydrolysis of SO_3 without and with H_2O within the temperature range of 280-320 K

Channel	*T*/K	280	290	298	300	310	320
Channel DSA_WM	$k_{DSA\_WM\_o}$	3.35×10^{-11}	3.53×10^{-11}	3.27×10^{-11}	3.19×10^{-11}	2.73×10^{-11}	2.29×10^{-11}
	$k_{DSA\_WM\_s}$	1.33×10^{-11}	1.13×10^{-11}	9.87×10^{-12}	9.53×10^{-12}	7.95×10^{-12}	6.59×10^{-12}
Channel SA_SA	$k_{SA\_SA\_o}$	1.39E-10	1.48E-10	1.45E-10	1.44E-10	1.39E-10	1.33E-10
	$k_{SA\_SA\_s}$	2.03E-11	1.80E-11	1.64E-11	1.61E-11	1.45E-11	1.31E-11
Channel SA	k_{SA}	6.22×10^{-24} (8.0×10^{-24})[a]	8.07×10^{-24} (1.1×10^{-23})[a]	1.02×10^{-23} (1.4×10^{-23})[a]	1.08×10^{-23} (1.4×10^{-23})[a]	1.49×10^{-23} (2.0×10^{-23})[a]	2.11×10^{-23} (3.0×10^{-23})[a]
Channel SA_WM	k_{SA_WM}	1.37×10^{-12}	1.17×10^{-12}	1.04×10^{-12} (4.08×10^{-12})[a]	1.01×10^{-12}	8.67×10^{-13}	7.49×10^{-13}

$k_{DSA\_WM\_o}$ and $k_{DSA\_WM\_s}$ are respectively the rate constants for the formation of $H_2S_2O_7$ from the reaction of $SO_3 + H_2SO_4$ with H_2O occurring through one-step and stepwise routes; k_{SA} and k_{SA_WM} are respectively the rate constants for the formation of H_2SO_4 without and with H_2O.

[a] The value was taken from reference (Bandyopadhyay, B., Kumar, P., and Biswas, P.: Ammonia Catalyzed Formation of Sulfuric Acid in Troposphere: The Curious Case of a Base Promoting Acid Rain, J. Phys. Chem. A, 121, 3101-3108, 10.1021/acs.jpca.7b01172, 2017.)

[b] The value was taken from reference (Torrent-Sucarrat, M., Francisco, J. S., and Anglada, J. M.: Sulfuric acid as autocatalyst in the formation of sulfuric acid, J. Am. Chem. Soc., 134, 20632-20644, 2012.)

Table S6 The rate constant ($cm^3 \cdot molecule^{-1} \cdot s^{-1}$) for the $SO_3 + H_2SO_4$ reaction for the $SO_3 + H_2SO_4$ reaction without and with H_2O within the temperature range of 280-320 K by using transition state theory

T/(K)	280 K	290 K	298 K	300 K	310 K	320 K
k_{DSA}	8.98×10^{-9}	4.38×10^{-9}	2.56×10^{-9}	2.25×10^{-9}	1.20×10^{-9}	6.72×10^{-10}
$k'_{DSA\_WM\_o}$	5.77×10^{-8}	2.59×10^{-8}	1.42×10^{-8}	1.23×10^{-8}	6.12×10^{-9}	3.18×10^{-9}
$k'_{DSA\_WM\_s}$	5.20×10^{-5}	2.44×10^{-5}	1.39×10^{-5}	1.21×10^{-5}	6.29×10^{-6}	3.42×10^{-6}

k_{DSA} is the rate constant for the $SO_3 + H_2SO_4$ reaction; $k_{DSA\_WM\_o}$ and $k_{DSA\_WM\_s}$ are respectively the rate constants for H_2O-assisted $SO_3 + H_2SO_4$ reaction occurring through one-step and stepwise routes.

As seen in Table S6, the rate constants for the $SO_3 + H_2SO_4$ reaction without and with H_2O by using transition state theory is significantly higher than the gas kinetic limit. In addition, as for the rate constants calculated by transition state theory (TST) coupled with the pre-equilibrium approximation, the rate constants for the $SO_3 + H_2SO_4$ reaction without and with H_2O showed appreciably high negative temperature dependence making the rate constants even larger at lower temperatures. This reveals that the TST coupled with pre-equilibrium approximation used in our calculation is truly obsolete and may not be appropriate. Thus, Using the Master Equation/Rice-Ramsperger-Kassel-Marcus (ME/RRKM) models, the kinetic calculations for the $SO_3 + H_2SO_4$ reaction without and with H_2O were performed by Bartis-Widom method in the MESMER program package (Master Equation Solver for Multi-Energy Well Reactions).

Part 3 Calculations of effective rate constants

Usually, the effective rate constants (*k*') is considered to be the relative efficiency of many atmospheric reactions (Liu et al., 2019; Sun et al., 2016; Ali et al., 2018; Ali et al., 2019) with water vapor. To better understand the competition between $H_2S_2O_7$ and H_2SO_4 formation in the atmospheric environment, it is necessary to compare the effective rate constants in different reaction. For the $H_2S_2O_7$ formation, the *k*' for the H_2O-assisted reaction (Channels DSA_WM) can be respectively expressed as:

$$k'_{DSA\_WM\_o} = k_{DSA\_WM\_o} \times K_{eq1} \times [H_2O] \quad (S3)$$

$$k'_{DSA\_WM\_s} = k_{DSA\_WM\_s} \times K_{eq2} \times [H_2O] \quad (S4)$$

In above formula, $k_{DSA\_WM\_o}$ and $k_{DSA\_WM\_s}$ were respectively denoted the bimolecular rate coefficient for Channels DSA_WM_o, DSA_WM_s and SA_WM; $[H_2O]$ and $[H_2SO_4]$ were respectively represented the concentration of H_2O and H_2SO_4 listed in Table S3; K_{eq1} and K_{eq2} is the equilibrium constant for the formation of complex $SO_3\cdots H_2O$ and $H_2SO_4\cdots H_2O$ shown in Table S2.

Reference

Ali, M. A., Balaganesh, M., and Lin, K.: Catalytic effect of a single water molecule on the OH + CH_2NH reaction, Phys. Chem. Chem. Phys., 20, 4297-4307, 2018.

Ali, M. A., M, B., and Jang, S.: Can a single water molecule catalyze the OH + CH_2CH_2 and OH + CH_2O reactions? Atmos. Environ., 207, 82-92, https://doi.org/10.1016/j.atmosenv.2019.03.025, 2019.

Liu, L., Zhong, J., Vehkamäki, H., Kurtén, T., Du, L., Zhang, X., Francisco, J. S., and Zeng, X. C.: Unexpected quenching effect on new particle formation from the atmospheric reaction of methanol with SO_3, Proc. Natl. Acad. Sci. U.S.A., 116, 24966-24971, 2019.

Sun, Y. Q., Wang, X., Bai, F.-Y., and Pan, X. M.: Theoretical study of the hydrolysis of HOSO + NO_2 as a source of atmospheric HONO: effects of H_2O or NH_3, Environ. Chem., 14, 19-30, 2016.

Table S7 The rate ratio between the SO_3 + H_2SO_4 reaction and the hydrolysis of SO_3 within the temperature range of 280-320 K at 0 km altitude

RH	[H_2SO_4]	280	290	298	300	310	320
20%RH	10^6	3.30×10^{-7}	1.40×10^{-8}	7.48×10^{-8}	5.98×10^{-8}	2.80×10^{-8}	1.41×10^{-9}
	10^7	4.23×10^{-6}	1.84×10^{-6}	1.01×10^{-6}	8.30×10^{-7}	4.00×10^{-7}	2.07×10^{-7}
	10^8	3.30×10^{-5}	1.40×10^{-5}	7.48×10^{-6}	5.98×10^{-6}	2.80×10^{-6}	1.41×10^{-7}
40%RH	10^6	1.05×10^{-7}	4.48×10^{-8}	2.25×10^{-8}	1.91×10^{-8}	8.90×10^{-9}	4.45×10^{-9}
	10^7	1.35×10^{-6}	5.90×10^{-7}	3.04×10^{-7}	2.65×10^{-7}	1.27×10^{-7}	6.54×10^{-8}
	10^8	1.05×10^{-5}	4.48×10^{-6}	2.25×10^{-6}	1.91×10^{-6}	8.90×10^{-7}	4.45×10^{-7}
60%RH	10^6	5.65×10^{-8}	2.41×10^{-8}	1.28×10^{-8}	1.03×10^{-8}	4.79×10^{-9}	2.39×10^{-9}
	10^7	7.24×10^{-7}	3.17×10^{-7}	1.72×10^{-7}	1.43×10^{-7}	6.84×10^{-8}	3.51×10^{-8}
	10^8	5.65×10^{-6}	2.41×10^{-6}	1.28×10^{-6}	1.03×10^{-6}	4.79×10^{-7}	2.39×10^{-7}
80%RH	10^6	3.73×10^{-8}	1.60×10^{-8}	8.05×10^{-9}	6.82×10^{-9}	3.16×10^{-9}	1.57×10^{-9}
	10^7	4.78×10^{-7}	2.10×10^{-7}	1.09×10^{-7}	9.47×10^{-8}	4.52×10^{-8}	2.32×10^{-8}
	10^8	3.73×10^{-6}	1.60×10^{-6}	8.05×10^{-7}	6.82×10^{-7}	3.16×10^{-7}	1.57×10^{-7}
100%RH	10^6	2.75×10^{-8}	1.17×10^{-8}	5.98×10^{-9}	5.01×10^{-9}	2.33×10^{-9}	1.16×10^{-9}
	10^7	3.53×10^{-7}	1.55×10^{-7}	8.08×10^{-8}	6.96×10^{-8}	3.33×10^{-8}	1.70×10^{-8}
	10^8	2.75×10^{-6}	1.17×10^{-6}	5.98×10^{-7}	5.01×10^{-7}	2.33×10^{-7}	1.16×10^{-7}

Table S8 The rate ratio between the SO_3 + H_2SO_4 reaction and the hydrolysis of SO_3 within the altitude range of 5-30 km in the atmospheres of Earth

H (km)	*T*(K)	P (Torr)	$[H_2O]^a$	$[H_2SO_4]^b$	k_{DSA}	$k_{DSA\_WM\_s}$	k_{SA_WM}	v_{DSA}/v_{SA}
5	259.30	406.75	2.43×10^{16}	6.00×10^{7}	3.16×10^{-12}	2.37×10^{-11}	1.91×10^{-12}	3.55×10^{-6}
10	229.70	202.16	4.92×10^{15}	8.30×10^{6} (5.1×10^{9})[c]	1.58×10^{-12}	2.25×10^{-11}	2.60×10^{-12}	6.56×10^{-5} (9.57×10^{-4})
15	212.60	91.20	1.96×10^{13}	2.40×10^{5}	1.10×10^{-13}	1.10×10^{-11}	3.07×10^{-12}	2.22×10^{-5}
20	215.50	41.04	9.56×10^{12}	4.20×10^{4}	1.50×10^{-13}	1.30×10^{-11}	2.89×10^{-12}	2.51×10^{-5}
25	218.60	19.00	2.50×10^{12}	4.59×10^{5}	1.56×10^{-13}	1.11×10^{-11}	2.75×10^{-12}	1.20×10^{-3}
30	223.70	8.36	2.62×10^{12}	2.88×10^{6}	1.49×10^{-13}	7.52×10^{-11}	2.55×10^{-12}	4.33×10^{-2}

k_{DSA}, $k_{DSA\_WM\_s}$ and k_{SA_WM} are respectively denoted the bimolecular rate coefficient for the H_2SO_4 + SO_3, $H_2SO_4\cdots H_2O$ + SO_3 and $SO_3\cdots H_2O$ + H_2O reactions. v_{DSA}/v_{SA} is the rate ratio between the SO_3 + SA reaction and H_2O-assisted hydrolysis of SO_3.

[a] The value was taken from reference (***J. Phys. Chem. A***, 2013, 117, 10381-10396.)

[b] The value was taken from reference (***J. Atmos. Sci.***, 1979, 36, 699-717.)

[c] The value was is the concentration of H_2SO_4 at the end and outside the aircraft engine and flight taken from reference (Geophys. Res. Lett., 2002, 29, 17-11-17-14.)

Part 4 The details of the equilibrium process for the droplet system with 191 water molecules

The droplet system with 191 water molecules has been equilibrated before SO_3 and H_2SO_4 was added at the water surface. Specifically, a nearly spherical droplet with 191 water molecules was firstly constructed by using the Packmol program (*J. Comput. Chem.*, 2009, 30, 2157-2164.) with a tolerance of 2.0 Å, namely, all atoms from different molecules will be at least 2.0 Å apart. Then, based on the resulting initial structure, the GROMACS software (*J. Comput. Chem.*, 2005, 26, 1701-1718.) with the general AMBER force field (GAFF) (*J. Comput. Chem.* 2004, 25, 1157-1174.) was used to simulate the droplet equilibrium process with two steps. In the first step, a water slab of 35 × 35 × 35 $Å^3$ containing 191 water molecules was built using periodic boundary conditions to avoid the effect of neighboring replicas. In the second step, the water slab was fully equilibrated for 1 ns under NVT ensemble (N, V and T represent the number of atoms, volume and temperature, respectively) to reach equilibrium state. The water molecules were described by the TIP3P model. The isothermal-isochoric (NVT) simulation was executed at 298 K for simulation system. The temperature was kept constant by the V-rescale thermostat coupling algorithm. The coupling time constant is 0.1 ps. Bond lengths were constrained by the LINCS algorithm. The cut-off distance of 1.2 nm was set for van der Waals (vdW) interactions. The Particle Mesh Ewald (PME) summation method was used to calculate the electrostatic interactions. During the whole simulation process, a time step of 2 fs was set and three-dimensional periodic boundary conditions were adopted. Next, to ensure the stability of the system, the droplets were pre-optimized using BOMD at 300 K for 10 ps prior to the simulation of the air-water interfacial reaction. Using the density functional theory (DFT) method, the electronic exchange-correlation term was described by the Becke-Lee-Yang-Parr (BLYP) functional. The Grimme's dispersion correction (D3) was applied to account for the weak dispersion interaction. The double-ζ Gaussian (DZVP-MOLOPT) basis set and the Goedecker-Teter-Hutter (GTH) norm-conserving pseudopotentials were adopted to treat the valence and the core electrons, respectively. The planewave cutoff energy is set to 280 Ry, and that for the Gaussian basis set is 40 Ry. And the SCF convergence criterion is 1.0E-5 Hartree. All simulations were performed in NVT ensemble with Nose-Hoover thermostat controlling the temperature. Finally, the SO_3 and H_2SO_4 molecule was added at the water surface after the droplet system with 191 water molecules was fully equilibrated.

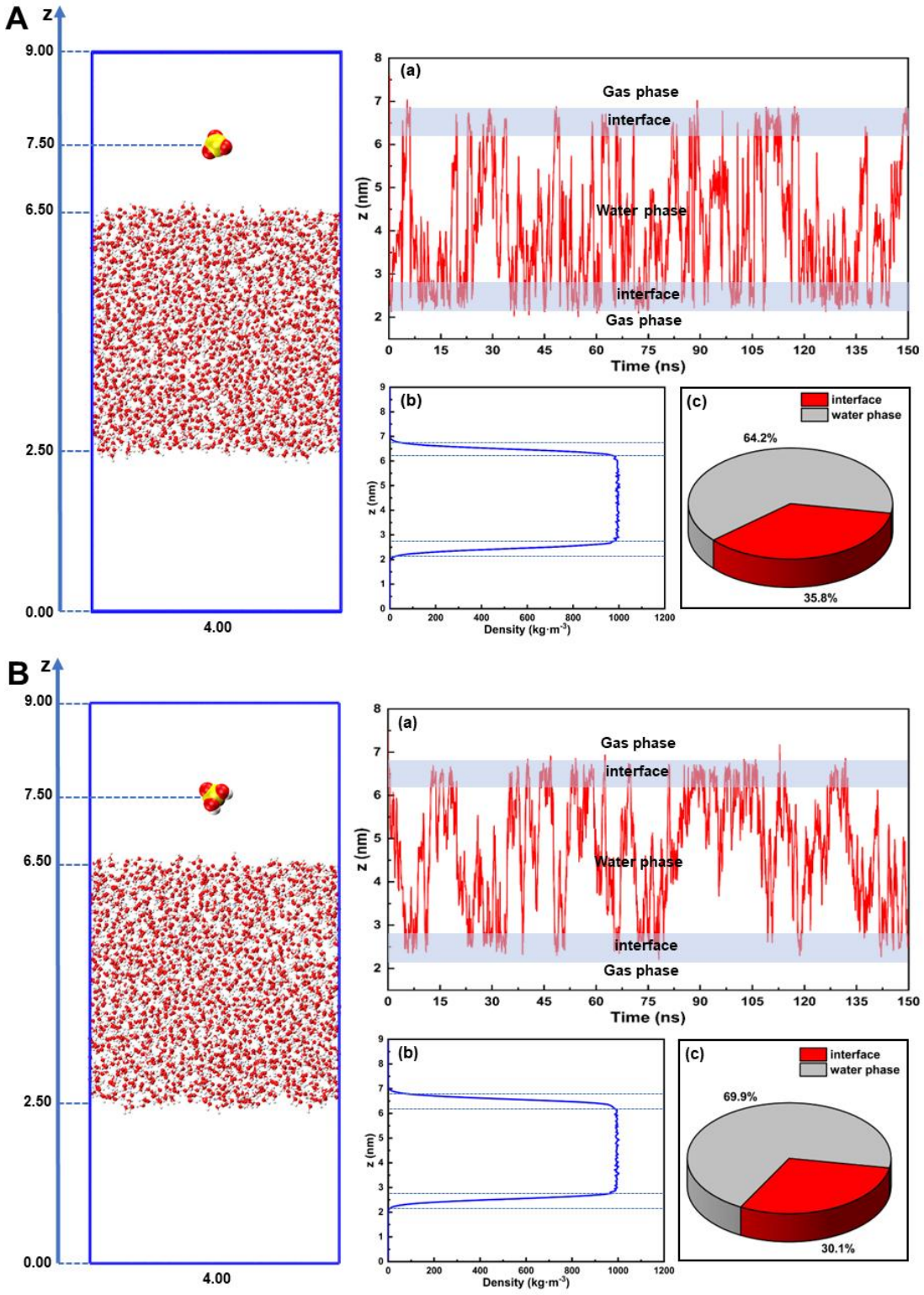
A
z
9.00
7.50
6.50
2.50
0.00
4.00
(a)
Gas phase
interface
Water phase
interface
Gas phase
z (nm)
Time (ns)
(b)
z (nm)
Density (kg·m-3)
(c)
interface
water phase
64.2%
35.8%
B
z
9.00
7.50
6.50
2.50
0.00
4.00
(a)
Gas phase
interface
Water phase
interface
Gas phase
z (nm)
Time (ns)
(b)
z (nm)
Density (kg·m-3)
(c)
interface
water phase
69.9%
30.1%

1

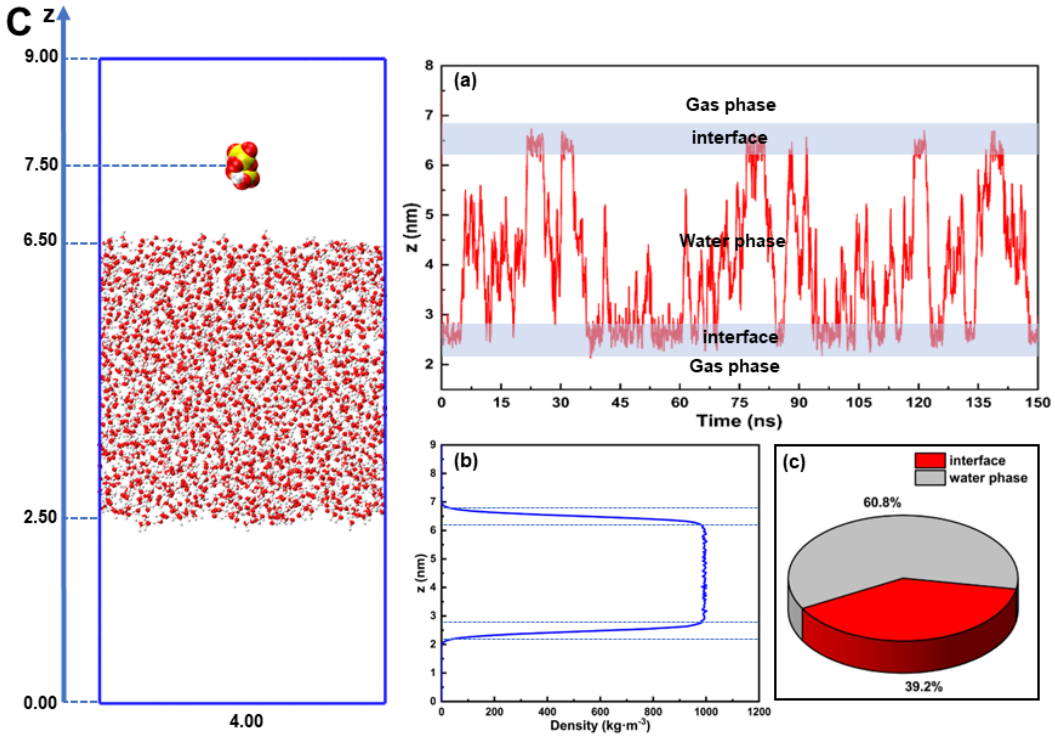

Figure S2 The z coordinates of SO_3 (A), H_2SO_4 (B) and $H_2S_2O_7$ (C) molecule as the function of simulation time, (a) the density profile of water (b) and the pie chart with the occurrence percentages (c) at the air-water interface and in water phase

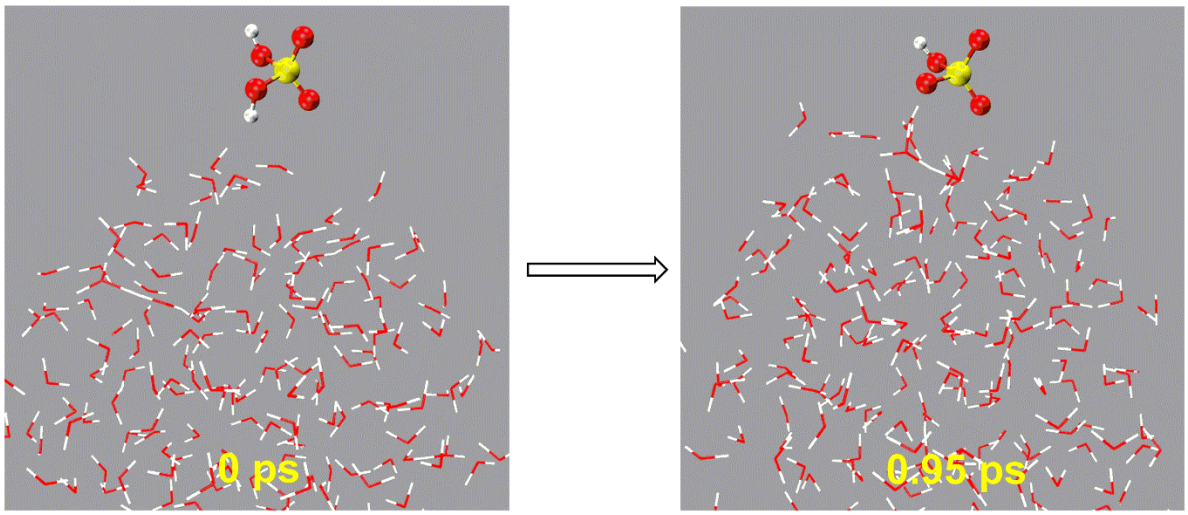

Figure S3 Snapshot structures taken from the BOMD simulations of H_2SO_4 reaction at the air-water interface. The white, red and yellow spheres represent H, O and S atoms, respectively.

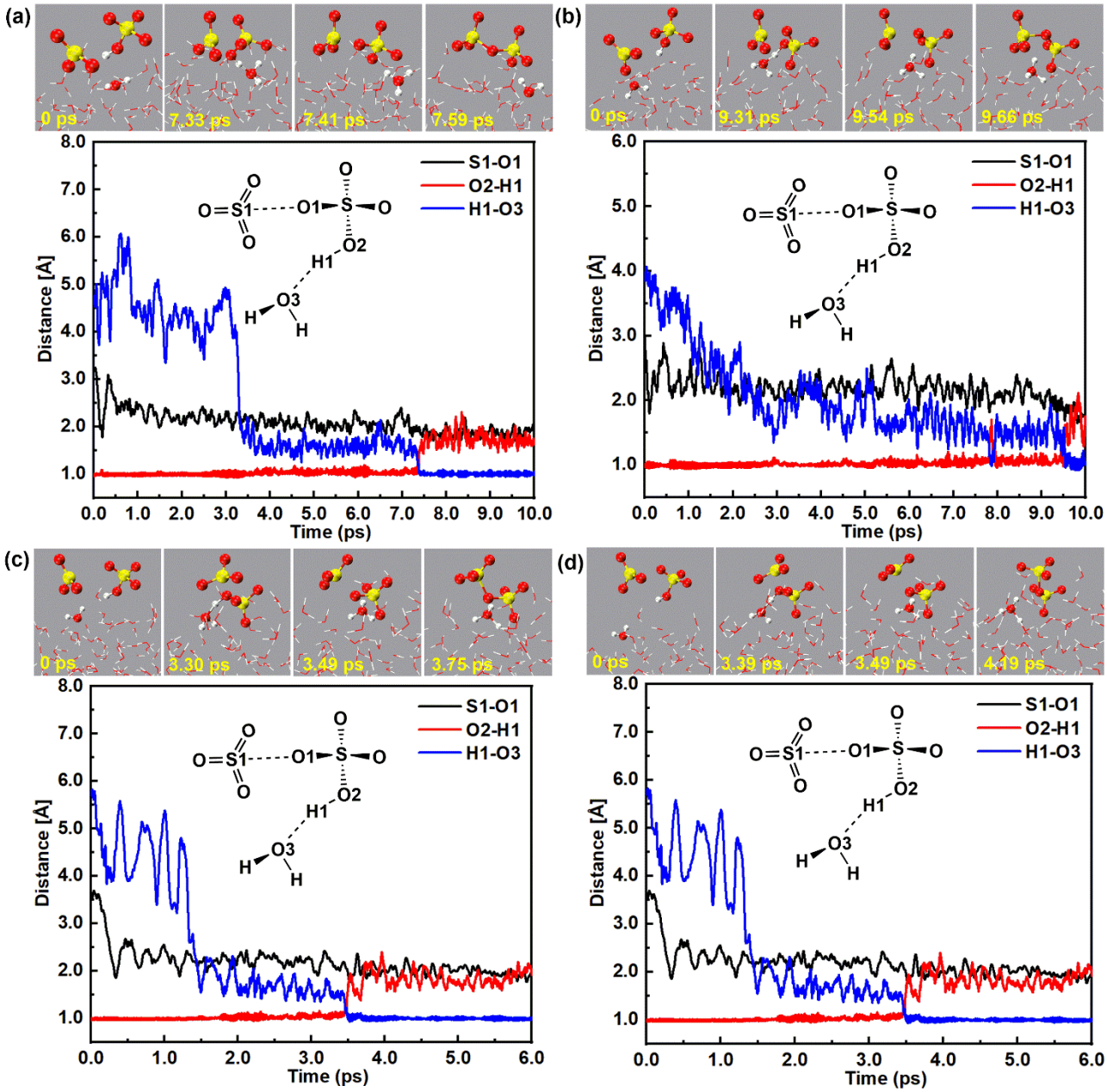

Figure S4 Two BOMD trajectories and snapshots for H_2O-induced the formation of $S_2O_7^{2-}$•••H_3O^+ ion pair from the reaction of SO_3 with HSO_4^- at the air-water interface (Top panel: Snapshot structures taken from the BOMD simulations, which illustrate H_2O-induced the formation of $S_2O_7^{2-}$•••H_3O^+ ion pair from the reaction of SO_3 with HSO_4^- at the air-water interface. Lower panel: time evolution of key bond distances (S-O1, O2-H1, and O3-H1) involved in the induced mechanism.)

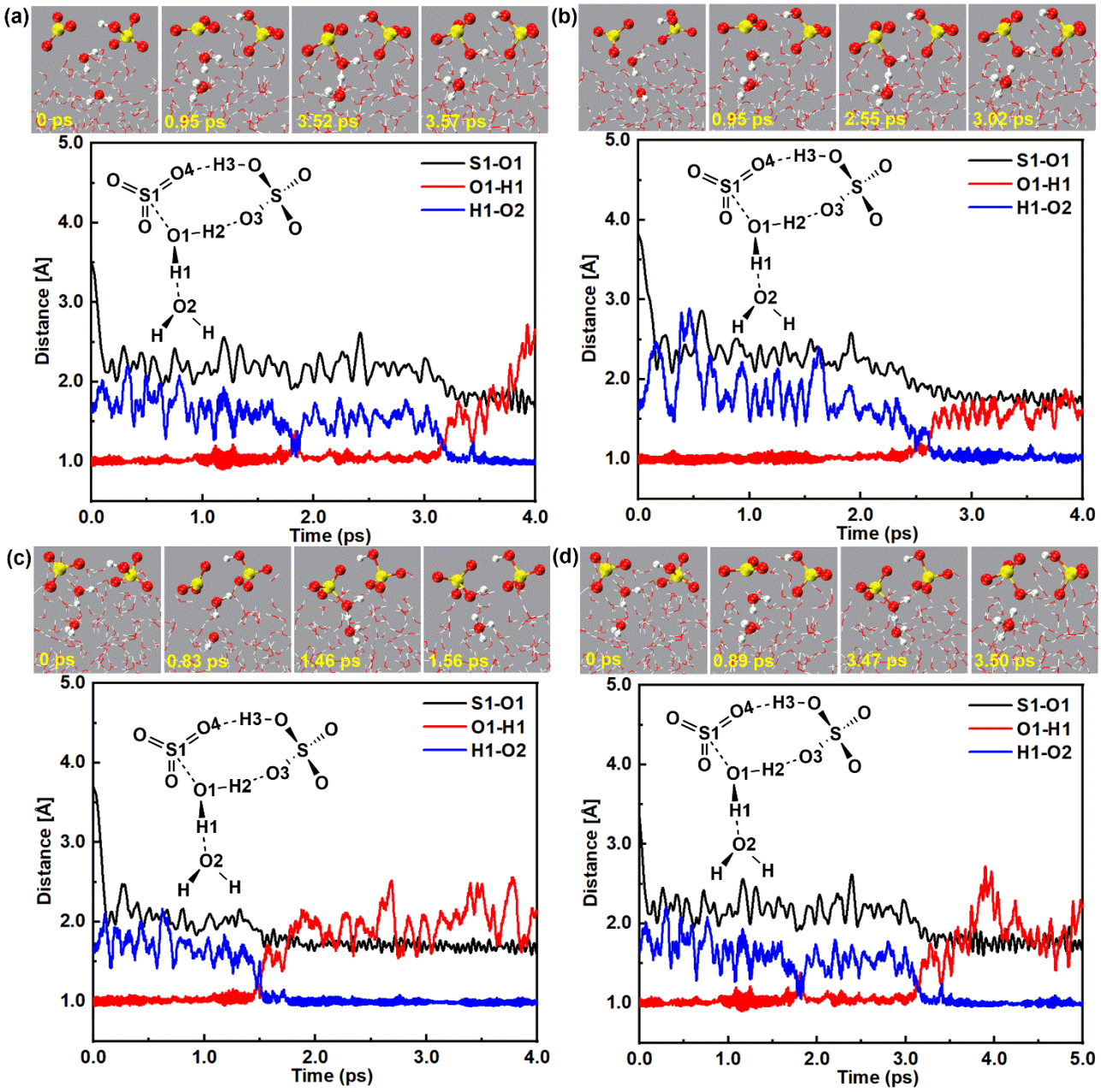

Figure S5 Two BOMD trajectories and snapshots for the direct HSO_4^--mediated formation of $HSO_4^-\cdots H_3O^+$ ion pair at the air water interface (Top panel: Snapshot structures taken from the BOMD simulations, which illustrate the direct HSO_4^--mediated formation of $HSO_4^-\cdots H_3O^+$ ion pair at the air water interface. Lower panel: time evolution of key bond distances (S1-O1, O1-H1 and H1-O2) involved in the hydration mechanism.)

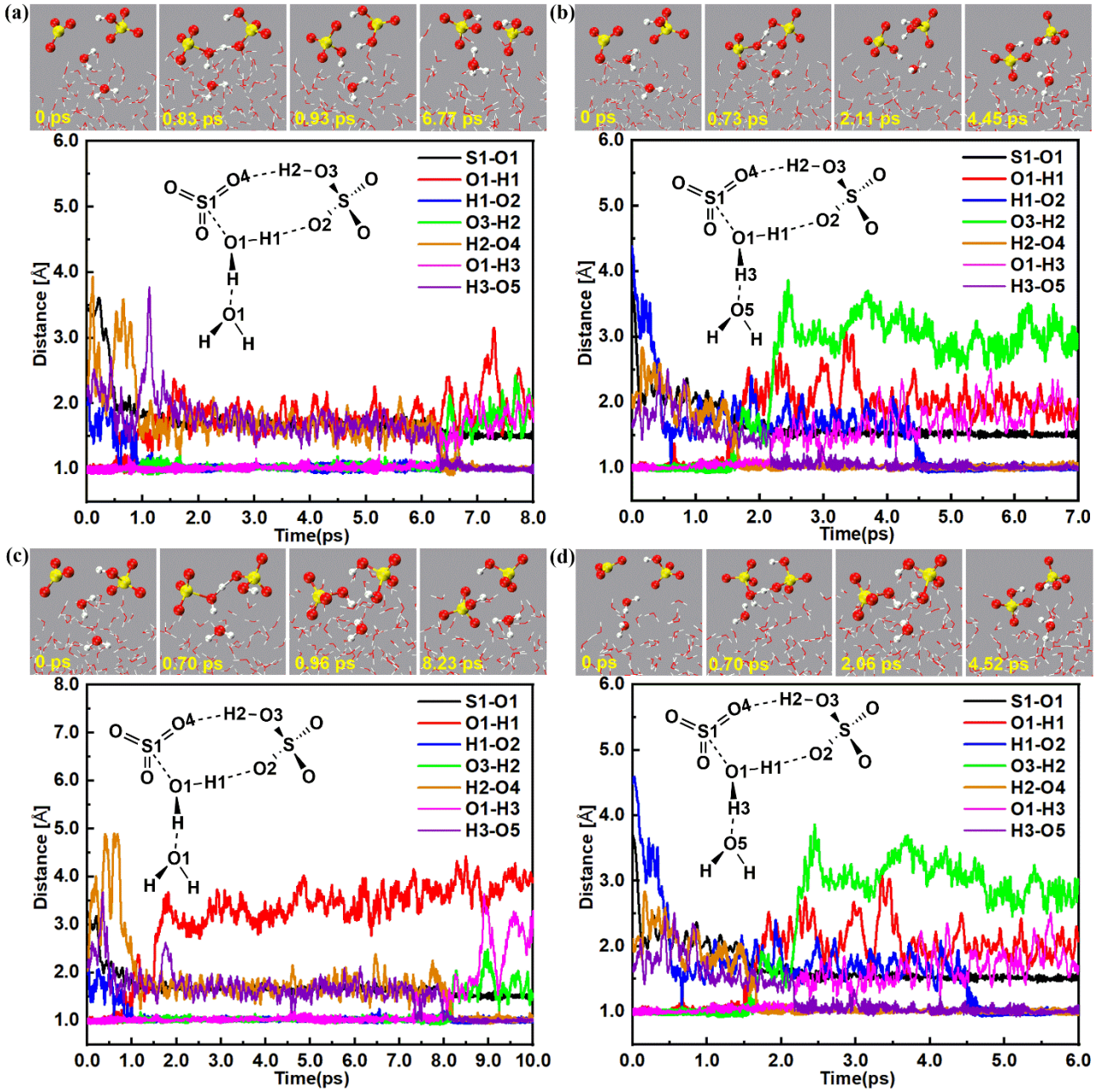

Figure S6 Two BOMD trajectories and snapshots for the indirect HSO_4^--mediated formation of $HSO_4^-\cdots H_3O^+$ ion pair at the air water interface (Top panel: Snapshot structures taken from the BOMD simulations, which illustrate the indirect HSO_4^--mediated formation of $HSO_4^-\cdots H_3O^+$ ion pair at the air water interface. Lower panel: time evolution of key bond distances (S1-O1, O1-H1 and H1-O2) involved in the hydration mechanism.)

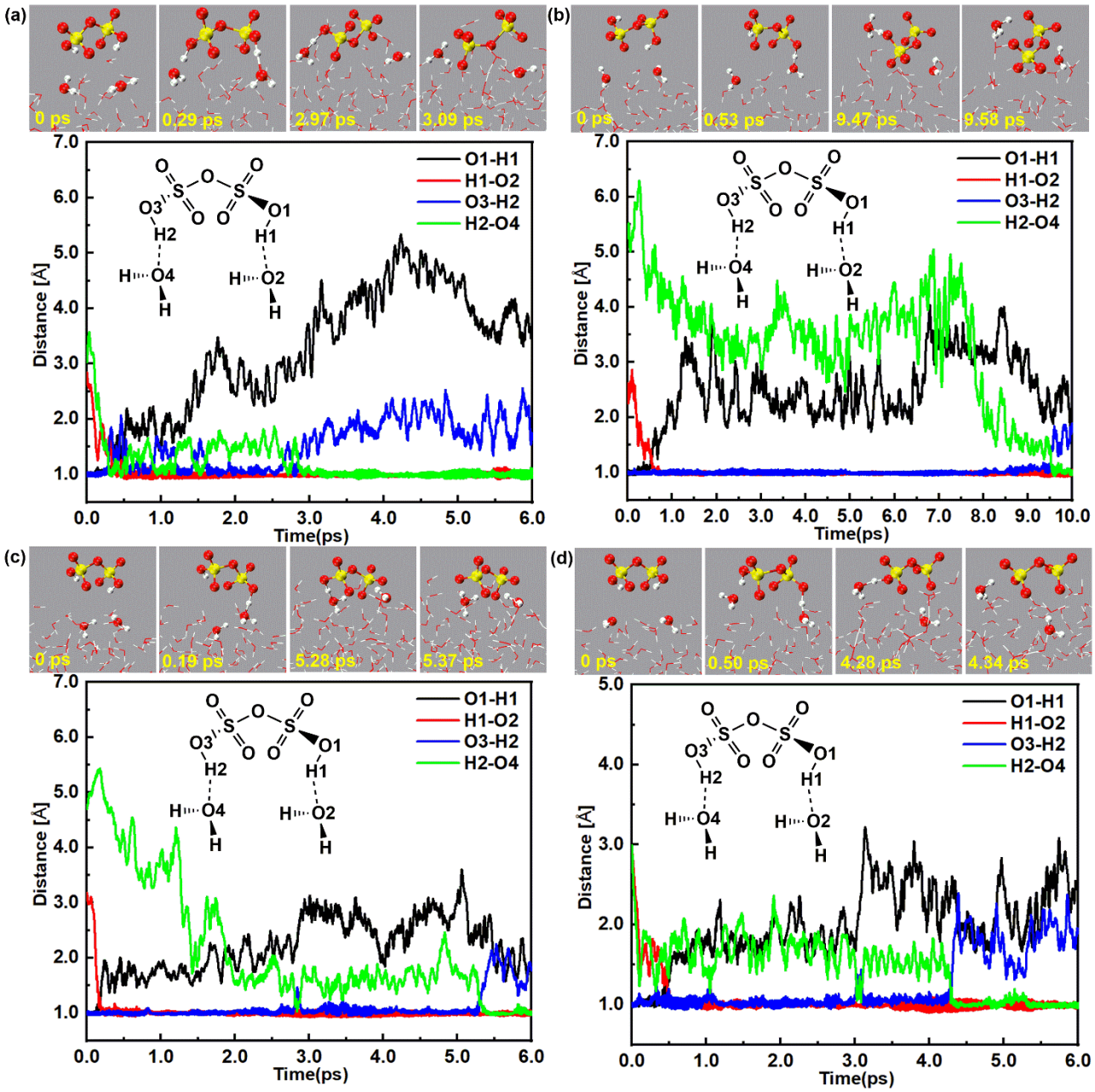

Figure S7 Two BOMD trajectories and snapshots for the deprotonation of $H_2S_2O_7$ at the air water interface (Top panel: Snapshot structures taken from the BOMD simulations, which illustrate the deprotonation of $H_2S_2O_7$ at the air water interface. Lower panel: time evolution of key bond distances (O1-H1, H1-O2, O3-H2 and H2-O4) involved in the hydration mechanism.)

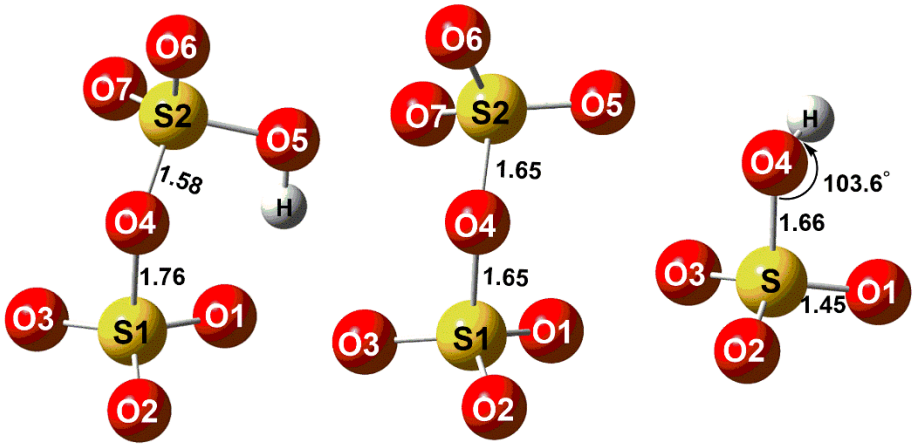

Figure S8 The optimized geometrical structures of $HS_2O_7^-$, $S_2O_7^{2-}$ and HSO_4^- ion at M06-2X/6-311++G(2*df*,2*pd*) level of theory

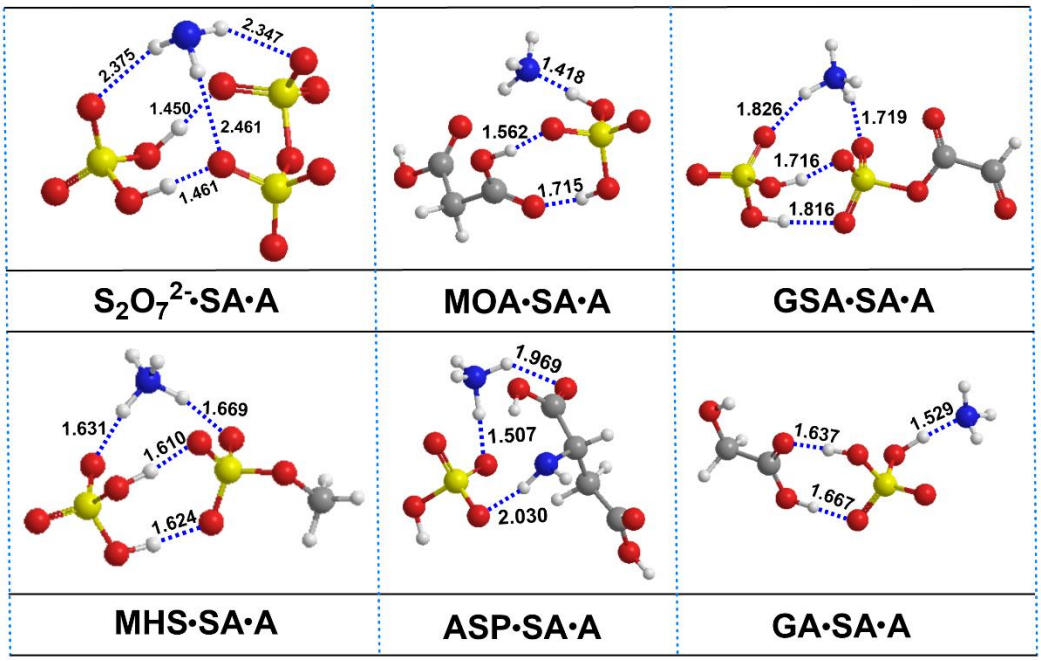

Figure S9 The most stable configurations of the $(SA)_1(A)_1(Acid)_1$ clusters identified at the M06-2X/6-311++G (2*df*,2*pd*) level of theory. SA^-, SA, A, MOA, GSA, MHS, ASP and GA are respectively $HS_2O_4^-$, H_2SO_4, NH_3, $HOOCCH_2COOH$, $HOCCOOSO_3H$, CH_3OSO_3H, $HOOCC(H)NH_2COOH$ and $HOCH_2COOH$.The lengths of hydrogen bonds are given in Å. (blue = nitrogen, yellow = sulfur, red = oxygen, gray = carbon, and white = hydrogen.)

Table S9 Gibbs free energy (ΔG, kcal·mol^{-1}), equilibrium constant (K_{eq}, cm^3·molecule^{-1}) and the concentrations of SA, SO_3 and DSA computed at the CCSD(T)-F12/cc-pVDZ-F12//M06-2X/6-311++G(2*df*,2*pd*) level of theory

ΔG	Altitude (km)	T (K)	K_{eq}	[SA]/(molecules·cm^{-3})
	0	298.15	1.14×10^{-20}	(3.70×10^{8})[a]
	5	259.30	1.66×10^{-17}	(6.00×10^{7})[a]
	10	229.70	3.97×10^{-16}	(5.10×10^{9})[b]
-1.6	15	212.60	3.85×10^{-16}	(2.40×10^{5})[a]
	20	215.50	2.51×10^{-15}	(4.20×10^{4})[a]
	25	218.60	1.66×10^{-15}	(4.59×10^{5})[a]
	30	223.70	8.50×10^{-16}	(2.88×10^{6})[a]

[a] The values were taken from reference (***J. Atmos. Sci.***, 1979, 36, 699-717.)

[b] The values were taken from reference (***Geophys. Res. Lett.***, 2002, 29, 1113.)

Part 5 Atmospheric concentrations of DSA under different SO_3 scenarios

The steady-state concentration of DSA was calculated using the calculated equilibrium constant listed in Eq. S5.

$$K_{eq3} = \frac{[DSA]}{[SO_3][SA]} \quad (S5)$$

where K_{eq3} is the equilibrium constant of DSA with respect to SO_3 and H_2SO_4 within the altitude range of 0-30 km shown in Table S9; [SO_3], [SA] and [DSA] are the concentrations of SO_3, H_2SO_4, and $H_2S_2O_7$, respectively. Although the concentration of sulfur trioxide remains unknown at different altitudes, experimental observations have shown that the concentration of sulfur trioxide can reach 10^6 molecules cm^{-3} in the troposphere. (Yao et al., 2020). Moreover, water vapor concentrations significantly decrease with increasing of altitude. Consequently, the concentration of sulfur trioxide should be higher in the stratosphere than in the troposphere (Long et al., 2022), and its concentration would increase as a result of geoengineered injection of SO_2 or SO_3. Besides, it is worth noting that H_2SO_4 can form at the end and outside the engine, and flight measurements in the exhaust plume have measured sulfuric acid abundances up to a value of 600 pptv. (Curtius et al., 2002). When an average flight altitude of 10 km is considered, this corresponds to a concentration of 5.1×10^9 molecules·cm^{-3}. Therefore, we have calculated the concentrations of DSA according to concentrations of sulfur trioxide in the range from 10^7 to 10^{14} molecules cm^{-3} and the concentrations of H_2SO_4 in the range of 10^4-10^9 molecules cm^{-3} as shown in Figure S9.

Reference:

Curtius, J., Arnold, F., and Schulte, P.: Sulfuric acid measurements in the exhaust plume of a jet aircraft in flight: Implications for the sulfuric acid formation efficiency, Geophys. Res. Lett., 29, 17-11-17-14, 2002.

Long, B., Xia, Y., Bao, J. L., Carmona-García, J., Gómez Martín, J. C., Plane, J. M. C., Saiz-Lopez, A., Roca-Sanjuán, D., and Francisco, J. S.: Reaction of SO3 with HONO2 and Implications for Sulfur Partitioning in the Atmosphere, J. Am. Chem. Soc., 144, 9172-9177, 10.1021/jacs.2c03499, 2022.

Yao, L., Fan, X., Yan, C., Kurtén, T., Daellenbach, K. R., Li, C., Wang, Y., Guo, Y., Dada, L., Rissanen, M. P., Cai, J., Tham, Y. J., Zha, Q., Zhang, S., Du, W., Yu, M., Zheng, F., Zhou, Y., Kontkanen, J., Chan, T., Shen, J., Kujansuu, J. T., Kangasluoma, J., Jiang, J., Wang, L., Worsnop, D. R., Petäjä, T., Kerminen, V. M., Liu, Y., Chu, B., He, H., Kulmala, M., and Bianchi, F.: Unprecedented Ambient Sulfur Trioxide (SO3) Detection: Possible Formation Mechanism and Atmospheric Implications, Environ. Sci. Technol. Lett., 7, 809-818, 10.1021/acs.estlett.0c00615, 2020.

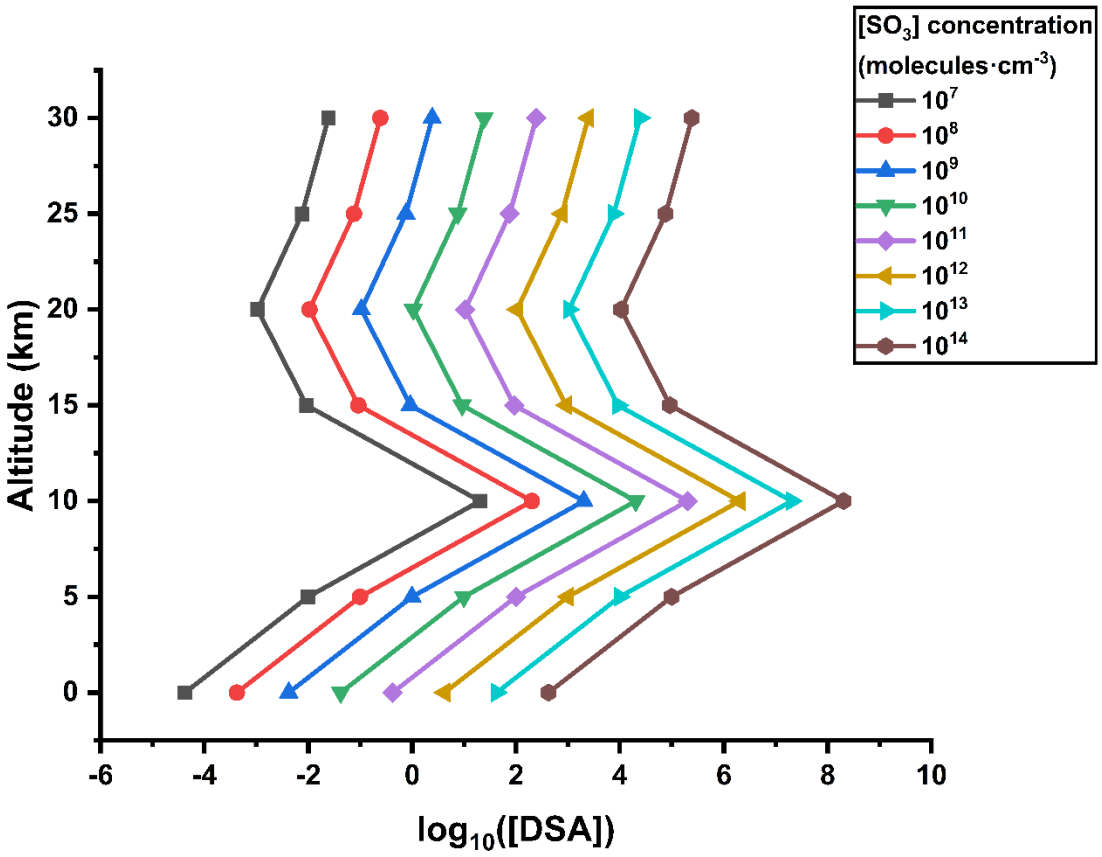

Figure S10 Concentration (unit: molecules·cm^{-3}) of DSA with respect to different concentrations of SO_3 as function of altitude. We consider the possible concentrations of SO_3 with the injection of SO_3.

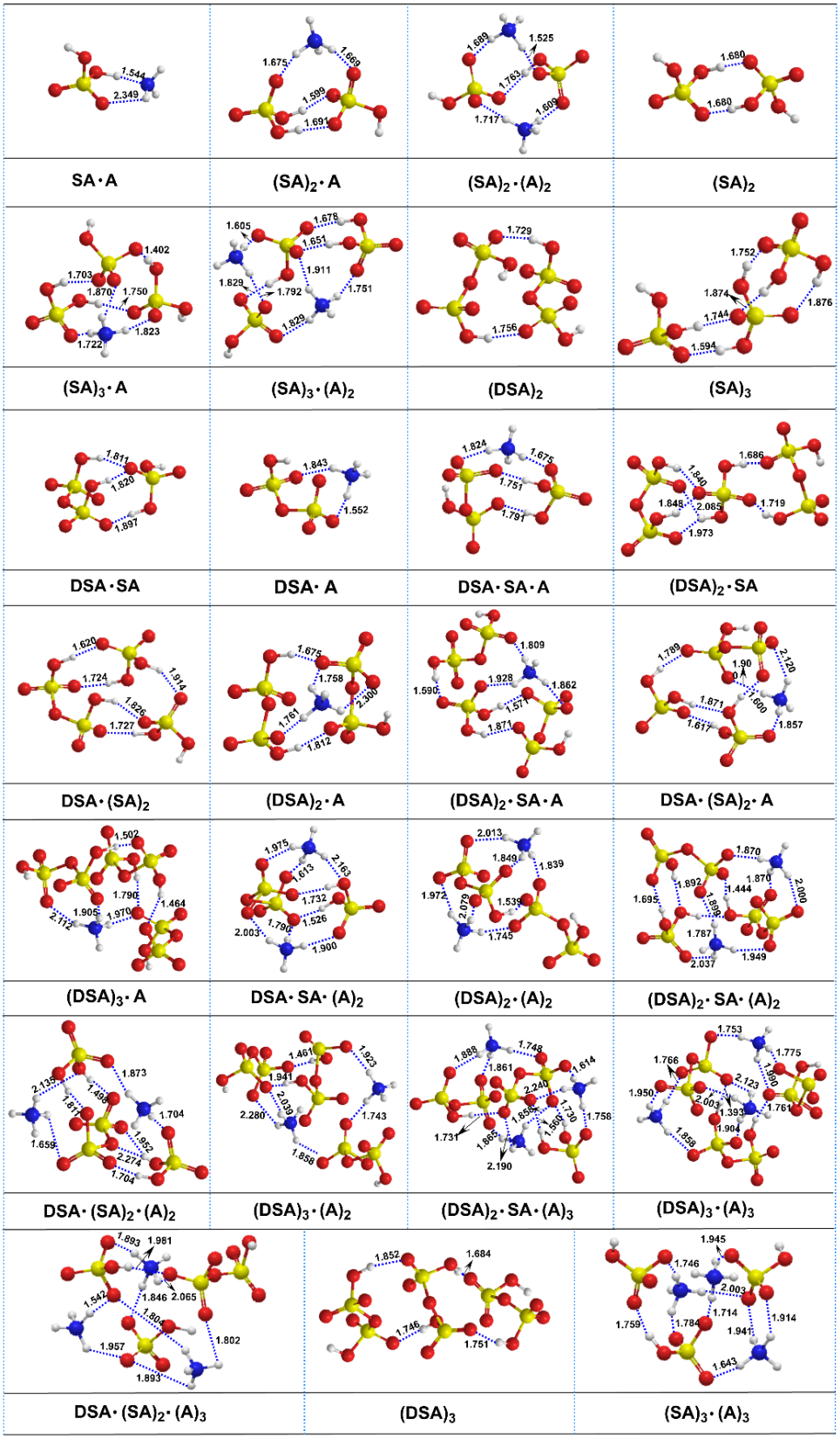

Figure S11 The most stable configurations of the DSA-SA-A-based clusters identified at the M06-2X/6-311++G(2*df*,2*pd*) level of theory. DSA, SA, A are the shorthand for disulfuric acid, sulfuric acid and ammonia, respectively. The lengths of hydrogen bonds are given in Å. (blue = nitrogen, yellow = sulfur, red = oxygen, gray = carbon, and white = hydrogen.)

Table S10 The Gibbs free energy ΔG (kcal·mol^{-1}) of formation of all clusters at pressure of 1 atm and the temperature range of 218.15-298.15 K, calculated at DLPNO-CCSD(T)/aug-cc-pVTZ//M06-2X/6-311++G(2*df*,2*pd*) level of theory

Clusters	T = 298.15 K	T = 278.15 K	T = 258.15 K	T = 238.15 K	T = 218.15 K
$(DSA)_2$	-5.0	-5.8	-6.7	-7.5	-8.4
$(DSA)_3$	-4.6	-6.2	-7.9	-9.6	-11.3
$(SA)_1{\cdot}(DSA)_1$	-4.7	-5.5	-6.3	-7.2	-8.0
$(SA)_1{\cdot}(DSA)_2$	-8.8	-10.4	-12.1	-13.7	-16.0
$(SA)_2{\cdot}(DSA)_1$	-6.8	-8.6	-10.4	-12.2	-14.0
$(DSA)_1{\cdot}(A)_1$	-15.3	-16.1	-16.9	-17.6	-18.4
$(DSA)_2{\cdot}(A)_1$	-24.8	-26.4	-28.0	-29.7	-31.3
$(DSA)_3{\cdot}(A)_1$	-32.3	-34.8	-37.4	-40.0	-42.5
$(DSA)_2{\cdot}(A)_2$	-41.9	-44.3	-46.7	-49.1	-51.5
$(SA)_1{\cdot}(DSA)_1{\cdot}(A)_1$	-25.9	-27.4	-29.0	-30.5	-32.0
$(SA)_1{\cdot}(DSA)_2{\cdot}(A)_1$	-32.8	-35.3	-37.8	-40.3	-43.3
$(SA)_2{\cdot}(DSA)_1{\cdot}(A)_1$	-31.9	-34.2	-36.6	-38.9	-41.3
$(SA)_1{\cdot}(DSA)_1{\cdot}(A)_2$	-37.9	-40.3	-42.8	-45.2	-47.7
$(SA)_1{\cdot}(DSA)_2{\cdot}(A)_2$	-49.1	-52.4	-55.7	-59.0	-62.3
$(SA)_2{\cdot}(DSA)_1{\cdot}(A)_2$	-48.4	-51.7	-55.0	-58.3	-61.6
$(SA)_2{\cdot}(DSA)_1{\cdot}(A)_3$	-61.3	-65.2	-69.1	-73.0	-77.0
$(SA)_1{\cdot}(DSA)_2{\cdot}(A)_3$	-73.9	-77.9	-81.8	-85.8	-89.8
$(DSA)_3{\cdot}(A)_3$	-69.5	-73.6	-77.6	-81.7	-85.8
$(DSA)_3{\cdot}(A)_2$	-51.6	-54.8	-58.1	-61.4	-64.7
$(SA)_2$	-7.8 (-8.4)	-8.6 (-9.1)	-9.1 (-9.8)	-9.8 (-10.5)	-10.5 (-11.1)
$(SA)_3$	-12.5 (-13.9)	-14.0 (-15.5)	-15.7 (-17.0)	-17.1 (-18.5)	-18.7 (-20.1)
$(SA)_1{\cdot}(A)_1$	-5.7 (-7.3)	-6.3 (-7.9)	-7.0 (-8.5)	-7.6 (-9.2)	-8.3 (-9.8)
$(SA)_2{\cdot}(A)_1$	-20.5 (-20.8)	-22.0 (-22.4)	-23.5 (-24.0)	-25.1 (-25.5)	-26.6 (-27.1)
$(SA)_2{\cdot}(A)_2$	-26.6 (-26.6)	-28.9 (-28.8)	-31.1 (-31.0)	-33.4 (-33.28)	-35.6 (-35.5)
$(SA)_3{\cdot}(A)_1$	-27.4 (-30.2)	-29.8 (-32.5)	-32.2 (-34.8)	-34.6 (-37.1)	-37.2 (-39.5)
$(SA)_3{\cdot}(A)_2$	-40.5 (-41.8)	-43.6 (-44.9)	-46.7 (-47.9)	-49.8 (-51.0)	-52.9 (-54.1)
$(SA)_3{\cdot}(A)_3$	-51.2 (-52.8)	-55.0 (-56.6)	-58.9 (-60.5)	-62.8 (-64.3)	-66.7 (-68.1)

The values in parentheses were taken from (Zhang, H., Kupiainen-Määttä, O., Zhang, X., Molinero, V., Zhang, Y., and Li, Z.: The enhancement mechanism of glycolic acid on the formation of atmospheric sulfuric acid–ammonia molecular clusters, J. Chem. Phys., 146, 184308, 10.1063/1.4982929, 2017.)

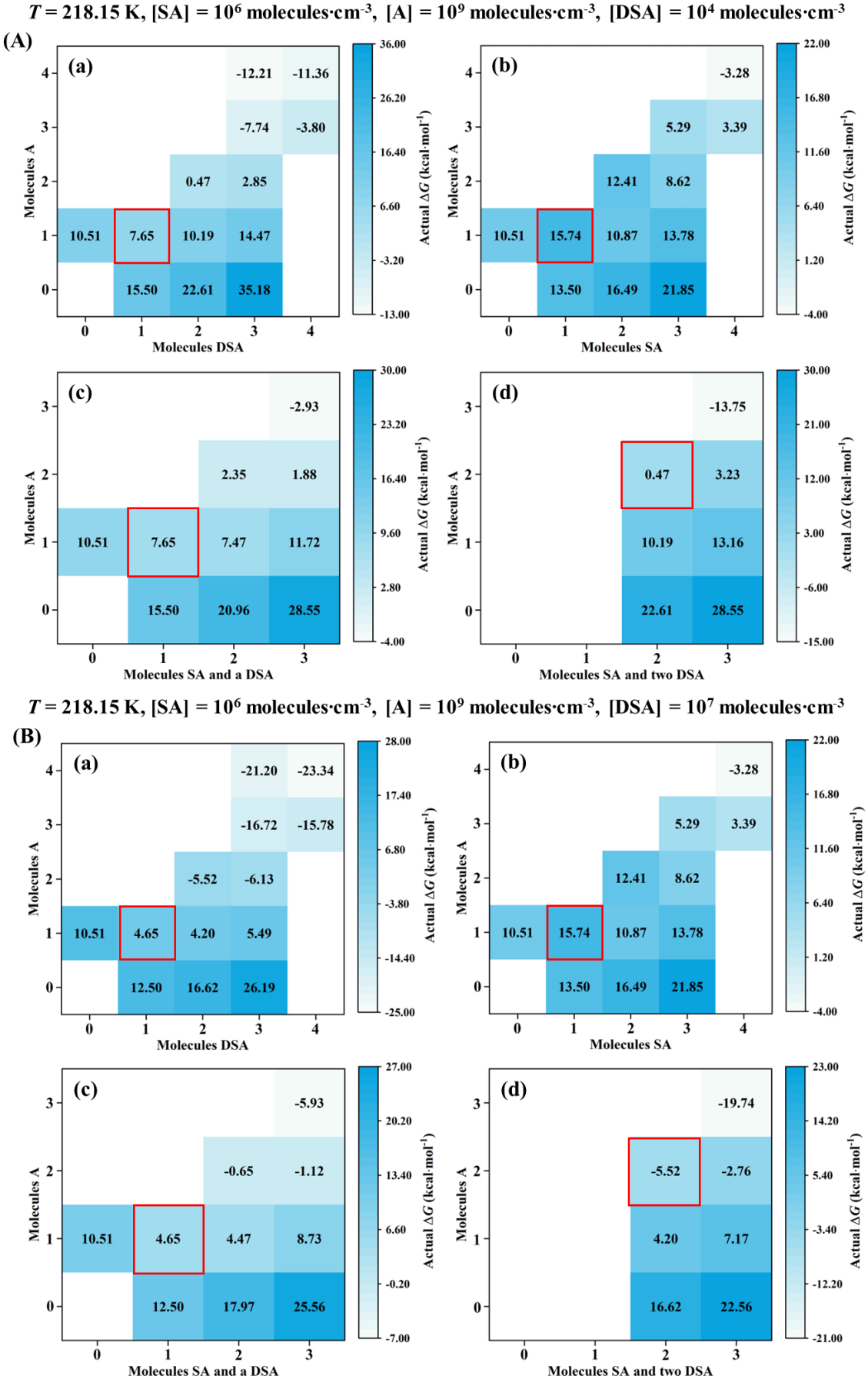
(A)
T = 218.15 K, [SA] = 10^6 molecules·cm^-3, [A] = 10^9 molecules·cm^-3, [DSA] = 10^4 molecules·cm^-3
(a)
-12.21
-11.36
-7.74
-3.80
0.47
2.85
10.51
7.65
10.19
14.47
15.50
22.61
35.18
Molecules A
Molecules DSA
Actual ΔG (kcal·mol^-1)
36.00
26.20
16.40
6.60
-3.20
-13.00
(b)
-3.28
5.29
3.39
12.41
8.62
10.51
15.74
10.87
13.78
13.50
16.49
21.85
Molecules SA
22.00
16.80
11.60
6.40
1.20
-4.00
(c)
-2.93
2.35
1.88
10.51
7.65
7.47
11.72
15.50
20.96
28.55
Molecules SA and a DSA
30.00
23.20
16.40
9.60
2.80
-4.00
(d)
-13.75
0.47
3.23
10.19
13.16
22.61
28.55
Molecules SA and two DSA
30.00
21.00
12.00
3.00
-6.00
-15.00
(B)
T = 218.15 K, [SA] = 10^6 molecules·cm^-3, [A] = 10^9 molecules·cm^-3, [DSA] = 10^7 molecules·cm^-3
(a)
-21.20
-23.34
-16.72
-15.78
-5.52
-6.13
10.51
4.65
4.20
5.49
12.50
16.62
26.19
Molecules DSA
28.00
17.40
6.80
-3.80
-14.40
-25.00
(b)
-3.28
5.29
3.39
12.41
8.62
10.51
15.74
10.87
13.78
13.50
16.49
21.85
Molecules SA
22.00
16.80
11.60
6.40
1.20
-4.00
(c)
-5.93
-0.65
-1.12
10.51
4.65
4.47
8.73
12.50
17.97
25.56
Molecules SA and a DSA
27.00
20.20
13.40
6.60
-0.20
-7.00
(d)
-19.74
-5.52
-2.76
4.20
7.17
16.62
22.56
Molecules SA and two DSA
23.00
14.20
5.40
-3.40
-12.20
-21.00

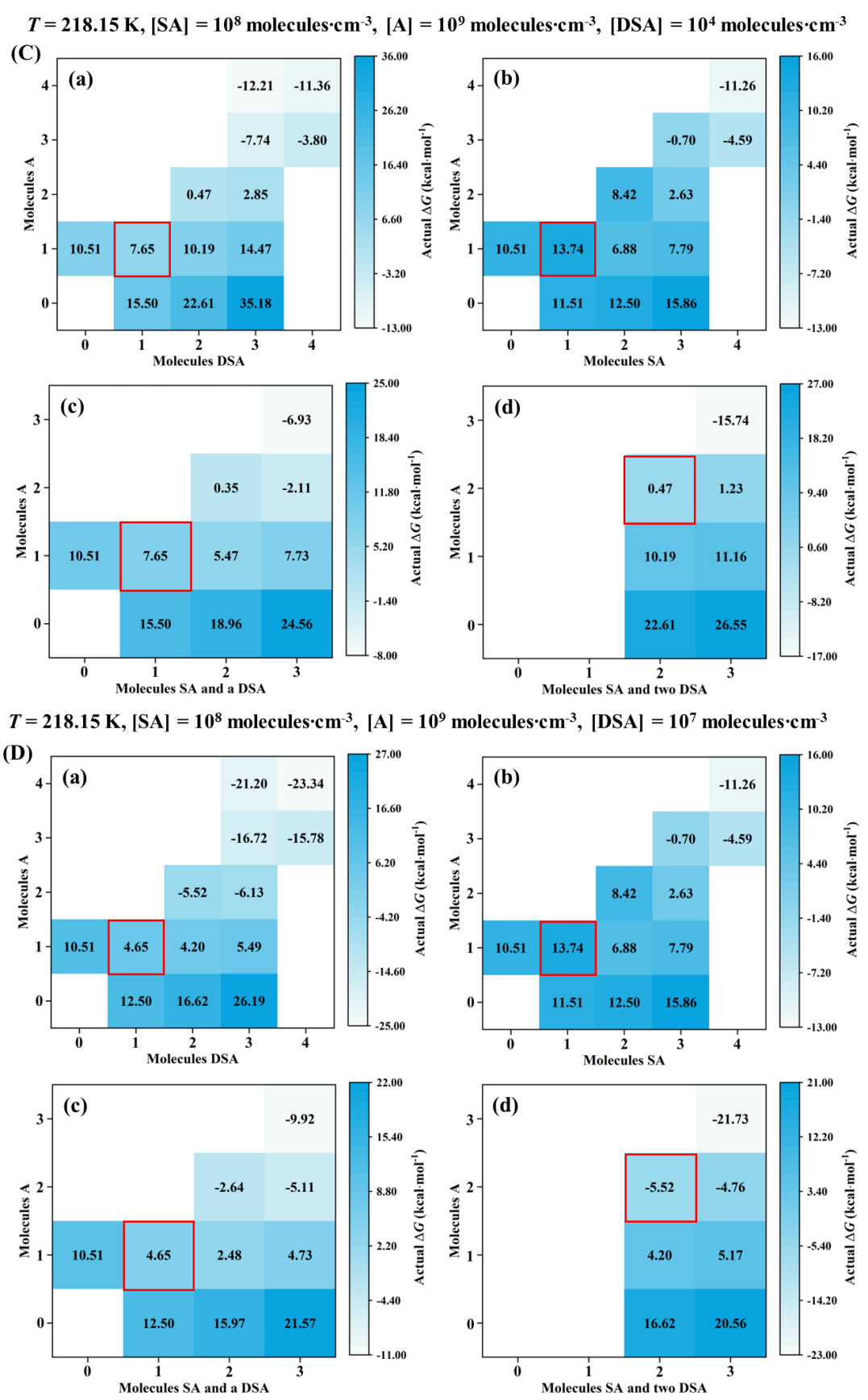

Figure S12 A typical actual Δ*G* surface at 218.15 K. [SA] is the concentration of sulfuric acid monomers, [A] the concentration of ammonia monomers and [DSA] is disulfuric acid

T = 238.15 K, [SA] = 10^6 molecules·cm^{-3}, [A] = 10^9 molecules·cm^{-3}, [DSA] = 10^4 molecules·cm^{-3}

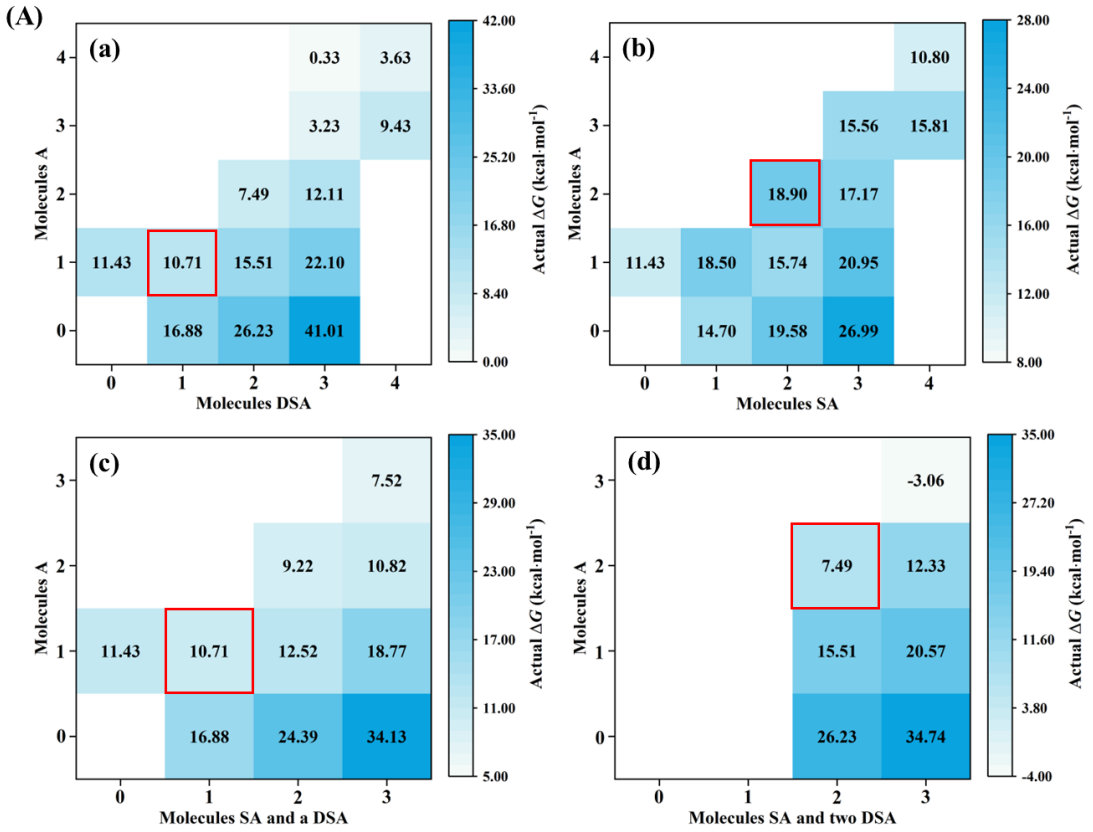

T = 238.15 K, [SA] = 10^6 molecules·cm^{-3}, [A] = 10^9 molecules·cm^{-3}, [DSA] = 10^7 molecules·cm^{-3}

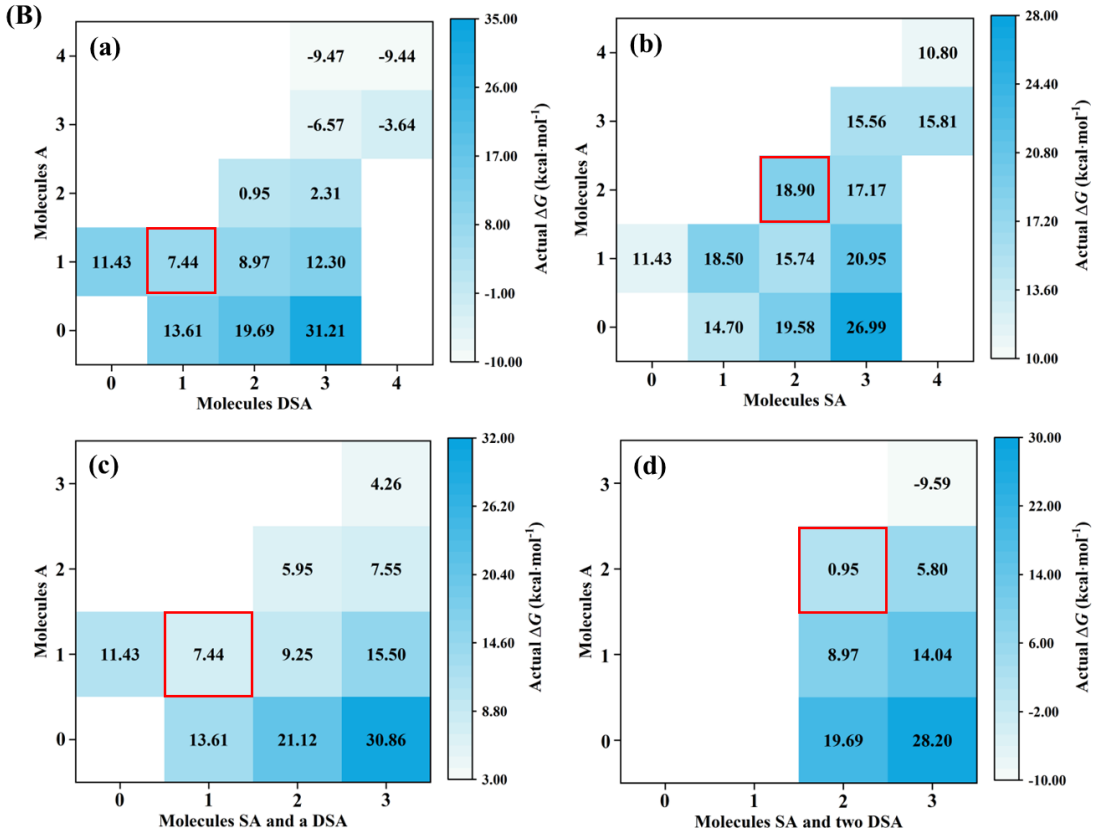

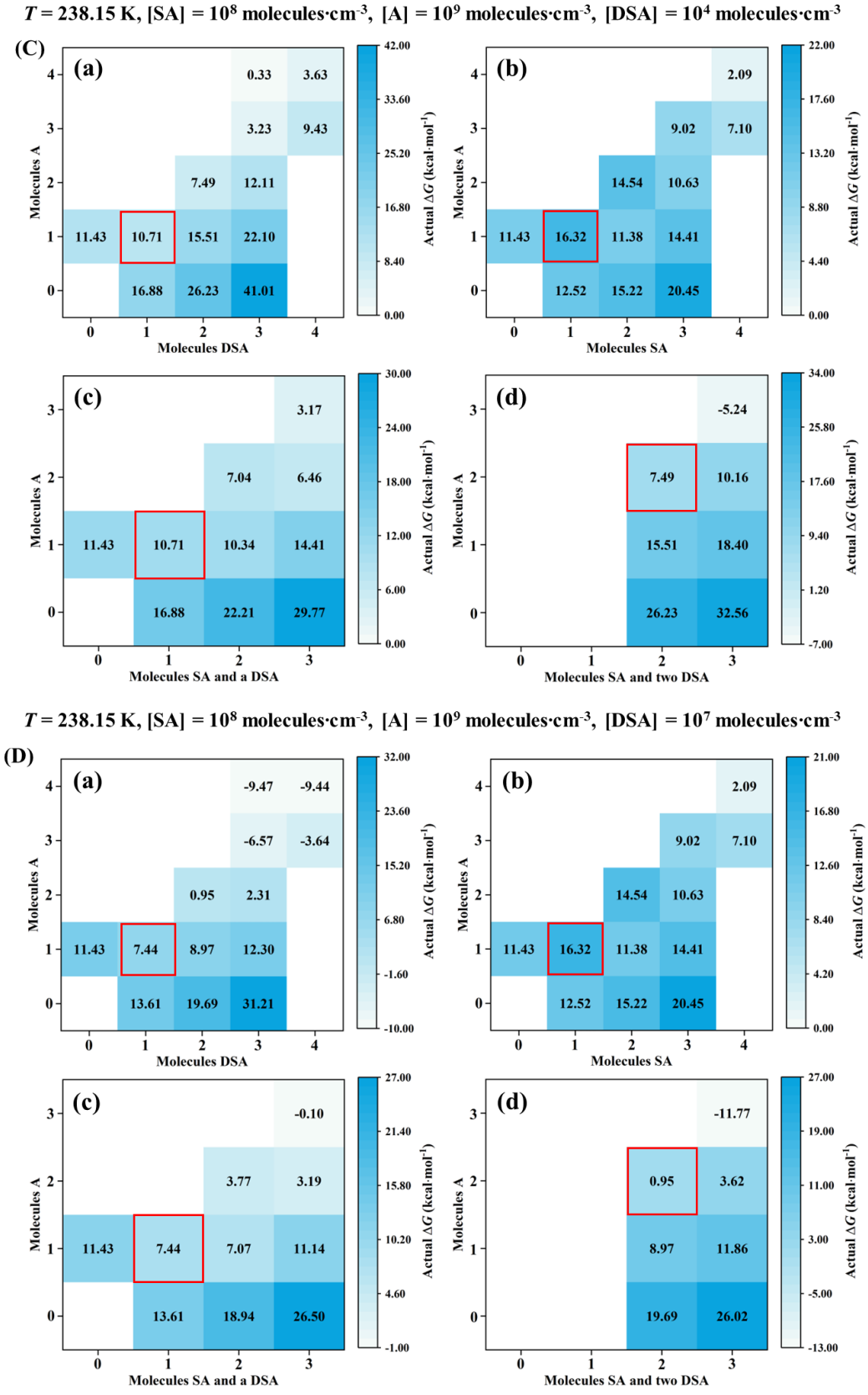

Figure S13 A typical actual Δ*G* surface at 238.15 K. [SA] is the concentration of sulfuric acid monomers, [A] the concentration of ammonia monomers and [DSA] is disulfuric acid

Part 6 Collision coefficients and evaporation coefficients

The collision rate coefficient $\beta_{i,j}$ between clusters i and j was calculated using hard-sphere collision theory (Chapman and Cowling, 1990) in Eq. (S5).

$$\beta_{i,j} = \pi(r_i + r_j)^2 \sqrt{\frac{8k_B T}{\pi\mu}} \quad \text{(S5)}$$

Where r_i is the radius of cluster i, defined as the sum of distance between the two farthest atom in cluster i and half of the van der Waals radii of these two atoms and given by Multiwfn_3.7 software (Lu and Chen, 2012); k_B is the Boltzmann constant; T is the temperature and $\mu = m_i \cdot m_j/(mi + mj)$ is the reduced mass.

The evaporation coefficient $\gamma_{(i+j) \to i}$ was computed using the corresponding collision coefficients and the Gibbs free energies of formation of the clusters as show in Eq. (S6).

$$\gamma_{(i+j)\to i} = \beta_{i,j} \frac{p_{ref}}{k_B T} \exp\left(\frac{\Delta G_{i+j} - \Delta G_i - \Delta G_j}{k_B T}\right) \quad \text{(S6)}$$

Where p_{ref} is the reference pressure (1 atm in current study) at which the Gibbs free energies have been calculated, and ΔG_{i+j} is the Gibbs free energy of formation of cluster i+j from monomers i and j.

Reference

Chapman, S., and Cowling, T. G.: The mathematical theory of non-uniform gases: an account of the kinetic theory of viscosity, thermal conduction and diffusion in gases, Cambridge university press, 1990.

Lu, T., and Chen, F.: Multiwfn: A multifunctional wavefunction analyzer, J. Comput. Chem., 33, 580-592, https://doi.org/10.1002/jcc.22885, 2012.

Part 7 Enhancement factor R

To figure out how DSA affects the kinetic clustering process, the potential influence of DSA to the SA-A-based particle formation was estimated by calculating the enhancement factor *R* in Eq (5).

$$R = \frac{J_{\text{SA-A-DSA}}}{J_{\text{SA-A}}} = \frac{J([\text{SA}] = x, [\text{A}] = y, [\text{DSA}] = z)}{J([\text{SA}] = x, [\text{A}] = y, [\text{DSA}] = 0)} \quad (5)$$

where $J_{\text{SA-A-DSA}}$ and $J_{\text{SA-A}}$ are represented the formation rate of SA-A-DSA and SA-A nucleating system, respectively. *x, y* and *z* are the atmospheric concentration of SA, A and DSA.

Table S10 Collision coefficients (β, $cm^3 \cdot s^{-1}$) for each cluster in the present study

Collisions	β, $cm^3 \cdot s^{-1}$				
	298.15 K	278.15 K	258.15 K	238.15 K	218.15 K
SA + A	1.65×10^{-10}	1.54×10^{-10}	1.43×10^{-10}	1.32×10^{-10}	1.20×10^{-10}
SA + DSA	7.02×10^{-11}	6.55×10^{-11}	6.08×10^{-11}	5.61×10^{-11}	5.14×10^{-11}
DSA + A	2.15×10^{-10}	2.00×10^{-10}	1.86×10^{-10}	1.71×10^{-10}	1.57×10^{-10}
SA + SA	6.81×10^{-11}	6.35×10^{-11}	5.90×10^{-11}	5.44×10^{-11}	4.98×10^{-11}
DSA + DSA	6.40×10^{-11}	5.97×10^{-11}	5.54×10^{-11}	5.11×10^{-11}	4.68×10^{-11}
$(SA)_2$ + A	3.03×10^{-10}	2.83×10^{-10}	2.62×10^{-10}	2.42×10^{-10}	2.22×10^{-10}
SA·A + SA	8.90×10^{-11}	8.31×10^{-11}	7.71×10^{-11}	7.11×10^{-11}	6.51×10^{-11}
$(SA)_2$·A + A	2.81×10^{-10}	2.62×10^{-10}	2.43×10^{-10}	2.25×10^{-10}	2.06×10^{-10}
$(DSA)_2$ + A	3.25×10^{-10}	3.03×10^{-10}	2.81×10^{-10}	2.59×10^{-10}	2.38×10^{-10}
DSA·A + DSA	6.95×10^{-11}	6.48×10^{-11}	6.01×10^{-11}	5.55×10^{-11}	5.08×10^{-11}
$(DSA)_2$·A + A	3.37×10^{-10}	3.15×10^{-10}	2.92×10^{-10}	2.70×10^{-10}	2.47×10^{-10}
$(SA)_2$ + DSA	8.05×10^{-11}	7.51×10^{-11}	6.97×10^{-11}	6.43×10^{-11}	5.89×10^{-11}
SA·DSA + SA	8.62×10^{-11}	8.04×10^{-11}	7.46×10^{-11}	6.89×10^{-11}	6.31×10^{-11}
$(DSA)_2$ + SA	8.65×10^{-11}	8.07×10^{-11}	7.49×10^{-11}	6.91×10^{-11}	6.33×10^{-11}
SA·DSA + DSA	7.13×10^{-11}	6.65×10^{-11}	6.17×10^{-11}	5.69×10^{-11}	5.21×10^{-11}
$(SA)_2$ + SA	9.26×10^{-11}	8.64×10^{-11}	8.02×10^{-11}	7.40×10^{-11}	6.77×10^{-11}
$(DSA)_2$ + DSA	6.88×10^{-11}	6.42×10^{-11}	5.96×10^{-11}	5.50×10^{-11}	5.04×10^{-11}
SA + $(SA)_2$·A	8.48×10^{-11}	7.91×10^{-11}	7.34×10^{-11}	6.78×10^{-11}	6.21×10^{-11}
$(SA)_3$ + A	3.93×10^{-10}	3.67×10^{-10}	3.41×10^{-10}	3.14×10^{-10}	2.88×10^{-10}
$(SA)_2$·$(A)_2$ + SA	9.26×10^{-11}	8.64×10^{-11}	8.02×10^{-11}	7.40×10^{-11}	6.78×10^{-11}
$(SA)_3$·A + A	3.13×10^{-10}	2.92×10^{-10}	2.71×10^{-10}	2.50×10^{-10}	2.29×10^{-10}
$(SA)_3$·$(A)_2$ + A	4.08×10^{-10}	3.80×10^{-10}	3.53×10^{-10}	3.26×10^{-10}	2.98×10^{-10}
$(DSA)_2$·A + DSA	7.00×10^{-11}	6.53×10^{-11}	6.06×10^{-11}	5.59×10^{-11}	5.12×10^{-11}
$(DSA)_3$ + A	4.90×10^{-10}	4.57×10^{-10}	4.24×10^{-10}	3.91×10^{-10}	3.58×10^{-10}
$(DSA)_2$·$(A)_2$ + DSA	7.76×10^{-11}	7.24×10^{-11}	6.72×10^{-11}	6.20×10^{-11}	5.68×10^{-11}
$(DSA)_3$·A + A	4.17×10^{-10}	3.89×10^{-10}	3.61×10^{-10}	3.33×10^{-10}	3.05×10^{-10}
$(DSA)_3$·$(A)_2$ + A	4.78×10^{-10}	4.46×10^{-10}	4.14×10^{-10}	3.82×10^{-10}	3.50×10^{-10}
DSA·A + SA	7.85×10^{-11}	7.32×10^{-11}	6.79×10^{-11}	6.27×10^{-11}	5.74×10^{-11}
SA·A + DSA	8.60×10^{-11}	8.02×10^{-11}	7.44×10^{-11}	6.87×10^{-11}	6.29×10^{-11}
SA·DSA + A	3.06×10^{-10}	2.86×10^{-10}	2.65×10^{-10}	2.45×10^{-10}	2.24×10^{-10}
SA·DSA·A + A	3.03×10^{-10}	2.83×10^{-10}	2.62×10^{-10}	2.42×10^{-10}	2.22×10^{-10}
SA·DSA·A + SA	8.43×10^{-11}	7.87×10^{-11}	7.30×10^{-11}	6.74×10^{-11}	6.17×10^{-11}

$(SA)_2 \cdot A + DSA$	7.33×10^{-11}	6.84×10^{-11}	6.35×10^{-11}	5.86×10^{-11}	5.36×10^{-11}
$(SA)_2 \cdot DSA + A$	3.80×10^{-10}	3.54×10^{-10}	3.29×10^{-10}	3.03×10^{-10}	2.78×10^{-10}
$SA \cdot DSA \cdot (A)_2 + SA$	8.09×10^{-11}	7.55×10^{-11}	7.00×10^{-11}	6.46×10^{-11}	5.92×10^{-11}
$(SA)_2 \cdot (A)_2 + DSA$	7.83×10^{-11}	7.30×10^{-11}	6.78×10^{-11}	6.25×10^{-11}	5.73×10^{-11}
$(SA)_2 \cdot DSA \cdot A + A$	3.25×10^{-10}	3.03×10^{-10}	2.82×10^{-10}	2.60×10^{-10}	2.38×10^{-10}
$(SA)_2 \cdot DSA \cdot (A)_2 + A$	4.22×10^{-10}	3.93×10^{-10}	3.65×10^{-10}	3.37×10^{-10}	3.08×10^{-10}
$(DSA)_2 \cdot A + SA$	8.88×10^{-11}	8.28×10^{-11}	7.69×10^{-11}	7.09×10^{-11}	6.49×10^{-11}
$SA \cdot DSA \cdot A + DSA$	6.92×10^{-11}	6.46×10^{-11}	5.99×10^{-11}	5.53×10^{-11}	5.06×10^{-11}
$SA \cdot (DSA)_2 + A$	3.31×10^{-10}	3.08×10^{-10}	2.86×10^{-10}	2.64×10^{-10}	2.42×10^{-10}
$(DSA)_2 \cdot (A)_2 + SA$	1.00×10^{-10}	9.34×10^{-11}	8.67×10^{-11}	8.00×10^{-11}	7.33×10^{-11}
$SA \cdot DSA \cdot (A)_2 + DSA$	6.61×10^{-11}	6.17×10^{-11}	5.72×10^{-11}	5.28×10^{-11}	4.84×10^{-11}
$SA \cdot (DSA)_2 \cdot A + A$	4.19×10^{-10}	3.91×10^{-10}	3.63×10^{-10}	3.35×10^{-10}	3.06×10^{-10}
$SA \cdot (DSA)_2 \cdot (A)_2 + A$	3.84×10^{-10}	3.58×10^{-10}	3.32×10^{-10}	3.06×10^{-10}	2.81×10^{-10}

Table S11 Evaporation rates (s^{-1}) of the studied clusters at different temperatures of 298.15, 278.15, 258.15, 238.15 and 218.15 K

Evaporation pathways	298.15 K	278.15 K	258.15 K	238.15 K	218.15 K
$(SA)_2 \rightarrow SA + SA$	3.36×10^3 (2.89×10^3)	3.81×10^2 (3.14×10^2)	3.07×10^1 (2.46×10^1)	1.61×10^0 (1.23×10^0)	4.91×10^{-2} (3.51×10^{-2})
$(SA)_3 \rightarrow (SA)_2 + SA$	7.99×10^5 (1.22×10^6)	9.55×10^4 (1.34×10^5)	8.20×10^3 (1.05×10^4)	4.64×10^2 (5.40×10^2)	1.54×10^1 (1.58×10^1)
$(SA)_1 \cdot (A)_1 \rightarrow SA + A$	2.67×10^5 (4.76×10^4)	4.19×10^4 (6.70×10^3)	4.92×10^3 (7.09×10^2)	4.03×10^2 (5.01×10^1)	2.08×10^1 (2.17×10^0)
$(SA)_2 \cdot (A)_1 \rightarrow (SA)_1 \cdot (A)_1 + SA$	3.32×10^{-2} (1.48×10^0)	1.08×10^{-3} (5.23×10^{-2})	2.07×10^{-5} (1.12×10^{-3})	2.05×10^{-7} (3.33×10^{-4})	8.64×10^{-10} (6.20×10^{-8})
$(SA)_2 \cdot (A)_1 \rightarrow A + (SA)_2$	3.72×10^0 (1.60×10^1)	1.68×10^{-1} (7.31×10^{-1})	4.69×10^{-3} (2.11×10^{-2})	7.20×10^{-5} (1.25×10^{-5})	5.16×10^{-7} (2.51×10^{-6})
$(SA)_3 \cdot (A)_1 \rightarrow (SA)_2 \cdot (A)_1 + SA$	1.63×10^4 (1.85×10^3)	1.53×10^3 (1.56×10^2)	9.93×10^1 (8.72×10^0)	4.02×10^0 (3.00×10^{-1})	4.95×10^{-2} (5.39×10^{-3})
$(SA)_3 \cdot (A)_1 \rightarrow A + (SA)_3$	1.07×10^{-1} (3.12×10^{-2})	3.81×10^{-3} (1.09×10^{-3})	8.04×10^{-5} (2.25×10^{-5})	8.84×10^{-7} (2.37×10^{-7})	2.34×10^{-9} (1.19×10^{-9})
$(SA)_2 \cdot (A)_2 \rightarrow (SA)_2 \cdot (A)_1 + A$	2.02×10^5 (1.37×10^6)	2.71×10^4 (2.07×10^5)	2.65×10^3 (2.32×10^4)	1.75×10^2 (1.80×10^3)	7.05×10^0 (8.49×10^1)
$(SA)_3 \cdot (A)_2 \rightarrow (SA)_2 \cdot (A)_2 + SA$	1.61×10^{-1} (9.75×10^{-2})	6.34×10^{-3} (3.53×10^{-3})	1.51×10^{-4} (7.48×10^{-5})	1.90×10^{-6} (8.44×10^{-7})	1.06×10^{-8} (4.16×10^{-9})
$(SA)_3 \cdot (A)_2 \rightarrow (SA)_3 \cdot (A)_1 + A$	2.04×10^0 (7.26×10^1)	1.14×10^{-1} (4.73×10^0)	4.10×10^{-3} (2.02×10^{-1})	8.43×10^{-5} (5.11×10^{-3})	1.55×10^{-6} (6.61×10^{-5})
$(SA)_3 \cdot (A)_3 \rightarrow (SA)_3 \cdot (A)_2 + A$	1.49×10^2	9.81×10^0	4.22×10^{-1}	1.07×10^{-2}	1.36×10^{-4} (2.93×10^{-4})
$(SA)_1 \cdot (DSA)_1 \rightarrow SA + DSA$	6.68×10^5	8.27×10^4	7.35×10^3	4.32×10^2	1.50×10^1
$(SA)_2 \cdot (DSA)_1 \rightarrow (SA)_1 \cdot (DSA)_1 + SA$	5.71×10^7	8.04×10^6	8.34×10^5	5.91×10^4	2.57×10^3
$(SA)_2 \cdot (DSA)_1 \rightarrow DSA + (SA)_2$	1.03×10^{10}	1.58×10^9	1.81×10^8	1.43×10^7	7.11×10^5
$(DSA)_1 \cdot (A)_1 \rightarrow DSA + A$	2.96×10^{-2}	1.17×10^{-3}	2.82×10^{-5}	3.64×10^{-7}	2.13×10^{-9}
$(SA)_1 \cdot (DSA)_1 \cdot (A)_1 \rightarrow SA + (DSA)_1 \cdot (A)_1$	3.67×10^1	2.48×10^0	1.10×10^{-1}	2.85×10^{-3}	3.77×10^{-5}
$(SA)_1 \cdot (DSA)_1 \cdot (A)_1 \rightarrow A + (SA)_1 \cdot (DSA)_1$	2.08×10^{-6}	4.49×10^{-8}	5.37×10^{-10}	3.07×10^{-12}	6.83×10^{-15}
$(SA)_1 \cdot (DSA)_1 \cdot (A)_1 \rightarrow DSA + (SA)_1 \cdot (A)_1$	3.41×10^{-6}	5.83×10^{-8}	5.28×10^{-10}	2.17×10^{-12}	3.23×10^{-15}
$(SA)_2 \cdot (DSA)_1 \cdot (A)_1 \rightarrow A + (SA)_2 \cdot (DSA)_1$	3.61×10^{-9}	6.26×10^{-11}	5.77×10^{-13}	2.42×10^{-15}	3.70×10^{-18}
$(SA)_2 \cdot (DSA)_1 \cdot (A)_1 \rightarrow DSA + (SA)_2 \cdot (A)_1$	7.26×10^0	4.28×10^{-1}	1.62×10^{-2}	3.49×10^{-4}	3.71×10^{-6}
$(SA)_1 \cdot (DSA)_1 \cdot (A)_2 \rightarrow A + (SA)_1 \cdot (DSA)_1 \cdot (A)_1$	1.18×10^1	5.29×10^{-1}	1.47×10^{-2}	2.25×10^{-4}	1.60×10^{-6}
$(SA)_2 \cdot (DSA)_1 \cdot (A)_2 \rightarrow SA + (SA)_1 \cdot (DSA)_1 \cdot (A)_2$	3.89×10^1	2.29×10^0	8.64×10^{-2}	1.87×10^{-3}	1.99×10^{-5}
$(SA)_2 \cdot (DSA)_1 \cdot (A)_2 \rightarrow A + (SA)_2 \cdot (DSA)_1 \cdot (A)_1$	6.55×10^{-3}	1.54×10^{-4}	2.02×10^{-6}	1.28×10^{-8}	3.24×10^{-11}
$(SA)_2 \cdot (DSA)_1 \cdot (A)_2 \rightarrow DSA + (SA)_2 \cdot (A)_2$	2.17×10^{-7}	2.25×10^{-9}	1.14×10^{-11}	2.36×10^{-14}	1.57×10^{-17}
$(SA)_2 \cdot (DSA)_1 \cdot (A)_3 \rightarrow A + (SA)_2 \cdot (DSA)_1 \cdot (A)_2$	3.08×10^0	2.14×10^{-1}	9.81×10^{-3}	2.68×10^{-4}	3.78×10^{-6}
$(DSA)_2 \rightarrow DSA + DSA$	3.56×10^5	4.18×10^4	3.50×10^3	1.93×10^2	6.20×10^0
$(SA)_1 \cdot (DSA)_2 \rightarrow SA + (DSA)_2$	$3.3. \times 10^6$	5.05×10^5	5.72×10^4	4.46×10^3	5.62×10^1

$(SA)_1\cdot(DSA)_2 \rightarrow DSA + (SA)_1\cdot(DSA)_1$	1.59×10^{6}	2.31×10^{5}	2.46×10^{4}	1.80×10^{3}	2.10×10^{1}
$(DSA)_2\cdot(A)_1 \rightarrow A + (DSA)_2$	2.52×10^{-5}	5.47×10^{-7}	6.55×10^{-9}	3.73×10^{-11}	8.24×10^{-14}
$(DSA)_2\cdot(A)_1 \rightarrow DSA + (DSA)_1\cdot(A)_1$	2.18×10^{2}	1.40×10^{1}	5.83×10^{-1}	1.41×10^{-2}	1.72×10^{-4}
$(SA)_1\cdot(DSA)_2\cdot(A)_1 \rightarrow SA + (DSA)_2\cdot(A)_1$	2.70×10^{3}	2.24×10^{2}	1.26×10^{1}	4.32×10^{-1}	2.04×10^{-3}
$(SA)_1\cdot(DSA)_2\cdot(A)_1 \rightarrow A + (SA)_1\cdot(DSA)_2$	3.09×10^{-8}	3.64×10^{-10}	2.16×10^{-12}	5.41×10^{-15}	4.47×10^{-18}
$(SA)_1\cdot(DSA)_2\cdot(A)_1 \rightarrow DSA + (SA)_1\cdot(DSA)_1\cdot(A)_1$	1.41×10^{4}	1.11×10^{3}	5.89×10^{1}	1.89×10^{0}	8.19×10^{-3}
$(DSA)_2\cdot(A)_2 \rightarrow A + (DSA)_2\cdot(A)_1$	2.13×10^{-3}	6.68×10^{-5}	1.22×10^{-6}	1.15×10^{-8}	4.57×10^{-11}
$(SA)_1\cdot(DSA)_2\cdot(A)_2 \rightarrow SA + (DSA)_2\cdot(A)_2$	1.51×10^{4}	1.25×10^{3}	7.09×10^{1}	2.45×10^{0}	4.58×10^{-2}
$(SA)_1\cdot(DSA)_2\cdot(A)_2 \rightarrow A + (SA)_1\cdot(DSA)_2\cdot(A)_1$	2.01×10^{-3}	6.02×10^{-5}	1.05×10^{-6}	9.21×10^{-9}	3.41×10^{-11}
$(SA)_1\cdot(DSA)_2\cdot(A)_2 \rightarrow DSA + (SA)_1\cdot(DSA)_1\cdot(A)_2$	1.17×10^{1}	6.51×10^{-1}	2.30×10^{-2}	4.60×10^{-4}	4.45×10^{-6}
$(SA)_1\cdot(DSA)_2\cdot(A)_3 \rightarrow A + (SA)_1\cdot(DSA)_2\cdot(A)_2$	5.72×10^{-9}	8.55×10^{-11}	6.65×10^{-13}	2.28×10^{-15}	2.76×10^{-18}
$(DSA)_3 \rightarrow (DSA)_2 + DSA$	3.48×10^{9}	8.08×10^{8}	1.49×10^{8}	2.05×10^{7}	1.94×10^{6}
$(DSA)_3\cdot(A)_1 \rightarrow A + (DSA)_3$	3.97×10^{-11}	2.74×10^{-13}	8.73×10^{-16}	1.06×10^{-18}	3.78×10^{-22}
$(DSA)_3\cdot(A)_1 \rightarrow DSA + (DSA)_2\cdot(A)_1$	3.50×10^{3}	2.58×10^{2}	1.26×10^{1}	3.67×10^{-1}	5.59×10^{-3}
$(DSA)_3\cdot(A)_2 \rightarrow A + (DSA)_3\cdot(A)_1$	7.22×10^{-5}	1.94×10^{-6}	2.95×10^{-8}	2.22×10^{-10}	6.77×10^{-13}
$(DSA)_3\cdot(A)_2 \rightarrow DSA + (DSA)_2\cdot(A)_2$	1.78×10^{2}	1.16×10^{1}	4.90×10^{-1}	1.21×10^{-2}	1.49×10^{-4}
$(DSA)_3\cdot(A)_3 \rightarrow A + (DSA)_3\cdot(A)_2$	8.19×10^{-4}	2.23×10^{-5}	3.46×10^{-7}	2.67×10^{-9}	8.48×10^{-12}

*****The values in parentheses were taken from (Liu, J., Liu, L., Rong, H., and Zhang, X.: The potential mechanism of atmospheric new particle formation involving amino acids with multiple functional groups, Phys. Chem. Chem. Phys., 23, 10184-10195, 10.1039/D0CP06472F, 2021.)

Table S12 Total evaporation coefficients ($\sum y$, s^{-1}) for each cluster in the present study

Clusters	$\sum y$, s^{-1}				
	298.15 K	278.15 K	258.15 K	238.15 K	218.15 K
SA·A	2.67×10^{5}	4.19×10^{4}	4.92×10^{3}	4.03×10^{2}	2.08×10^{1}
SA·DSA	6.68×10^{5}	8.27×10^{4}	7.35×10^{3}	4.32×10^{2}	1.50×10^{1}
A·DSA	2.96×10^{-2}	1.17×10^{-3}	2.82×10^{-5}	3.64×10^{-7}	2.13×10^{-9}
$(SA)_2$	3.36×10^{3}	3.81×10^{2}	3.07×10^{1}	1.61×10^{0}	4.91×10^{-2}
$(DSA)_2$	3.56×10^{5}	4.18×10^{4}	3.50×10^{3}	1.93×10^{2}	6.20×10^{0}
$(SA)_2$·A	$3.75E \times 10^{0}$	1.69×10^{-1}	4.71×10^{-3}	7.22×10^{-5}	5.17×10^{-7}
$(SA)_2$·$(A)_2$	2.02×10^{5}	2.71×10^{4}	2.65×10^{3}	1.75×10^{2}	7.05×10^{0}
A·$(DSA)_2$	2.18×10^{2}	1.40×10^{1}	5.83×10^{-1}	1.41×10^{-2}	1.72×10^{-4}
$(A)_2$·$(DSA)_2$	2.13×10^{-3}	6.68×10^{-5}	1.22×10^{-6}	1.15×10^{-8}	4.57×10^{-11}
$(SA)_2$·DSA	1.03×10^{10}	1.59×10^{9}	1.82×10^{8}	1.44×10^{7}	7.14×10^{5}
SA·$(DSA)_2$	4.90×10^{6}	7.36×10^{5}	8.18×10^{4}	6.26×10^{3}	7.72×10^{1}
$(SA)_3$	7.99×10^{5}	9.55×10^{4}	8.20×10^{3}	4.64×10^{2}	1.54×10^{1}
$(DSA)_3$	3.48×10^{9}	8.08×10^{8}	1.49×10^{8}	2.05×10^{7}	1.94×10^{6}
$(SA)_3$·A	1.63×10^{4}	1.53×10^{3}	9.93×10^{1}	4.02×10^{0}	4.95×10^{-2}
$(SA)_3$·$(A)_2$	2.20×10^{0}	1.21×10^{-1}	4.25×10^{-3}	8.62×10^{-5}	1.56×10^{-6}
$(SA)_3$·$(A)_3$	1.49×10^{2}	9.81×10^{0}	4.22×10^{-1}	1.07×10^{-2}	1.36×10^{-4}
A·$(DSA)_3$	3.50×10^{3}	2.58×10^{2}	1.26×10^{1}	3.67×10^{-1}	5.59×10^{-3}
$(A)_2$·$(DSA)_3$	1.45×10^{3}	9.80×10^{1}	4.28×10^{0}	1.08×10^{-1}	1.41×10^{-3}
$(A)_3$·$(DSA)_3$	2.70×10^{-3}	7.59×10^{-5}	1.22×10^{-6}	9.82×10^{-9}	3.24×10^{-11}
SA·A·DSA	3.67×10^{1}	2.48×10^{0}	1.10×10^{-1}	2.85×10^{-3}	3.77×10^{-5}
SA·$(A)_2$·DSA	1.18×10^{1}	5.29×10^{-1}	1.47×10^{-2}	2.25×10^{-4}	1.60×10^{-6}
SA_2·A·DSA	7.84×10^{4}	8.84×10^{3}	7.06×10^{2}	3.67×10^{1}	1.10×10^{0}
$(SA)_2$·$(A)_2$·DSA	3.89×10^{1}	2.29×10^{0}	8.64×10^{-2}	1.87×10^{-3}	1.99×10^{-5}
$(SA)_2$·$(A)_3$·DSA	4.23×10^{8}	1.27×10^{8}	3.16×10^{7}	6.14×10^{6}	8.75×10^{5}
SA·A·$(DSA)_2$	1.68×10^{4}	1.34×10^{3}	7.14×10^{1}	2.32×10^{0}	1.02×10^{-2}
SA·$(A)_2$·$(DSA)_2$	1.51×10^{4}	1.26×10^{3}	7.09×10^{1}	2.46×10^{0}	4.58×10^{-2}
SA·$(A)_3$·$(DSA)_2$	5.72×10^{-9}	8.55×10^{-11}	6.65×10^{-13}	2.28×10^{-15}	2.76×10^{-18}

Table S13 The formation rate J of DSA at the conditions of T = 218.15 K, [SA] = 10^6-10^8 molecules·cm^{-3}, [A] = 10^7-10^{11} molecules·cm^{-3}, and [DSA] = 0, 10^4-10^7 molecules·cm^{-3}. SA, A and DSA represent sulfuric acid, ammonia and disulfuric acid, respectively

[SA]	[A]	[DSA] = 0	[DSA] = 10^4	[DSA] = 10^5	[DSA] = 10^6	[DSA] = 10^7
[SA] = 10^6	[A] = 10^7	3.66×10^{-5}	4.05×10^{-5}	4.63×10^{-4}	1.04×10^{-1}	4.14×10^{1}
[SA] = 10^6	[A] = 10^8	5.33×10^{-3}	6.30×10^{-3}	1.10×10^{-1}	2.70×10^{1}	3.28×10^{3}
[SA] = 10^6	[A] = 10^9	6.50×10^{-2}	2.01×10^{-1}	2.47×10^{1}	3.14×10^{3}	4.21×10^{4}
[SA] = 10^6	[A] = 10^{10}	1.52×10^{-1}	2.72×10^{1}	3.34×10^{3}	4.53×10^{4}	2.11×10^{5}
[SA] = 10^6	[A] = 10^{11}	1.21×10^{0}	5.26×10^{3}	7.12×10^{4}	3.32×10^{5}	1.17×10^{6}
[SA] = 10^7	[A] = 10^7	3.20×10^{-1}	3.22×10^{-1}	3.57×10^{-1}	2.96×10^{0}	3.69×10^{2}
[SA] = 10^7	[A] = 10^8	4.44×10^{1}	4.47×10^{1}	5.13×10^{1}	5.12×10^{2}	2.74×10^{4}
[SA] = 10^7	[A] = 10^9	4.79×10^{2}	4.97×10^{2}	1.06×10^{3}	2.76×10^{4}	3.74×10^{5}
[SA] = 10^7	[A] = 10^{10}	1.02×10^{3}	1.77×10^{3}	2.99×10^{4}	3.96×10^{5}	2.02×10^{6}
[SA] = 10^7	[A] = 10^{11}	6.17×10^{3}	5.11×10^{4}	5.82×10^{5}	3.11×10^{6}	1.15×10^{7}
[SA] = 10^8	[A] = 10^7	1.78×10^{3}	1.78×10^{3}	1.80×10^{3}	1.97×10^{3}	5.01×10^{3}
[SA] = 10^8	[A] = 10^8	1.05×10^{5}	1.05×10^{5}	1.06×10^{5}	1.11×10^{5}	2.18×10^{5}
[SA] = 10^8	[A] = 10^9	5.60×10^{5}	5.60×10^{5}	5.64×10^{5}	6.41×10^{5}	2.03×10^{6}
[SA] = 10^8	[A] = 10^{10}	9.10×10^{5}	9.17×10^{5}	1.00×10^{6}	2.33×10^{6}	1.38×10^{7}
[SA] = 10^8	[A] = 10^{11}	2.96×10^{6}	3.12×10^{6}	4.69×10^{6}	1.87×10^{7}	9.41×10^{7}

Table S14 The formation rate J of DSA at the conditions of T = 238.15 K, [SA] = 10^6-10^8 molecules·cm^{-3}, [A] = 10^7-10^{11} molecules·cm^{-3}, and [DSA] = 0, 10^4-10^7 molecules·cm^{-3}. SA, A and DSA represent sulfuric acid, ammonia and disulfuric acid, respectively

[SA]	[A]	[DSA] = 0	[DSA] = 10^4	[DSA] = 10^5	[DSA] = 10^6	[DSA] = 10^7
[SA] = 10^6	[A] = 10^7	1.14×10^{-8}	1.71×10^{-6}	1.93×10^{-4}	4.09×10^{-2}	1.75E+01
[SA] = 10^6	[A] = 10^8	4.51×10^{-6}	6.10×10^{-4}	8.08×10^{-2}	2.22×10^{1}	2.72×10^{3}
[SA] = 10^6	[A] = 10^9	5.48×10^{-4}	1.03×10^{-1}	2.32×10^{1}	2.92×10^{3}	3.74×10^{4}
[SA] = 10^6	[A] = 10^{10}	2.02×10^{-2}	2.62×10^{1}	3.18×10^{3}	4.12×10^{4}	1.89×10^{5}
[SA] = 10^6	[A] = 10^{11}	1.18×10^{-1}	3.64×10^{3}	4.62×10^{4}	2.11×10^{5}	7.40×10^{5}
[SA] = 10^7	[A] = 10^7	1.26×10^{-4}	2.68×10^{-4}	1.18×10^{-2}	1.23×10^{0}	1.78×10^{2}
[SA] = 10^7	[A] = 10^8	4.58×10^{-2}	8.85×10^{-2}	3.57×10^{0}	3.51×10^{2}	2.25×10^{4}
[SA] = 10^7	[A] = 10^9	5.22×10^{0}	1.07×10^{1}	4.39×10^{2}	2.45×10^{4}	3.31×10^{5}
[SA] = 10^7	[A] = 10^{10}	1.70×10^{2}	7.43×10^{2}	2.76×10^{4}	3.64×10^{5}	1.82×10^{6}
[SA] = 10^7	[A] = 10^{11}	8.26×10^{2}	3.19×10^{4}	4.06×10^{5}	2.03×10^{6}	7.31×10^{6}
[SA] = 10^8	[A] = 10^7	1.74×10^{0}	1.80×10^{0}	2.52×10^{0}	2.36×10^{1}	1.26×10^{3}
[SA] = 10^8	[A] = 10^8	4.46×10^{2}	4.58×10^{2}	5.87×10^{2}	3.68×10^{3}	9.84×10^{4}
[SA] = 10^8	[A] = 10^9	2.83×10^{4}	2.89×10^{4}	3.49×10^{4}	1.39×10^{5}	1.57×10^{6}
[SA] = 10^8	[A] = 10^{10}	3.29×10^{5}	3.36×10^{5}	4.32×10^{5}	1.86×10^{6}	1.27×10^{7}
[SA] = 10^8	[A] = 10^{11}	8.15×10^{5}	9.07×10^{5}	2.30×10^{6}	1.39×10^{7}	6.46×10^{7}

Table S15 The formation rate J of DSA at the conditions of T = 258.15 K, [SA] = 10^6-10^8 molecules·cm^{-3}, [A] = 10^7-10^{11} molecules·cm^{-3}, and [DSA] = 0, 10^4-10^7 molecules·cm^{-3}. SA, A and DSA represent sulfuric acid, ammonia and disulfuric acid, respectively

[SA]	[A]	[DSA] = 0	[DSA] = 10^4	[DSA] = 10^5	[DSA] = 10^6	[DSA] = 10^7
[SA] = 10^6	[A] = 10^7	5.58×10^{-13}	2.64×10^{-8}	1.18×10^{-5}	1.00×10^{-2}	7.42×10^{0}
[SA] = 10^6	[A] = 10^8	5.34×10^{-10}	2.72×10^{-5}	1.20×10^{-2}	7.96×10^{0}	1.36×10^{3}
[SA] = 10^6	[A] = 10^9	3.75×10^{-7}	3.05×10^{-2}	1.21×10^{1}	1.90×10^{3}	2.79×10^{4}
[SA] = 10^6	[A] = 10^{10}	9.02×10^{-5}	2.28×10^{1}	2.91×10^{3}	3.82×10^{4}	1.76×10^{5}
[SA] = 10^6	[A] = 10^{11}	6.67×10^{-3}	3.37×10^{3}	4.21×10^{4}	1.92×10^{5}	6.73×10^{5}
[SA] = 10^7	[A] = 10^7	6.50×10^{-9}	1.32×10^{-6}	2.01×10^{-4}	8.73×10^{-2}	5.76×10^{1}
[SA] = 10^7	[A] = 10^8	6.16×10^{-6}	1.34×10^{-3}	2.01×10^{-1}	6.89×10^{1}	1.09×10^{4}
[SA] = 10^7	[A] = 10^9	4.01×10^{-3}	1.28×10^{0}	1.66×10^{2}	1.58×10^{4}	2.49×10^{5}
[SA] = 10^7	[A] = 10^{10}	8.50×10^{-1}	4.07×10^{2}	2.44×10^{4}	3.35×10^{5}	1.69×10^{6}
[SA] = 10^7	[A] = 10^{11}	5.81×10^{1}	2.86×10^{4}	3.70×10^{5}	1.84×10^{6}	6.65×10^{6}
[SA] = 10^8	[A] = 10^7	1.53×10^{-4}	2.04×10^{-4}	4.33×10^{-3}	6.03×10^{-1}	2.02×10^{2}
[SA] = 10^8	[A] = 10^8	1.30×10^{-1}	1.88×10^{-1}	4.22×10^{0}	4.63×10^{2}	4.08×10^{4}
[SA] = 10^8	[A] = 10^9	5.22×10^{1}	9.63×10^{1}	1.99×10^{3}	7.84×10^{4}	1.23×10^{6}
[SA] = 10^8	[A] = 10^{10}	6.14×10^{3}	1.13×10^{4}	1.16×10^{5}	1.55×10^{6}	1.16×10^{7}
[SA] = 10^8	[A] = 10^{11}	1.81×10^{5}	3.03×10^{5}	1.81×10^{6}	1.27×10^{7}	5.87×10^{7}

Table S16 The formation rate J of DSA at the conditions of T = 278.15 K, [SA] = 10^6-10^8 molecules·cm^{-3}, [A] = 10^7-10^{11} molecules·cm^{-3}, and [DSA] = 0, 10^4-10^7 molecules·cm^{-3}. SA, A and DSA represent sulfuric acid, ammonia and disulfuric acid, respectively

[SA]	[A]	[DSA] = 0	[DSA] = 10^4	[DSA] = 10^5	[DSA] = 10^6	[DSA] = 10^7
[SA] = 10^6	[A] = 10^7	8.97×10^{-19}	7.12×10^{-9}	7.07×10^{-6}	6.91×10^{-3}	5.49×10^{0}
[SA] = 10^6	[A] = 10^8	8.97×10^{-16}	7.10×10^{-6}	6.91×10^{-3}	5.49×10^{0}	1.15×10^{3}
[SA] = 10^6	[A] = 10^9	8.96×10^{-13}	6.94×10^{-3}	5.50×10^{0}	1.15×10^{3}	1.88×10^{4}
[SA] = 10^6	[A] = 10^{10}	8.81×10^{-10}	5.61×10^{0}	1.17×10^{3}	1.94×10^{4}	1.01×10^{5}
[SA] = 10^6	[A] = 10^{11}	7.59×10^{-7}	1.34×10^{3}	2.38×10^{4}	1.37×10^{5}	5.61×10^{5}
[SA] = 10^7	[A] = 10^7	9.09×10^{-15}	5.60×10^{-8}	5.39×10^{-5}	5.25×10^{-2}	4.17×10^{1}
[SA] = 10^7	[A] = 10^8	9.09×10^{-12}	5.59×10^{-5}	5.27×10^{-2}	4.18×10^{1}	8.98×10^{3}
[SA] = 10^7	[A] = 10^9	9.07×10^{-9}	5.46×10^{-2}	4.20×10^{1}	9.00×10^{3}	1.67×10^{5}
[SA] = 10^7	[A] = 10^{10}	8.89×10^{-6}	4.41×10^{1}	9.18×10^{3}	1.72×10^{5}	9.70×10^{5}
[SA] = 10^7	[A] = 10^{11}	7.36×10^{-3}	1.08×10^{4}	2.12×10^{5}	1.32×10^{6}	5.54×10^{6}
[SA] = 10^8	[A] = 10^7	1.03×10^{-10}	2.22×10^{-7}	1.64×10^{-4}	1.55×10^{-1}	1.23×10^{2}
[SA] = 10^8	[A] = 10^8	1.03×10^{-7}	2.21×10^{-4}	1.60×10^{-1}	1.23×10^{2}	2.81×10^{4}
[SA] = 10^8	[A] = 10^9	1.02×10^{-4}	2.17×10^{-1}	1.28×10^{2}	2.83×10^{4}	7.74×10^{5}
[SA] = 10^8	[A] = 10^{10}	9.58×10^{-2}	1.77×10^{2}	3.01×10^{4}	8.04×10^{5}	6.91×10^{6}
[SA] = 10^8	[A] = 10^{11}	5.85×10^{1}	4.98×10^{4}	1.06×10^{6}	9.42×10^{6}	4.90×10^{7}

Table S17 The formation rate J of DSA at the conditions of T = 298.15 K, [SA] = 10^6-10^8 molecules·cm^{-3}, [A] = 10^7-10^{11} molecules·cm^{-3}, and [DSA] = 0, 10^4-10^7 molecules·cm^{-3}. SA, A and DSA represent sulfuric acid, ammonia and disulfuric acid, respectively

[SA]	[A]	[DSA] = 0	[DSA] = 10^4	[DSA] = 10^5	[DSA] = 10^6	[DSA] = 10^7
[SA] = 10^6	[A] = 10^7	2.62×10^{-24}	5.25×10^{-11}	5.25×10^{-8}	5.24×10^{-5}	5.15×10^{-2}
[SA] = 10^6	[A] = 10^8	2.62×10^{-21}	5.25×10^{-8}	5.24×10^{-5}	5.15×10^{-2}	4.33×10^{1}
[SA] = 10^6	[A] = 10^9	2.62×10^{-18}	5.25×10^{-5}	5.16×10^{-2}	4.33×10^{1}	7.91×10^{3}
[SA] = 10^6	[A] = 10^{10}	2.62×10^{-15}	5.17×10^{-2}	4.34×10^{1}	7.91×10^{3}	7.92×10^{4}
[SA] = 10^6	[A] = 10^{11}	2.62×10^{-12}	4.44×10^{1}	7.98×10^{3}	7.95×10^{4}	3.33×10^{5}
[SA] = 10^7	[A] = 10^7	2.62×10^{-20}	4.08×10^{-10}	4.07×10^{-7}	4.06×10^{-4}	3.99×10^{-1}
[SA] = 10^7	[A] = 10^8	2.62×10^{-17}	4.08×10^{-7}	4.06×10^{-4}	3.99×10^{-1}	3.34×10^{2}
[SA] = 10^7	[A] = 10^9	2.62×10^{-14}	4.07×10^{-4}	3.99×10^{-1}	3.34×10^{2}	6.63×10^{4}
[SA] = 10^7	[A] = 10^{10}	2.62×10^{-11}	4.02×10^{-1}	3.35×10^{2}	6.64×10^{4}	7.55×10^{5}
[SA] = 10^7	[A] = 10^{11}	2.62×10^{-8}	3.43×10^{2}	6.69×10^{4}	7.58×10^{5}	3.28×10^{6}
[SA] = 10^8	[A] = 10^7	2.64×10^{-16}	1.29×10^{-9}	1.25×10^{-6}	1.25×10^{-3}	1.22×10^{0}
[SA] = 10^8	[A] = 10^8	2.64×10^{-13}	1.29×10^{-6}	1.25×10^{3}	1.22×10^{0}	1.02×10^{3}
[SA] = 10^8	[A] = 10^9	2.64×10^{-10}	1.28×10^{-3}	1.23×10^{0}	1.02×10^{3}	2.45×10^{5}
[SA] = 10^8	[A] = 10^{10}	2.64×10^{-7}	1.26×10^{0}	1.02×10^{3}	2.45×10^{5}	5.06×10^{6}
[SA] = 10^8	[A] = 10^{11}	2.63×10^{-4}	1.07×10^{3}	2.47×10^{5}	5.08×10^{6}	2.89×10^{7}

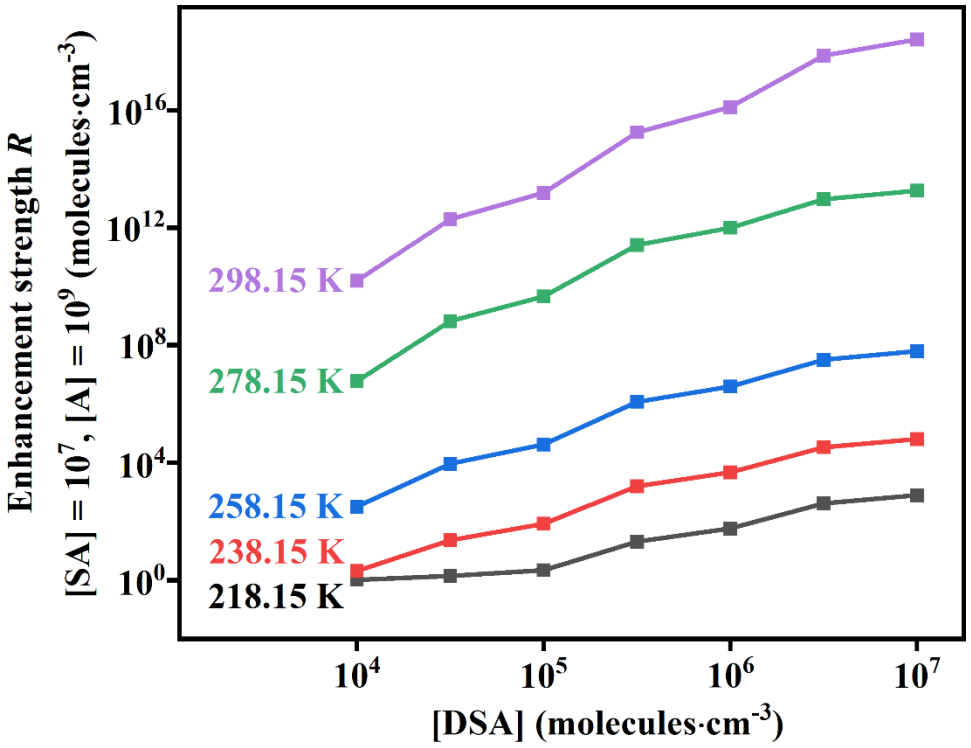

Figure S14 The enhancement strength *R* of DSA as a function of [DSA] from 10^4 to 10^7 molecules·cm^{-3} under different temperatures (218.15, 238.15, 258.15, 278.15 and 298.15 K) where [SA] = 10^7 molecules·cm^{-3} and [A] = 10^9 molecules·cm^{-3}

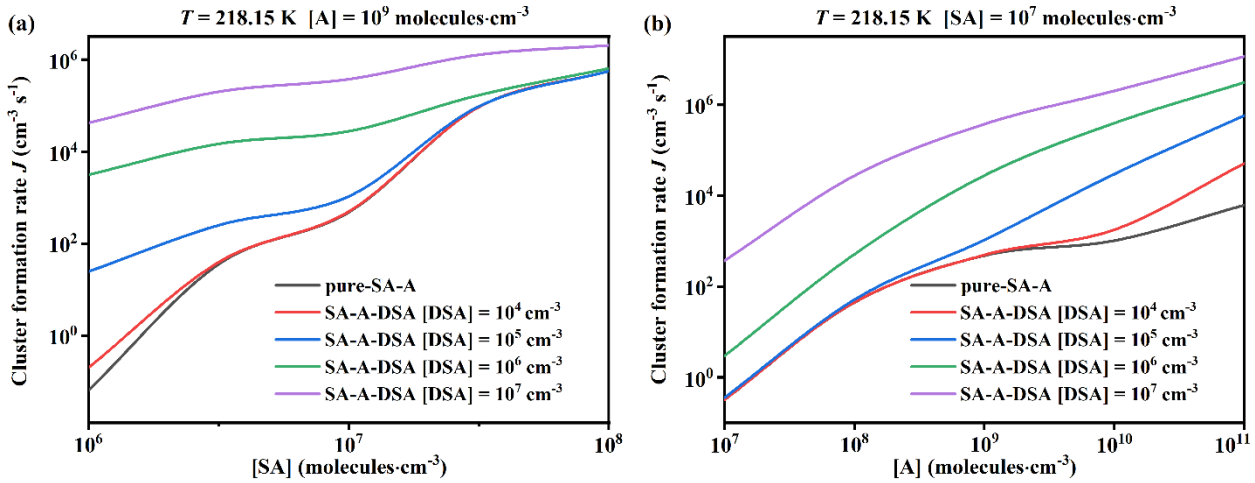

Figure S15 Simulated cluster formation rates J (cm^{-3} s^{-1}) as a function of (a) [SA], (b) [A], with different concentrations of disulfuric acid [DSA] of 10^4 (red), 10^5 (blue), 10^6 (green) ,10^7 (purple) and 0 molecules·cm^{-3} (black, pure-SA-A), at T = 218.15 K

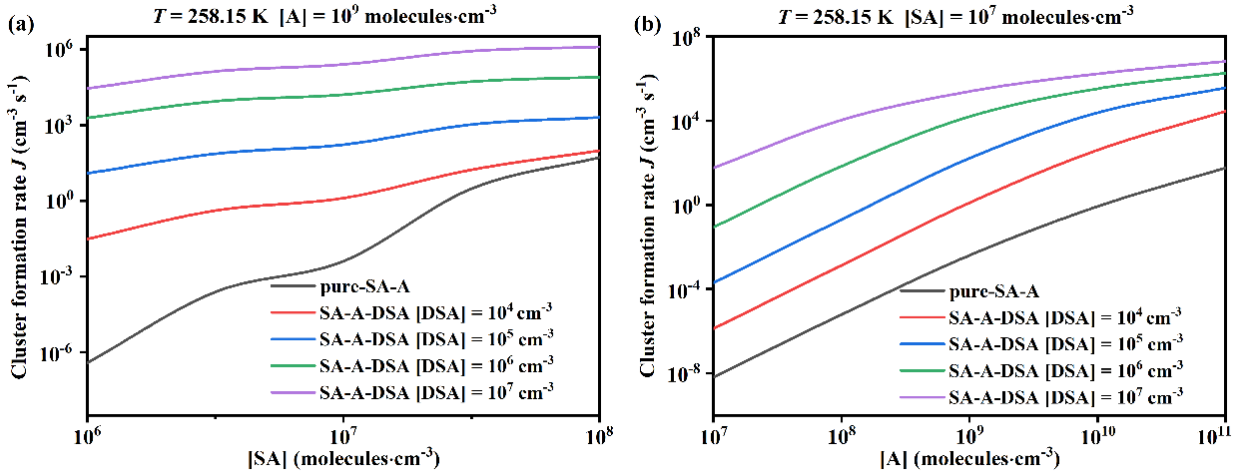

Figure S16 Simulated cluster formation rates J (cm^{-3} s^{-1}) as a function of (a) [SA], (b) [A], with different concentrations of disulfuric acid [DSA] of 10^4 (red), 10^5 (blue), 10^6 (green) ,10^7 (purple) and 0 molecules·cm^{-3} (black, pure-SA-A), at T = 258.15 K

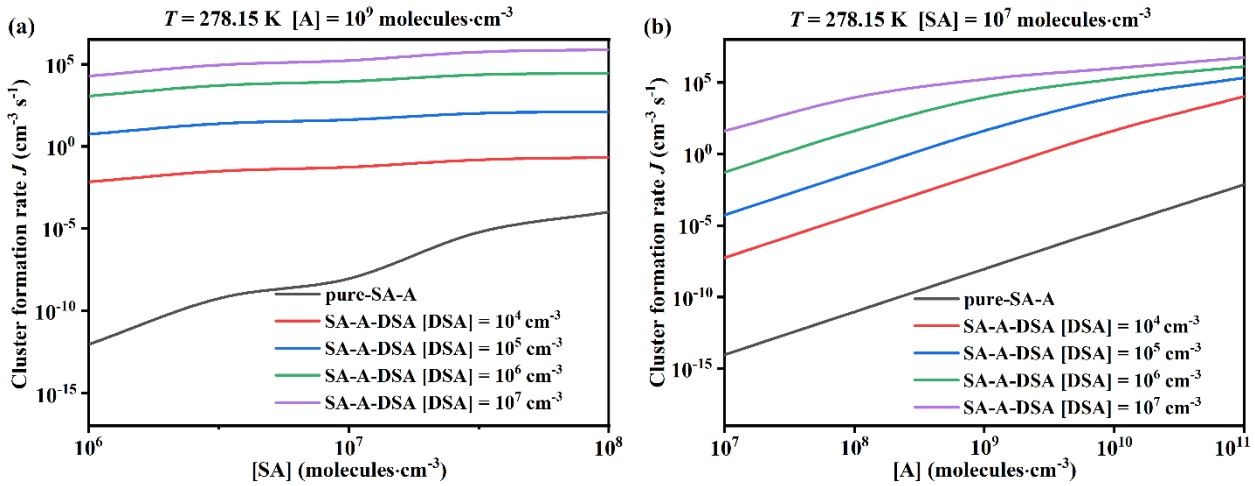

Figure S17 Simulated cluster formation rates J (cm^{-3} s^{-1}) as a function of (a) [SA], (b) [A], with different concentrations of disulfuric acid [DSA] of 10^4 (red), 10^5 (blue), 10^6 (green) ,10^7 (purple) and 0 molecules·cm^{-3} (black, pure-SA-A), at T = 278.15 K

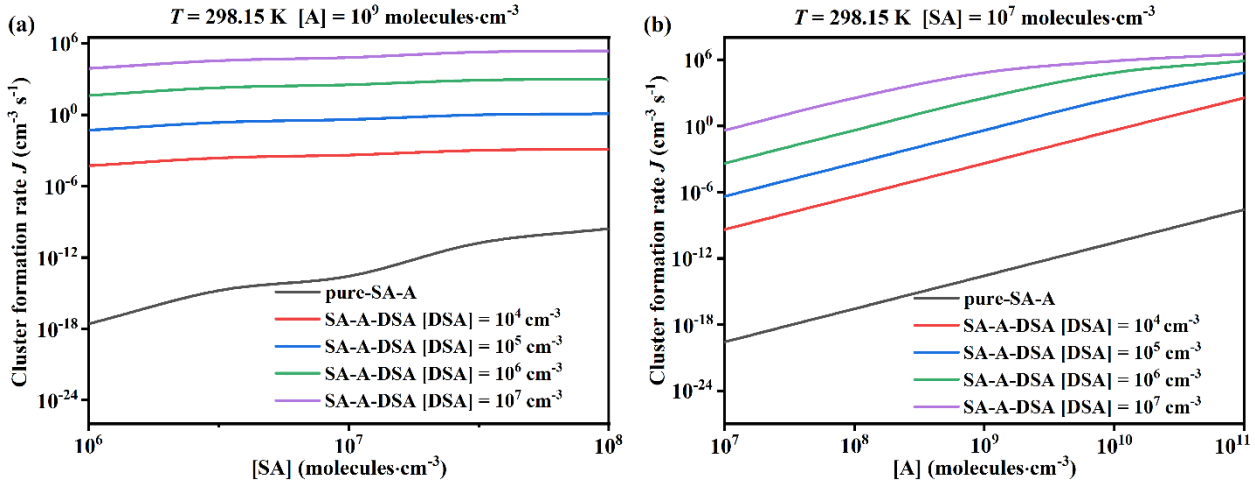

Figure S18 Simulated cluster formation rates J (cm^{-3} s^{-1}) as a function of (a) [SA], (b) [A], with different concentrations of disulfuric acid [DSA] of 10^4 (red), 10^5 (blue), 10^6 (green) ,10^7 (purple) and 0 molecules·cm^{-3} (black, pure-SA-A), at T = 298.15 K

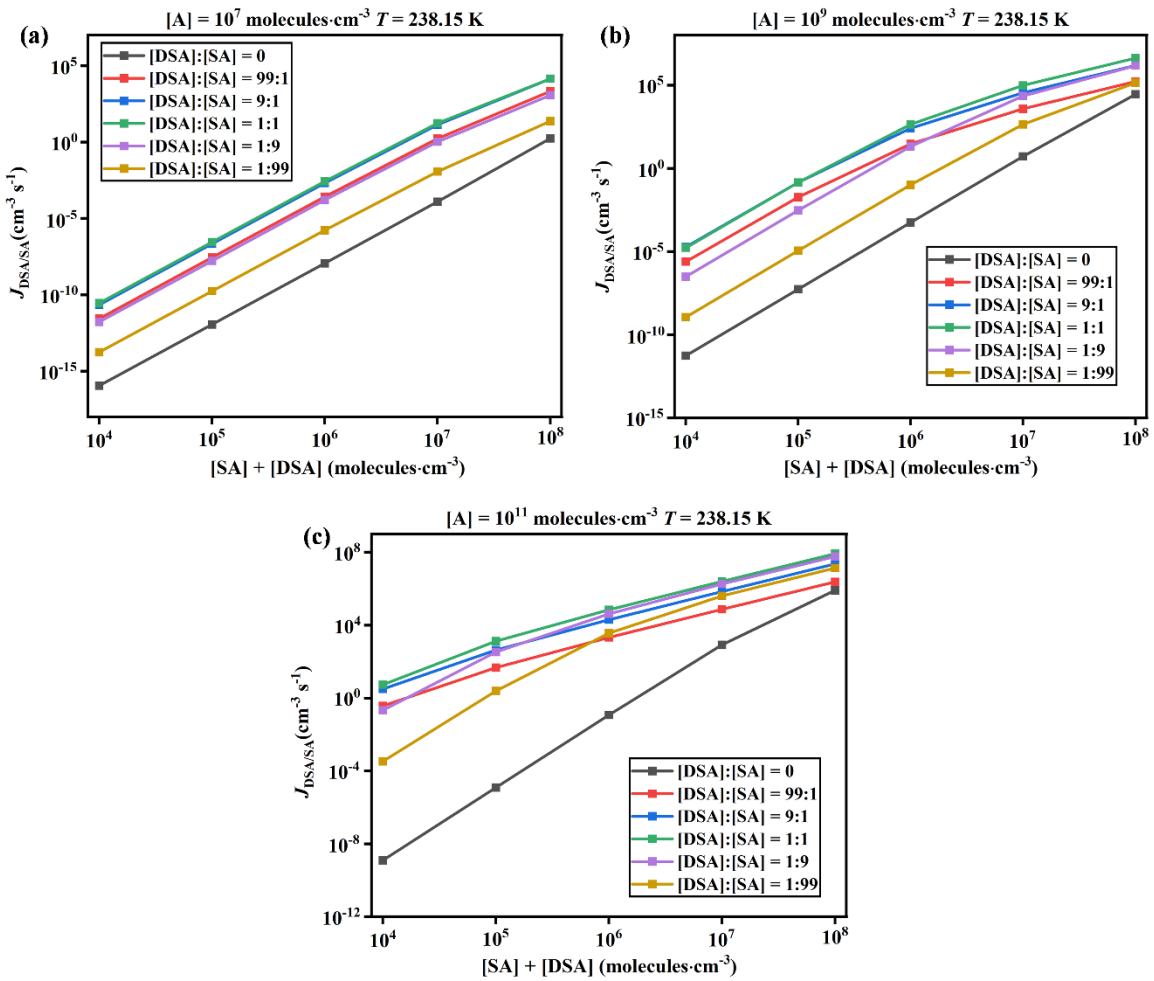

Figure S19 Particle formation rates (J, $cm^{-3}\cdot s^{-1}$) with varying ratios of [DSA]:[SA] at 238.15 K under different A concentrations ((a)10^7 molecules·cm^{-3}, (b)10^9 molecules·cm^{-3}, (c)10^{11} molecules·cm^{-3}). [DSA] + [SA] = 10^4-10^8 molecules·cm^{-3}

As shown in Figure S19(a), at lower atmospheric concentration of A (10^7 molecules·cm^{-3}), the formation rate $J_{DSA/SA}$ at 1% substitution ([DSA]:[SA] = 1:99) was higher than that at unsubstituted condition ([DSA]:[SA] = 0:100). Similarly, $J_{DSA/SA}$ at 10% substitution ([DSA]:[SA] = 1:9) was higher than that at 1% substitution. Moreover, $J_{DSA/SA}$ at 50% substitution ([DSA]:[SA] = 1:1) reach a maximum value (1.41×10^4 $cm^{-3}\cdot s^{-1}$), which is larger by 4-5 orders of magnitude than the value at unsubstituted condition. These results at lower atmospheric concentration of A show that the enhancement strength of DSA on the particle formation rate of SA-A-based clusters increases with the increasing of the percentage of substitution.

At medium (10^9 molecules·cm^{-3}) and higher (10^{11} molecules·cm^{-3}) atmospheric concentration of A, $J_{DSA/SA}$ at 50% substitution ([DSA]:[SA] = 1:1) reaches a maximum value. As compared with $J_{DSA/SA}$ at unsubstituted condition, the value of $J_{DSA/SA}$ at 50% substitution ([DSA]:[SA] = 1:1) enhanced by 10 and 11 orders of magnitude, respectively. However, as the percentage of substitution (> 50%) increases, the value of $J_{DSA/SA}$ at medium and higher [A] decreases. This may be due to the fact that in the pure A-DSA nucleation system, large stable clusters $(A)_3\cdot(DSA)_3$ can only be formed by mutual collisions of A·DSA clusters. So, DSA has the same "acid" molecular properties as SA in the SA-A-DSA ternary nucleation system. We predicted that DSA is a relatively stronger nucleation precursor than SA.

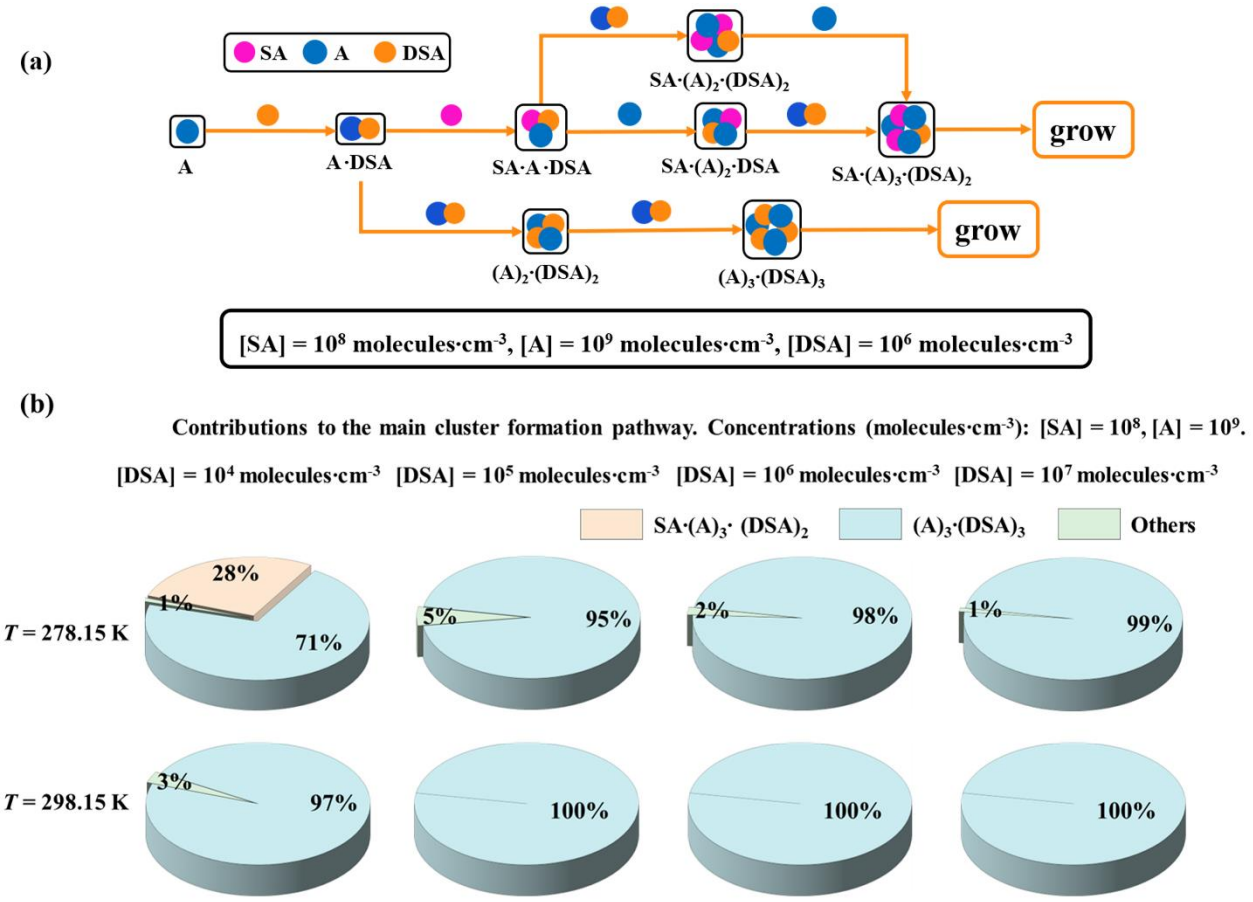

Figure S20 (a) The main pathways of clusters growing out of the research system under the conditions where 278.15 K, and 298.15 K, [SA] = 10^8 molecules·cm^{-3}, [A] = 10^9 molecules·cm^{-3}, and [DSA] = 10^6 molecules·cm^{-3}; (b) The contribution of different concentrations of DSA to the main cluster formation pathway at 278.15 K, and 298.15 K is shown in the pie charts.

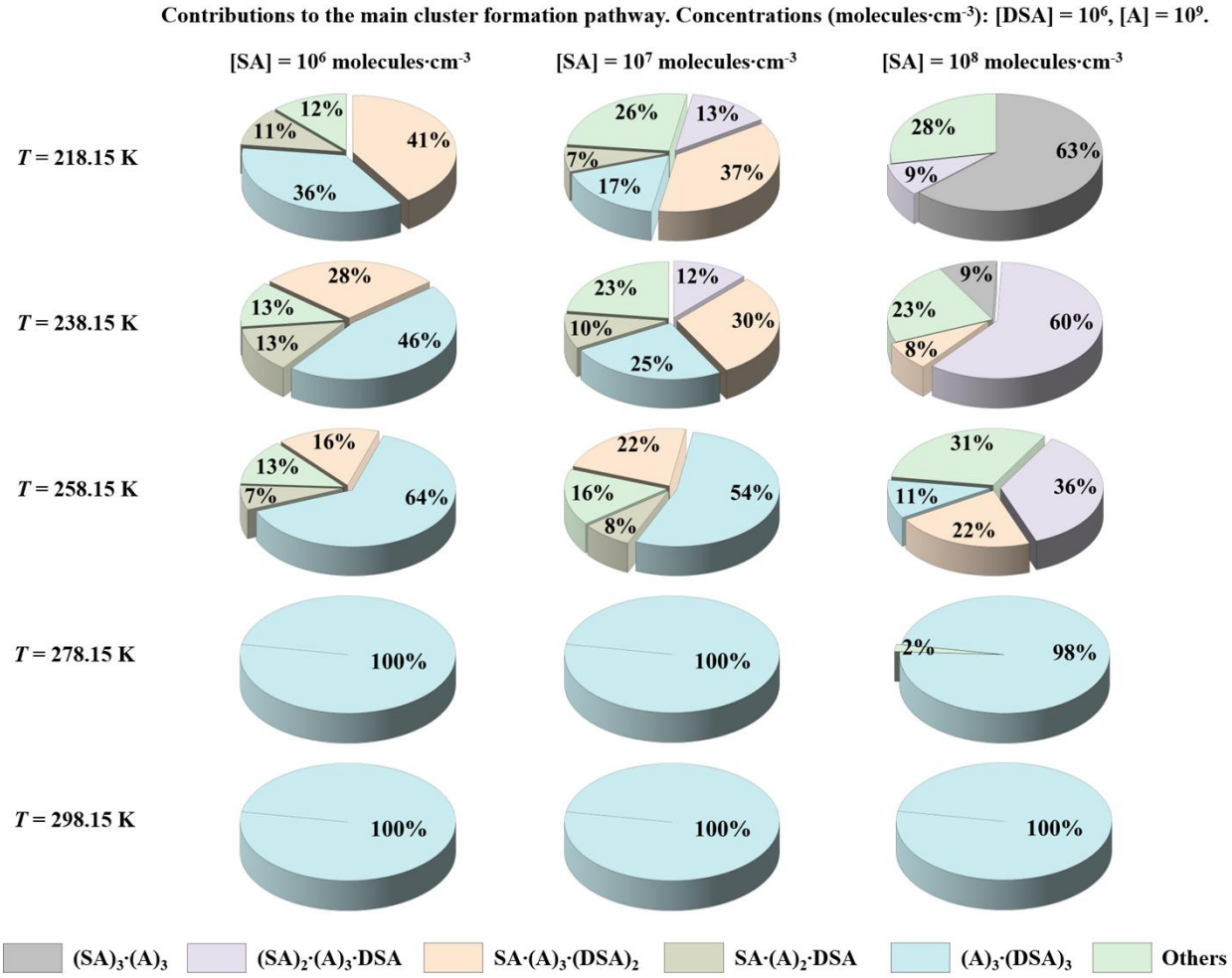

Figure S21 The contribution of different concentrations of SA to the major cluster formation pathways at different temperatures (218.15 K, 238.15 K, 258.15 K, 278.15 K, and 298.15 K) and at [DSA] = 10^6 molecules·cm^{-3}, [A] = 10^9 molecules·cm^{-3} is shown in the pie charts.

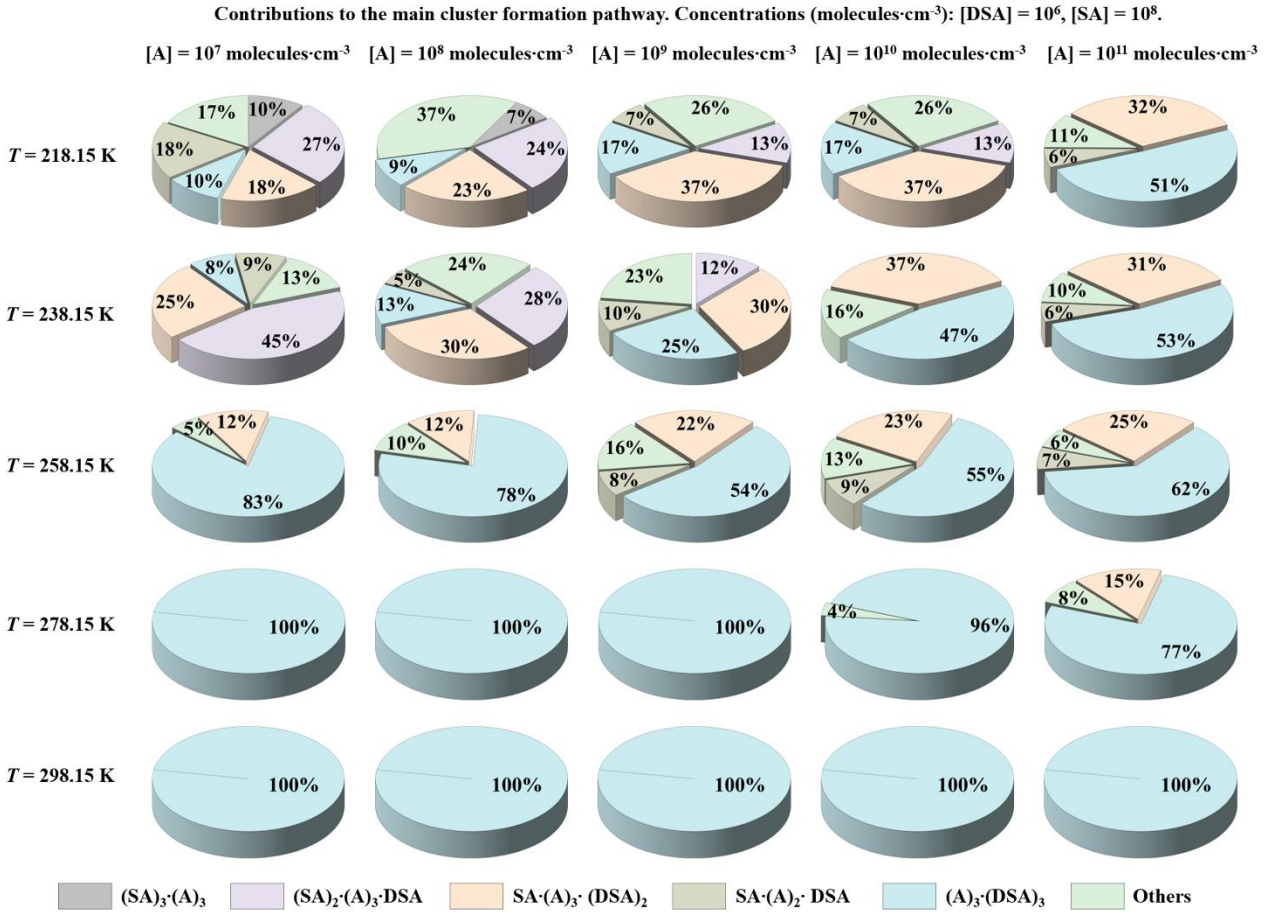

Figure S22 The contribution of different concentrations of A to the major cluster formation pathways at different temperatures (218.15 K, 238.15 K, 258.15 K, 278.15 K, and 298.15 K) and at [DSA] = 10^6 molecules·cm^{-3}, [SA] = 10^8 molecules·cm^{-3} is shown in the pie charts.

Table S18 Cartesian coordinates of all molecules and clusters in the studied system.

SA:

Atoms	X	Y	Z
S	-0.00000100	-0.00000100	-0.15756700
O	0.67306500	0.67306500	-0.81983600
O	-0.67307500	-0.67307500	-0.81979800
O	1.01736800	1.01736800	0.84358200
O	-1.01735800	-1.01735800	0.84357500
H	1.70169100	1.70169100	1.07043800
H	-1.70167800	-1.70167800	1.07045700

A:

Atoms	X	Y	Z
N	0.00000000	0.11911400	0.00000000
H	-0.93235000	-0.27807200	0.00000000
H	0.46617500	-0.27786300	0.80753900
H	0.46617500	-0.27786300	-0.80753900

DSA:

Atoms	X	Y	Z
S	-1.43510900	-0.13598100	0.03492700
O	-2.38705700	-0.43102000	1.02932100
O	-1.24778700	-0.89230600	-1.14721200
O	-1.54051800	1.38764200	-0.28976900
S	1.38684600	0.12449200	0.06491400
O	1.11188700	1.05840000	-0.97277300
O	1.64540800	-1.25084900	-0.64070300
O	2.34997600	0.33819800	1.07741600
O	0.01087600	-0.15789900	0.86275800
H	-0.84560200	1.61939600	-0.93204600
H	2.07552800	-1.85290200	-0.01771400

$(SA)_1 \cdot (A)_1$:

Atoms	X	Y	Z
S	-0.59732600	-0.11330300	0.09028200
O	0.11386900	-0.09250800	1.33053100
O	-1.77725300	-0.88882800	-0.09102500
O	0.38323700	-0.42810500	-1.05987100
O	-0.97903500	1.41306500	-0.18279600
H	1.35885500	-0.23109000	-0.73760300
H	-1.72492000	1.42300400	-0.79399800
N	2.71575100	0.04051200	-0.05360200
H	3.15679600	0.92252300	-0.28222700

H	3.40929600	-0.69086300	-0.14794300
H	2.42039100	0.07670700	0.91776700

$(SA)_1 \cdot (DSA)_1$:

Atoms	X	Y	Z
S	-2.47894500	-0.27718400	-0.07642800
O	-1.96942000	-0.69986700	1.32142600
O	-3.71936500	-0.91541600	-0.30294600
O	-1.39496600	-0.39448700	-1.03015800
O	-2.68689900	1.27963100	0.02947600
H	0.13413900	-1.35148000	-1.27363600
H	-3.55012600	1.46532400	0.42365200
S	1.71348900	-1.27742400	0.10594200
O	2.93138800	-1.97706900	0.17828500
O	1.10381000	-1.47119600	-1.31475600
O	0.67953600	-1.42141800	1.07950900
S	1.13845700	1.55591000	0.08489700
O	0.10562700	1.27156800	1.02340900
O	0.55626500	1.50979600	-1.35863100
O	1.99771500	2.66524800	0.18881000
O	2.17216200	0.28353900	0.05759200
H	-0.99604700	-0.58635500	1.38700300
H	-0.27344600	0.98808800	-1.36114300

$(SA)_1 \cdot (DSA)_1 \cdot (A)_1$:

Atoms	X	Y	Z
N	0.13203900	-0.69865100	2.57081600
H	-0.09820600	0.24085300	2.88663600
H	0.94687800	-0.61472500	1.91851700
H	0.36650600	-1.29661600	3.35702000
S	-1.36558700	-1.43866900	-0.41236900
O	-1.93814100	-2.27300500	-1.40003200
O	-2.05721700	-1.34463300	0.88102700
O	0.07046500	-1.46827700	-0.22323000
S	-1.64689100	1.38540600	-0.13002500
O	-0.51624200	1.25992200	0.76902000
O	-2.95619100	1.18333900	0.69692800
O	-1.78524200	2.53966300	-0.92557400
O	-1.64573200	0.12543300	-1.08303700
H	-0.67833000	-1.06704400	2.04175900
H	-2.98291100	0.24564200	0.98396400
S	2.84196800	0.16905200	-0.13063300
O	4.17836600	0.57355300	-0.33440900
O	2.40700700	-0.23359000	1.19157800

O	2.54895000	-0.98628800	-1.13465400
O	1.88912300	1.31567200	-0.60376200
H	1.63256100	-1.30885000	-0.99865200
H	1.05622000	1.30436200	-0.08737600

$(SA)_1 \cdot (DSA)_1 \cdot (A)_2$:

Atoms	X	Y	Z
N	0.18558600	-0.42777500	2.69341100
H	0.42446900	0.41891100	2.13776300
H	0.22002000	-0.23493600	3.68889300
H	-0.77044100	-0.65607300	2.38916300
S	1.50115100	-1.38977600	-0.01360500
O	1.96564300	-1.72651000	-1.33444200
O	0.06199800	-1.08823200	0.00995300
O	1.91464000	-2.21104900	1.09420700
S	1.56569400	1.50356200	-0.05508300
O	0.35142500	1.60111000	0.79620900
O	1.20883500	1.38127000	-1.45768000
O	2.59905500	2.41327900	0.28396600
O	2.20419300	0.04782600	0.39472500
H	0.83092700	-1.18798700	2.43214500
H	0.21262400	0.35027500	-2.19677800
N	-0.21950900	-0.47968000	-2.68577800
H	0.42816900	-1.25280800	-2.47932300
H	-1.13410900	-0.66252500	-2.26849900
H	-0.29905600	-0.31804400	-3.68415100
S	-2.73864200	0.13718200	0.13240900
O	-2.33692000	-0.04611600	1.50407700
O	-4.06757200	0.49138800	-0.19509100
O	-2.44593300	-1.22129500	-0.64152200
O	-1.75846000	1.12418900	-0.55316500
H	-1.57732400	-1.54280100	-0.31762000
H	-0.92428500	1.29579400	0.01554000

$(SA)_1 \cdot (DSA)_2$:

Atoms	X	Y	Z
S	-0.13767500	-0.19715200	0.54525800
O	-0.42207900	-0.86585500	-0.82014700
O	1.04200900	-0.83307100	1.05116300
O	-1.32800500	-0.19667000	1.36133700
O	0.13514300	1.29151800	0.24366200
H	-2.91156200	-1.13032000	1.55389200
H	1.03801800	1.39817800	-0.15275000
S	-4.24938800	-1.33970400	-0.04918500
O	-5.44989800	-2.06032700	-0.17755700

O	-3.87733800	-1.24265900	1.46229700
O	-3.07393000	-1.64456800	-0.79753900
S	-3.65868400	1.46022300	-0.45922500
O	-2.48142200	1.03228800	-1.14047400
O	-3.32838200	1.69077400	1.04492400
O	-4.47160300	2.51468100	-0.91136100
O	-4.69233600	0.19551500	-0.37449900
H	-1.35522900	-0.72140200	-1.09153900
H	-2.50681500	1.21314800	1.27796200
S	3.72256900	1.38395500	0.20360800
O	3.64169600	2.20232700	1.34451500
O	2.62269000	1.26632800	-0.71430700
O	5.01531700	1.72818200	-0.57990200
S	4.25886000	-1.36865400	-0.29821200
O	4.98229300	-0.86284300	-1.41906500
O	2.81420000	-1.62226000	-0.77565200
O	4.75478800	-2.39492500	0.52939100
O	4.04465200	-0.10690900	0.75229600
H	5.18141100	1.04151100	-1.25808700
H	2.16089400	-1.55201000	-0.03802000

$(SA)_1 \cdot (DSA)_2 \cdot (A)_1$:

Atoms	X	Y	Z
N	-1.03477100	-1.42131200	2.23680900
H	-1.12479800	-1.61683800	3.22835100
H	-1.02403900	-0.40937600	2.05950300
H	-0.13593600	-1.76980700	1.87236500
S	-2.19075800	-1.64299100	-0.90140900
O	-2.28576800	-2.33434400	-2.13022700
O	-2.92530400	-2.18564200	0.24468400
O	-0.88408400	-1.14090100	-0.49689600
S	-3.68951300	0.63285700	-0.05946400
O	-2.70238300	0.72145300	0.99671100
O	-4.85219400	-0.29167500	0.41526500
O	-4.23884800	1.81821000	-0.58951400
O	-3.05939400	-0.19546700	-1.24856300
H	-1.80709100	-1.83095200	1.69067400
H	-4.48747100	-1.19327100	0.53514400
S	0.15228100	1.95387800	0.53584900
O	1.27606900	2.82182300	0.32007600
O	0.26759000	0.92056200	1.52846900
O	-0.25845800	1.33727700	-0.81415400
O	-1.02023000	2.91465900	0.88504600
H	-0.46549600	0.35646300	-0.72440200
H	-1.82682100	2.37519200	1.01264400

S	2.70599300	-1.36719900	0.84693600
O	1.53748600	-2.07068700	1.25335000
O	3.48880900	-0.61750600	1.75521000
O	3.56491500	-2.40057400	0.05893500
S	3.31947100	0.57499500	-1.12424400
O	4.51717300	-0.19412300	-1.22251200
O	3.56072300	1.67250700	-0.08237600
O	2.60229600	1.03068700	-2.24998800
O	2.20362900	-0.38844900	-0.34690900
H	4.30165600	-1.92828500	-0.37622400
H	2.71759900	2.19893600	0.06872900

$(SA)_1 \cdot (DSA)_2 \cdot (A)_2$:

Atoms	X	Y	Z
N	2.39985100	-2.97995600	0.60863900
H	2.17249700	-2.21230000	1.25885300
H	2.57937300	-3.84211400	1.11296400
H	1.60459000	-3.08625700	-0.04273300
S	3.31532100	-0.21618600	-0.95088900
O	3.58748000	0.62663000	-2.08297800
O	1.98642200	-0.80122700	-0.93595000
O	4.34509900	-1.10208900	-0.48385400
S	2.33992100	0.78348200	1.55891700
O	2.53468400	-0.55602700	2.03829900
O	0.88097200	0.87157200	0.98400900
O	2.56748000	1.90201600	2.39036100
O	3.20779200	1.01301900	0.25964700
H	3.23400600	-2.65890000	0.09906500
H	0.47258700	-0.07798300	0.88607700
N	0.81514100	1.54421200	-2.05391900
H	0.65845800	2.21477100	-1.29197200
H	0.30450100	1.87433700	-2.86894500
H	1.81990700	1.42934000	-2.25445900
S	-0.70849400	-1.79353700	-0.45413700
O	-0.07798500	-3.01896600	-0.85366300
O	-0.27175700	-1.31509900	0.86688700
O	-0.83967000	-0.74372800	-1.42950700
S	-3.47843400	-1.35259700	0.22474100
O	-3.52221500	-0.25603700	-0.69939800
O	-3.05481600	-0.80518700	1.62040800
O	-4.57870700	-2.21569500	0.38950700
O	-2.26460300	-2.32654000	-0.16495100
H	0.42797600	0.62807900	-1.77000500
H	-2.60391400	0.05457400	1.51595600
S	-1.88607500	2.69154700	-0.16408000

O	-0.65403000	3.41090800	-0.29487200
O	-3.12494300	3.33110600	0.05919000
O	-1.69047700	1.63600100	1.01999500
O	-1.93571200	1.76832800	-1.42330600
H	-0.73585700	1.59045200	1.23386600
H	-2.51499400	0.98098000	-1.27315900

$(SA)_1 \cdot (DSA)_2 \cdot (A)_3$:

Atoms	X	Y	Z
N	-2.51999000	-2.10255300	1.68586100
H	-2.66179000	-1.94588000	0.67966300
H	-2.88384800	-3.00536300	1.96981700
H	-1.51136500	-2.01395400	1.90962400
S	-2.73989300	1.10681500	1.23034100
O	-2.38587200	2.48758500	1.45205300
O	-1.65059400	0.29235300	0.71447900
O	-3.53154300	0.46062000	2.24748400
S	-3.81546900	0.17596300	-1.25519500
O	-3.67324900	-1.13779200	-0.69403000
O	-2.54198900	0.54713500	-2.06140500
O	-4.93861000	0.50740900	-2.04414200
O	-3.80396100	1.25309900	-0.07405800
H	-3.02102900	-1.32637600	2.14822300
H	-1.71148000	0.16036600	-1.69197600
N	4.28888900	-2.20923500	-0.37897100
H	3.90506700	-2.44111100	-1.29262600
H	5.08427200	-2.79218000	-0.14274400
H	4.54173900	-1.20721700	-0.38478000
S	1.10942300	-1.46982700	1.37569600
O	0.15094400	-1.78817000	2.40158700
O	1.42114800	-0.04776800	1.23348500
O	2.29522500	-2.30630200	1.39074000
S	0.69839600	-1.26214200	-1.47194400
O	2.15541900	-1.04750100	-1.39728200
O	0.00674800	0.01401300	-1.54204200
O	0.26632900	-2.29456200	-2.34625300
O	0.29343300	-1.87714900	0.02076000
H	3.50472000	-2.30252900	0.32175800
H	0.05203000	2.06645500	-0.77843200
N	0.15956600	2.27891000	0.21401300
H	0.36619600	1.36859900	0.65698600
H	0.94159700	2.91453100	0.35014800
H	-0.72450100	2.63213900	0.61640100
S	3.81394200	1.73522600	-0.19005900
O	4.59950600	0.52861500	-0.11261600

O	4.41694100	2.96511800	-0.53974200
O	3.12055100	1.96111700	1.20416100
O	2.60644900	1.47467000	-1.13553900
H	2.67064600	1.12637400	1.46726000
H	2.43113500	0.47981800	-1.23816300

$(DSA)_1 \cdot (A)_1$:

Atoms	X	Y	Z
N	1.39103700	2.49577300	0.05425100
H	0.36403100	2.43206600	0.07924100
H	1.70913000	3.36997100	-0.34808000
H	1.75204800	2.36086900	0.99506100
S	1.23309500	-0.70744200	-0.02208000
O	1.74993600	-2.02510400	0.01713200
O	1.05815300	0.00463100	1.24344400
O	1.75554200	0.17671500	-1.05951900
S	-1.52632100	0.03673600	-0.12635900
O	-1.06629500	1.37280200	-0.39993600
O	-1.61646800	-0.16517600	1.42380200
O	-2.72809900	-0.42868500	-0.69974800
O	-0.38253900	-0.98851200	-0.52357100
H	1.67058800	1.62863800	-0.51876000
H	-0.70326600	-0.10404300	1.77497600

$(SA)_2$:

Atoms	X	Y	Z
S	-2.01322700	-0.06909400	0.12032000
O	-1.03993500	0.02070700	1.17305600
O	-3.33344600	-0.50822700	0.37973100
O	-2.03861500	1.38798500	-0.49770200
H	-2.80898000	1.47208500	-1.07474100
O	-1.44840100	-0.93353400	-1.03975000
H	-0.49362800	-0.70536900	-1.17055400
O	1.03990200	-0.02023300	-1.17304000
S	2.01323800	0.06911400	-0.12030200
O	1.44861400	0.93342700	1.03995600
O	3.33355800	0.50799300	-0.37963200
O	2.03830500	-1.38810900	0.49739500
H	0.49378000	0.70547900	1.17068500
H	2.80879500	-1.47259300	1.07421100

$(SA)_2 \cdot (A)_1$:

Atoms	X	Y	Z
S	-1.75156900	-0.35106400	-0.05309700

O	-1.08755700	0.22332400	1.13077400
O	-0.97588400	-1.41957800	-0.65807100
O	-3.09267400	-1.03007100	0.46440300
H	-2.87930000	-1.91566500	0.78109800
O	-2.22526600	0.68973700	-0.94849600
H	-1.40930200	2.07376900	-0.49615300
O	1.36347800	1.03234300	-0.60427700
S	2.05584200	-0.10297800	-0.02123500
O	1.42781100	-0.37315300	1.37706700
O	3.46255300	-0.06302900	0.11092600
O	1.68407300	-1.36217100	-0.85448200
H	0.44072100	-0.19621900	1.34104900
H	0.69686100	-1.43307500	-0.90284700
N	-0.68866100	2.67273600	-0.01622200
H	0.21057600	2.15515800	-0.14127600
H	-0.92046500	2.68070400	0.97367200
H	-0.63909600	3.61164500	-0.39543300

$(SA)_2 \cdot (DSA)_1$:

Atoms	X	Y	Z
S	-0.38040400	2.37720100	-0.13492600
O	0.95898800	2.43967100	-0.65606200
O	-1.01498400	3.53934700	0.35802100
O	-0.44607500	1.24514500	0.94980400
O	-1.23762100	1.73931800	-1.28917300
H	0.45992400	0.91391300	1.14848700
H	-2.16452700	1.66024100	-0.98698100
S	3.03468600	-0.04900600	0.38831200
O	4.36227200	-0.37422900	0.71647800
O	2.10425900	0.44800300	1.35549600
O	2.99023300	0.81161800	-0.88013400
S	0.86885900	-1.78465100	-0.33732000
O	0.53272600	-0.55361100	-1.23971400
O	0.23489600	-1.62448100	0.94063200
O	0.77924400	-3.01106800	-1.02731300
O	2.43502400	-1.49119900	-0.17509300
H	2.17795700	1.39648200	-0.87701700
H	-1.39391400	-1.26302900	1.38570900
S	-2.96705500	-0.64644500	0.14770400
O	-3.36927100	0.71968200	0.16497100
O	-2.35708900	-1.08137700	1.50688100
O	-2.10529400	-1.10763400	-0.91020900
O	-4.29625200	-1.47255000	0.13445800
H	-0.44432900	-0.46082900	-1.30637800
H	-4.10093900	-2.41344200	0.02347800

$(SA)_2 \cdot (DSA)_1 \cdot (A)_1$:

Atoms	X	Y	Z
N	-2.03199700	1.98480500	-1.64025700
H	-1.40392200	1.17426900	-1.74782000
H	-1.53675100	2.66815700	-1.04061700
H	-2.25526800	2.38840900	-2.54470100
S	-2.59331100	-0.03211400	1.00826000
O	-3.13042900	-0.41251300	2.25993300
O	-3.43575700	-0.15204100	-0.17559500
O	-1.79000600	1.18171000	0.95612300
S	-1.06821400	-1.75031000	-0.69886200
O	-0.83454200	-0.61428400	-1.53861000
O	-2.38448600	-2.46812600	-1.12841000
O	-0.08021100	-2.76573000	-0.57650200
O	-1.39196900	-1.26092000	0.76403200
H	-2.86794900	1.63509300	-1.16362500
H	-3.11850900	-1.82768600	-1.02985200
S	0.99253100	2.58597200	-0.06545800
O	2.31430600	3.06556300	0.07615000
O	-0.13468500	3.47523500	-0.12881100
O	0.76055700	1.55675500	1.10954800
O	0.83323900	1.68485500	-1.33551900
H	-0.21588200	1.35518400	1.17860100
H	1.37762100	0.85706100	-1.23959500
S	2.92117500	-1.17009800	0.17926700
O	2.11734600	-0.52247000	-0.83473000
O	4.32691400	-1.04191600	0.16236900
O	2.57646400	-2.68366900	0.17346500
O	2.33759300	-0.74343400	1.57442000
H	1.63178400	-2.79781200	-0.05997800
H	1.90330300	0.12639500	1.49517100

$(SA)_2 \cdot (DSA)_1 \cdot (A)_2$:

Atoms	X	Y	Z
N	0.37554800	-1.94641900	-1.19044400
H	1.10152200	-1.78793200	-0.45780800
H	0.49176900	-2.87550900	-1.58466100
H	-0.56877500	-1.85210700	-0.78569300
S	0.01581700	1.31307000	-1.30660200
O	-0.27709000	2.72030900	-1.27608500
O	-1.17174400	0.48116700	-1.11612100
O	0.90357700	0.82369400	-2.34019100
S	0.31077000	0.68614600	1.50570400
O	-0.32304200	-0.62580800	1.37308800

O	-0.64625700	1.74801000	1.74019400
O	1.49705000	0.71297700	2.31264800
O	0.95896800	0.98338000	0.01051100
H	0.49603500	-1.23497000	-1.91794500
H	-2.03214000	2.09923600	0.89843200
N	-2.72325200	2.43947000	0.18581000
H	-2.14321900	2.79726600	-0.58475100
H	-3.27583900	1.63896600	-0.13185000
H	-3.32038800	3.16488700	0.56963900
S	-3.41466400	-1.30065100	0.07381000
O	-2.37658300	-2.17078600	-0.41370200
O	-4.67380900	-1.80520200	0.46861500
O	-3.71357400	-0.22862500	-1.07018900
O	-2.83273700	-0.40995400	1.20157200
H	-2.86015200	-0.04355200	-1.50688500
H	-1.81381500	-0.52518900	1.27121100
S	3.66868100	-0.79997200	0.02627400
O	2.50831000	-1.54112300	0.47078700
O	4.92447100	-1.44102500	-0.06521800
O	3.78546500	0.46683400	0.91790700
O	3.37802700	-0.22512800	-1.40741800
H	2.97442700	0.56466400	1.47705500
H	2.56660500	0.31564000	-1.45246500

$(SA)_2 \cdot (DSA)_1 \cdot (A)_3$:

Atoms	X	Y	Z
S	-1.80849800	-1.01399400	1.02474100
O	-0.54273300	-1.58061900	0.58457100
O	-2.15158000	-0.11014500	-0.36807300
O	-2.91535200	-1.92415700	1.14355100
O	-1.66344800	-0.03750700	2.07929300
H	0.10055600	0.11328700	2.41451400
H	1.48544900	-0.43593600	3.21530000
N	1.13424800	0.05518400	2.40052800
H	1.54080900	0.99730700	2.30895300
H	1.40510500	-0.43611500	1.52817400
H	5.13196300	0.54475400	-0.22677100
N	4.23247000	0.99212800	-0.36818300
H	3.43218600	0.27879700	-0.29620900
H	4.00222100	1.69398800	0.34514400
H	0.83981600	-0.90516900	-2.26305100
N	0.27505000	-0.10532700	-1.94439400
H	-0.52814700	0.07914700	-2.53904700
H	-0.05264100	-0.35783800	-1.00606300
S	2.56157100	-2.02383300	-0.47451600

O	2.19644000	-0.61865600	-0.08319200
O	3.97940400	-2.22043500	-0.40538000
O	1.94156800	-2.91038100	0.69375600
O	1.88028700	-2.38416200	-1.70168600
H	0.97260000	-2.85702100	0.62166600
H	0.86658600	0.73570200	-1.83018600
S	1.38361100	2.60826200	0.07654500
O	0.83332600	3.92721700	0.10887600
O	1.89358600	2.14005400	-1.21373700
O	2.32460900	2.28321700	1.16224600
O	0.13333700	1.59669600	0.36321000
H	4.16749000	1.44454800	-1.27605700
H	-0.65278500	2.12465900	0.55465700
O	-4.19406000	0.99054300	0.45010500
S	-3.66425200	0.35803100	-0.70272000
O	-4.35878500	-1.01987600	-0.95511300
H	-4.23211000	-1.57151500	-0.15602900
O	-3.54789600	1.00596800	-1.95785900

$(SA)_2 \cdot (A)_2$:

Atoms	X	Y	Z
S	-1.99375600	0.03950600	-0.14679700
O	-1.96770800	1.49843900	-0.07048200
O	-3.42358600	-0.32337200	-0.76178300
O	-1.06994700	-0.54333200	-1.10365000
O	-1.92152200	-0.59640400	1.16575700
H	-0.60468900	2.18376200	0.65313600
H	-4.09078700	0.17534600	-0.27653000
S	2.10772600	-0.06533300	-0.21735300
O	1.97293600	-1.43365000	-0.71671300
O	1.24928600	0.86001100	-1.20138700
O	1.39488600	0.04212900	1.09037500
O	3.41196200	0.51312500	-0.22105800
H	0.78789600	-2.09192900	0.15000000
H	0.39594100	0.39985400	-1.36649500
N	0.14396100	-2.41317300	0.93378300
H	-0.18316600	-3.36112700	0.78560100
H	0.68671400	-2.34759800	1.79018800
H	-0.66121400	-1.75146700	1.00977700
N	0.35234900	2.40999100	1.00848400
H	0.31970800	3.00004000	1.83116400
H	0.83110500	1.45569800	1.19383700
H	0.87614100	2.85816600	0.26091400

$(DSA)_2$:

Atoms	X	Y	Z
S	-1.41878100	1.52046200	0.51265300
O	-2.69600800	1.97749800	0.90202900
O	-0.39509500	2.40403200	0.05763000
O	-0.75177200	0.64196100	1.62143800
S	-2.65392900	-0.79452000	-0.54100600
O	-2.73115000	-1.07079200	0.85848300
O	-1.80259400	-1.85627700	-1.27089700
O	-3.78153000	-0.49664300	-1.32645800
O	-1.57710700	0.46231900	-0.69698500
H	-1.38737800	-0.03921100	1.91527500
H	-1.03860300	-2.10977000	-0.70346300
S	1.43272500	-1.42786500	0.61381900
O	0.20872500	-2.15792100	0.53160200
O	1.89523500	-0.87495500	1.82812300
O	2.52147400	-2.31436100	-0.06327000
S	2.44729400	0.86296800	-0.70395500
O	3.67656900	0.18828700	-0.45870600
O	2.18502300	1.79960000	0.49286900
O	2.11650400	1.45421600	-1.94014200
O	1.23916000	-0.25844100	-0.48932200
H	3.36139800	-1.81848000	-0.08343700
H	1.28815800	2.20254100	0.39631900

$(DSA)_2 \cdot (A)_1$:

Atoms	X	Y	Z
N	0.28528300	-0.68180100	2.62406700
H	-0.59378800	-1.13366900	2.31464700
H	0.27206000	-0.49647800	3.62203400
H	1.08812700	-1.25863900	2.37430700
S	2.45668400	0.93644500	0.59608300
O	3.40054900	1.94222600	0.28413100
O	2.88064400	-0.20857200	1.38851400
O	1.12728500	1.39851800	1.01624900
S	1.59351700	-1.22494400	-1.03439800
O	0.55866300	-1.39660200	-0.03502300
O	2.83912900	-2.06307100	-0.60091300
O	1.30960300	-1.50589800	-2.38480900
O	2.14918600	0.25504200	-0.93662500
H	0.41679800	0.19733500	2.08473200
H	3.18096000	-1.68329900	0.23376100
S	-2.62296000	-0.90586300	0.49237100
O	-3.99582000	-0.64698900	0.31863500
O	-2.14273900	-1.62725200	1.63872500
O	-2.07298100	-1.52366700	-0.81588400

S	-1.62075800	1.49496400	-0.72878600
O	-0.69288400	0.85266600	-1.58919300
O	-0.96024200	2.64782100	0.05389400
O	-2.91553400	1.88093100	-1.12983600
O	-1.77844600	0.47042000	0.60248800
H	-1.09207600	-1.59167200	-0.75677100
H	-0.04463700	2.37114300	0.31995000

$(DSA)_2 \cdot (A)_2$:

Atoms	X	Y	Z
N	-1.06283000	-1.26663900	-2.50840500
H	-1.03918100	-0.27055900	-2.23900800
H	-0.93182000	-1.37741500	-3.50867400
H	-0.31890200	-1.75008900	-1.97521000
S	-2.88270300	-0.93204000	0.22299100
O	-3.46280900	-1.35269200	1.47136300
O	-1.44198300	-1.10220700	0.14781000
O	-3.57241900	-1.23958000	-0.99990400
S	-2.05086500	1.78124200	-0.28564000
O	-1.74922600	1.32294100	-1.61454500
O	-0.76685900	1.62319600	0.59530600
O	-2.59651700	3.06573600	-0.06175900
O	-3.05509900	0.76889200	0.41330200
H	-1.98732000	-1.60247400	-2.21041200
H	-0.07675000	1.04680300	0.12022500
N	-1.01628000	-0.40345700	2.75278200
H	-1.11800500	0.53300700	2.34765300
H	-0.77687200	-0.34249400	3.73772300
H	-1.90170500	-0.91090200	2.60434400
S	1.45886600	-1.03894800	-0.09597300
O	1.15452900	-2.15175700	-0.95485600
O	0.99445000	0.25561700	-0.64545200
O	1.20086400	-1.20109900	1.31265500
S	3.85701600	0.43994700	0.16932600
O	3.21297600	0.98589600	1.31245400
O	3.53451600	1.31556600	-1.09382700
O	5.23236900	0.12652400	0.12019500
O	3.09922200	-0.94489200	-0.23284300
H	-0.25515200	-0.86263700	2.20874100
H	2.57035800	1.44710200	-1.12645100S

$(SA)_3$:

Atoms	X	Y	Z
S	0.16483700	1.30605100	-0.06336500
O	-0.10407000	0.08451900	-0.80968300
O	1.37746300	1.98145900	-0.39595600
H	3.11822700	1.29813100	-0.24755100
O	0.10199300	0.97627800	1.45441800
O	-1.00412300	2.28075600	-0.20277700
O	3.82969200	0.63311300	-0.17992300
S	3.19659800	-0.77206100	0.08974300
O	4.25644700	-1.69047600	0.22901900
O	2.44151500	-1.08907800	-1.24922900
O	-2.42010200	-1.31989300	-1.02508800
H	1.52576000	-0.75359300	-1.20077100
H	-1.54359000	-0.87259000	-1.03690100
O	2.19850800	-0.63473100	1.12400800
O	-3.16961700	0.85361300	-0.19755800
H	0.83407900	0.33942600	1.63195900
H	-1.87447800	1.78339100	-0.18874100
O	-4.64837000	-1.13962700	-0.15465900
S	-3.36281200	-0.56330400	-0.04568500
O	-2.73563400	-0.88198700	1.36909700
H	-3.02757700	-1.75731700	1.65756900

$(SA)_3 \cdot (A)_1$:

Atoms	X	Y	Z
N	-0.04172000	0.31393500	2.50407500
H	-0.90969100	0.06818900	1.98691100
H	0.71310500	-0.29441000	2.15097000
H	-0.17125100	0.19382600	3.50277600
S	1.01542600	1.97849500	-0.14077200
O	-0.00526000	0.92850100	-0.23378200
O	1.18656600	2.48449400	1.19635500
H	0.24693700	1.27641200	2.27050300
O	2.24337900	1.55803500	-0.83387100
S	-2.86205700	-0.43166700	-0.10848500
O	-2.02181500	-1.23225400	-1.15389300
O	-2.63228000	1.05375200	-0.53246700
O	-4.23147800	-0.71882200	-0.30442500
O	-2.26109000	-0.64315900	1.19033600
H	-1.13058000	-1.44136000	-0.79715800
H	-1.66222100	1.22940700	-0.48893400
S	1.72178700	-1.63935800	-0.07740200
O	2.65109800	-2.91101100	-0.14869600
O	2.16645600	-0.85899500	-1.30276100
O	0.37004900	-2.12000700	-0.20621800

O	2.07535500	-0.93817900	1.12542500
H	2.14919700	-3.63570300	-0.54219400
H	2.22674400	0.18299300	-1.10444000
O	0.47811700	3.22500900	-0.96825000
H	0.67455700	3.08467700	-1.90245400

$(SA)_3 \cdot (A)_2$:

Atoms	X	Y	Z
N	0.04080800	0.04080800	0.08780100
H	-0.76321900	-0.76321900	-0.54706000
H	0.93979000	0.93979000	-0.41363000
H	0.08931200	0.08931200	0.74907100
N	-2.34151400	-2.34151400	1.67098900
H	-3.28639200	-3.28639200	1.34957300
H	-2.17630400	-2.17630400	2.58799900
H	-2.22980100	-2.22980100	1.68130600
S	-3.01773500	-3.01773500	-0.12741300
O	-2.49434500	-2.49434500	-1.04838500
O	-2.99705800	-2.99705800	-0.66645800
O	-2.44011400	-2.44011400	1.21337500
H	-1.33804100	-1.33804100	-1.42890100
S	0.27373000	0.27373000	-0.39748000
O	-0.35916500	-0.35916500	-1.49334800
O	1.58046200	1.58046200	-0.89844300
O	-0.64753600	-0.64753600	-0.22470400
O	0.32340100	0.32340100	0.84468800
H	-0.13168800	-0.13168800	0.59204600
H	-1.66304700	-1.66304700	0.95201500
O	-4.55140600	-4.55140600	0.11903600
H	-4.94495500	-4.94495500	-0.73381900
S	3.42424600	3.42424600	0.12698000
O	3.89261900	3.89261900	-0.32505500
O	2.62104500	2.62104500	1.44668900
O	4.56295900	4.56295900	0.47398200
O	2.48760400	2.48760400	-0.85833400
H	3.09999000	3.09999000	-0.64371300
H	1.79771600	1.79771600	1.24585300

$(SA)_3 \cdot (A)_3$:

Atoms	X	Y	Z
S	2.60141600	-1.19585400	0.09028500
O	1.48413400	-2.08386400	0.36783500
O	3.92882800	-2.09122400	0.15651500
O	2.64333500	-0.67818000	-1.26933200

H	3.92528500	-2.56696900	0.99505500
S	-2.73331100	-1.02693500	0.00470300
O	-2.78264800	0.26465500	0.66745400
O	-4.06497900	-1.75400600	0.51531200
O	-2.83320700	-0.99509200	-1.44855000
H	-4.30626800	-2.41338000	-0.14407300
S	-0.34333100	2.24129800	0.02140700
O	0.26545600	0.92835600	-0.28703000
O	-0.60525300	2.36316200	1.44529000
O	-1.71298000	2.30527000	-0.74363100
O	0.44986700	3.32229000	-0.55386900
H	1.94532200	2.65273900	-0.68157200
O	2.75488900	-0.16732100	1.12583000
N	-0.07985100	-0.27110800	2.17282900
N	2.80483500	2.03905400	-0.63408200
N	-0.08936400	-1.27196600	-1.83994300
H	3.65956600	2.54992200	-0.82231000
H	2.84235300	1.58042200	0.28701900
H	2.70046200	1.23535100	-1.26789800
H	-2.30374600	1.63719400	-0.32205100
H	0.20145100	-1.90642500	-1.08397800
H	0.51392500	-1.39430700	-2.64518600
H	-1.09237500	-1.39308200	-2.03483900
H	0.03941600	-0.31894800	-1.44051300
H	0.91162700	-0.26388400	1.90403900
H	-0.59002500	-0.90705900	1.52372800
H	-0.45080700	0.69119800	2.04875500
H	-0.19333800	-0.58822500	3.12877200
O	-1.60662500	-1.84665700	0.45914400

$(DSA)_3$:

Atoms	X	Y	Z
S	0.20058700	-1.09702200	-1.15759400
O	-0.75267800	-1.23915500	-2.18655000
O	1.41227700	-1.85381200	-1.13531800
O	0.61345500	0.37737400	-0.92256800
S	-0.65836100	-0.58956900	1.57248700
O	-0.96210400	0.75850000	1.24735200
O	0.77513700	-0.71673600	2.11662200
O	-1.54732800	-1.36272000	2.37363400
O	-0.58860700	-1.48732000	0.21606500
H	-0.16170800	0.97743800	-1.06934500
H	1.27191500	0.13194600	1.97015700
S	3.16751900	1.44593000	0.66771900
O	2.11537600	1.54845200	1.62857800

O	3.09683700	2.04295000	-0.61014100
O	4.47876400	1.84417900	1.40927300
S	4.47540600	-0.76257600	-0.53237500
O	5.54265900	0.17809900	-0.57016500
O	3.70722500	-0.64915700	-1.86685400
O	4.62866300	-2.09812000	-0.10838500
O	3.34601500	-0.15791000	0.52269500
H	5.23016800	1.73824800	0.79697400
H	2.88860200	-1.19670800	-1.80949100
S	-2.98114400	1.49977200	-0.86663300
O	-1.70753200	1.67676000	-1.48070000
O	-3.40748300	2.24270700	0.25560300
O	-4.02611000	1.56313900	-2.02210500
S	-4.31055300	-0.72598200	0.27882700
O	-5.45430200	-0.01498400	-0.18075800
O	-4.04308800	-0.27092900	1.73470100
O	-4.13280000	-2.11690900	0.12305200
O	-3.01137400	-0.09004300	-0.51251800
H	-4.90978200	1.38516300	-1.65097100
H	-3.27849100	-0.75983900	2.11165600

$(DSA)_3 \cdot (A)_1$:

Atoms	X	Y	Z
N	0.23627200	-1.96073500	-0.71711400
H	0.83135000	-1.22419300	-1.11189500
H	-0.47464300	-2.24639700	-1.39057000
H	0.84398700	-2.72280400	-0.41636300
S	2.99428800	-1.48147900	1.19230900
O	3.76092700	-1.69912900	2.35965600
O	2.97618200	-2.50494100	0.15723500
O	1.65954800	-0.91023800	1.36184900
S	3.73770700	0.04348500	-1.10731600
O	2.32973500	0.00638000	-1.45803700
O	4.43420500	-1.21505500	-1.70193400
O	4.49012600	1.18658900	-1.44125800
O	3.86007400	-0.19336100	0.44978000
H	-0.24547700	-1.57048500	0.10341800
H	4.05873700	-2.00721700	-1.26167300
S	-0.48334000	1.55748600	-1.35759100
O	-1.49019000	2.53697800	-1.24910900
O	-0.65340400	0.31538200	-2.03458400
O	0.83077100	2.24481400	-1.79209600
S	0.01972700	2.04173200	1.42562100
O	0.90228500	3.08888000	1.08400800
O	0.56881200	1.04469200	2.43433600

O	-1.32676800	2.37093800	1.82356100
O	-0.09671100	1.01675700	0.15251600
H	1.54102900	1.56537600	-1.84574600
H	1.12685400	0.27775100	2.03071400
S	-3.44921300	-0.97270500	-1.36363300
O	-2.57837800	-2.10286000	-1.27881300
O	-3.54011100	-0.14399100	-2.49453500
O	-4.89306500	-1.38041200	-0.94914900
S	-2.82890800	-0.63503300	1.37361800
O	-3.87627900	-1.58120200	1.57208600
O	-3.10315200	0.61193200	2.19430100
O	-1.46587100	-1.04753600	1.46941300
O	-3.03189700	0.01798200	-0.12242900
H	-4.87209300	-1.81925600	-0.07695900
H	-2.36253400	1.31580500	2.08637700

$(DSA)_3 \cdot (A)_2$:

Atoms	X	Y	Z
N	-0.66041100	-0.35858300	2.45263400
H	-0.30164800	0.60118200	2.51435900
H	0.13690500	-1.01375200	2.54886000
H	-1.38635500	-0.52973500	3.14244300
S	-1.08763400	-2.42013500	-0.81829300
O	-0.92506100	-3.58220100	-1.60844000
O	-0.86045500	-2.52573600	0.61572200
O	-0.77571200	-1.13423700	-1.37235000
S	-3.63437000	-1.56988600	0.31981100
O	-2.93540100	-0.28391100	0.50457700
O	-3.31331600	-2.40553400	1.60697800
O	-5.03221700	-1.52992000	0.13787400
O	-2.93960200	-2.33469900	-0.81200200
H	-1.04527300	-0.49920600	1.51155700
H	-2.40339600	-2.76174800	1.49687500
S	0.20530000	2.89462700	0.88943800
O	1.33714400	2.94939200	0.04788300
O	0.25296000	2.44757400	2.24293500
O	-0.47544400	4.30079600	0.80227100
S	-1.89470000	2.50362500	-1.01860100
O	-2.85501800	3.33046000	-0.37814900
O	-2.42405800	1.15660600	-1.45459100
O	-1.02185200	3.01980200	-2.01885500
O	-0.91574300	1.93183600	0.22655000
H	-1.33788000	4.30929600	1.24666100
H	-2.69974100	0.53578500	-0.65607200
N	1.03465500	0.82325900	-2.03991000

H	1.99624500	0.81698700	-2.37849300
H	0.58203500	1.72379100	-2.20998000
H	0.48427800	0.06373300	-2.44290500
S	1.98658500	-1.16394100	0.77541700
O	1.74077900	-1.79002200	2.04717000
O	2.01465000	-2.00086400	-0.40316200
O	1.23499400	0.07459300	0.60205500
S	4.46328600	-0.37101000	-0.34654800
O	3.66416400	0.38622300	-1.26134800
O	4.67308900	-1.81475700	-0.90706300
O	5.70869100	0.10406900	0.11341300
O	3.58026100	-0.66051100	0.96366800
H	1.08766400	0.63388100	-1.01491300
H	3.78917200	-2.21710600	-1.02815300

$(DSA)_3 \cdot (A)_3$:

Atoms	X	Y	Z
N	-4.05000800	2.05521800	0.68059200
H	-3.51014800	1.42083700	1.29826600
H	-4.55280800	2.75404100	1.21663400
H	-3.38727800	2.49070700	0.02183800
S	-3.70982800	-0.79855400	-0.86879100
O	-3.66545400	-1.69780000	-1.98856500
O	-2.76191800	0.30192500	-0.92989400
O	-4.99946600	-0.42280700	-0.34966700
S	-2.19912800	-1.18221100	1.52852400
O	-2.92812600	-0.05873700	2.06711100
O	-0.90602200	-0.76319600	0.90343800
O	-1.98048700	-2.29294200	2.42532700
O	-3.04115800	-1.82073900	0.33668500
H	-4.68990400	1.43023600	0.17066800
H	-0.79618900	0.61522700	0.73434400
N	-0.77890000	-1.27179600	-2.07383100
H	-0.63766100	-1.47892800	-1.07740500
H	-0.00235800	-1.68416000	-2.59828100
H	-1.69853700	-1.62968500	-2.35914900
S	-0.68175800	2.36840500	-0.60726100
O	-1.86423600	3.14656200	-0.81611300
O	-0.72484300	1.67789900	0.75509400
O	-0.21230200	1.49259200	-1.63105400
S	2.01698600	3.16437800	-0.02098600
O	2.40645300	2.09568000	-0.86715700
O	1.92740500	2.67623700	1.45088900
O	2.60206900	4.44669600	-0.03629300
O	0.42311600	3.50710000	-0.33158100

H	-0.77981000	-0.24798400	-2.15438400
H	1.88253400	1.69281500	1.46370400
N	0.77094500	-2.44957600	2.36645400
H	0.94880600	-2.77060300	1.39942200
H	-0.24778300	-2.51949200	2.55866400
H	1.33412300	-2.97011600	3.03025900
S	3.17416700	-0.52117500	0.62509800
O	4.31012800	0.31723600	0.61852700
O	3.47541800	-1.90225100	1.33214900
O	1.97394100	-0.05823100	1.29584500
S	2.24319400	-2.53933000	-1.24683200
O	1.09604000	-2.68755800	-0.36751100
O	3.37940900	-3.35653200	-0.91858700
O	1.91850000	-2.32776700	-2.62215400
O	2.83816600	-0.93693100	-0.84147900
H	1.04413800	-1.46166300	2.35613700
H	3.86739000	-2.53385600	0.69063500

1